The Effects of Extra Yarn Gripping on Fabric Ballistic Performance

A thesis submitted to the University of Manchester for the degree of

Doctor of Philosophy

In the Faculty of Science and Engineering

2017

Nan Wang

School of Materials

Table of Contents

LIST OF FIGURES

LIST OF TABLES

ABSTRACT

The development of weaponry drives the demand for advanced body armour materials. The heavy weight of currently fielded armour systems and subsequent reduction in wearer's mobility has highlighted the need for light-weight personal armour systems. The primary objective of body armour research is to focus on the development of lightweight and wearable garments that effectively resist ballistic impact with low-cost. This research is concentrated on manipulating the inter-yarn friction in the ballistic fabrics by means of weaving technology in order to improve the energy absorption of the ballistic panels.

By using textile techniques, 5 novel fabrics with enhanced yarn gripping insertion were designed and created utilising wrapping angles between the warp and weft yarns in the fabrics in this research. It was revealed that the increased wrapping angle provides higher inter-yarn friction over the normal wrapping angle by yarn pull-out tests and the pull-out force can be increased up to 128%. Ballistic performance of the engineered fabrics was evaluated experimentally by ballistic penetration tests with designed layer arrangement. The improvement based on average energy absorption for the fabric was found relating to the impact location on the engineered fabrics but such discretion disappeared for fabric panels containing larger number of fabric layers. It was found that the leno insertion method among the other methods (cramming and double pick) showed superior ballistic performance to the rest of the engineered structures and the conventional plain woven fabrics in the V_{50} test. It was established that optimal layer arrangement for layers of fabrics with leno insertion for ballistic performance was achieved by offsetting the leno insertion lines among the adjacent layers of fabrics.

FE model was established using ABAQUS® software for numerical analysis to achieve further and more comprehensive understanding of the influence of the inter-yarn friction on the ballistic performance of fabrics and panels based on the use of fabrics with leno insertions. The optimal leno gap was found to be 4 cm which was related to the highest impact energy absorption. EV_{50} evaluation of panels made from the engineered fabrics confirmed the optimal design. Impact locations for panels with different designs were also studied numerically as an extension of the findings obtained from ballistic tests, and it confirmed leno insertion facilitates energy absorption in the plain area.

DECLARATION

No portion of the work referred to in the thesis has been submitted in support of an allocation for another degree or qualification of this or any other university.

COPYRIGHT STATEMENT

ACKNOWLEDGEMENT

I sincerely thank Dr Xiaogang Chen for his supervision, help and guidance throughout the whole research project.

Special thanks go to the financial support from by the UK DSTL, and the School of Materials, the University of Manchester, who partially contributed to my tuition fees. Appreciations also go to Teijin Aramid for providing Twaron® yarns for this research.

I also would like to thank Mr Tom Kerr, Mr John Payne and Mr Mark Chadwick of the Weaving Laboratory for their technical support, in making my ballistic fabrics at the University of Manchester.

My gratitude extends to the colleagues in the Textiles division in the School of Materials for providing good working atmosphere.

I also wish to express my appreciation to the members of the ballistic materials research team, including Dr Yi Zhou, Dr Yanyan Chu, Dr Yanfei Yang, Dr Shengnan Min, Dr Yue Xu, Mr Yuan Chai, Mr Haoxian Zeng, and Mr Zishun Yuan for their selfless friendship.

Thanks also go to my kindest husband Dr Qian Ma, who often had valuable discussions on my research and gave me support and encouragement throughout my whole study period.

Finally, I would like to express my deepest gratitude to my dearest parents for their patience, encouragement, moral support and most importantly financial support during my PhD study.

PUBLICATIONS

1. Xiaogang Chen, Yanyan Chu, Nan Wang, Study on inter-yarn friction and engineering of ballistic fabrics, *Proceedings to 14th AUTEX World Textile Conference*, 26th to 28th May 2014, Bursa, Turkey

2. Xiaogang Chen, Yanyan Chu, Nan Wang, Inter-yarn friction and engineering of woven fabrics for ballistic protection, *Proceedings to the 7th Cross-Strait Symposium on Textile Science and Technology*, 5th to 10th May 2014, Fujen University, Taipei, Taiwan

Chapter 1 Introduction

1.1 Background and the Problem

Modern ballistic body armour is widely used by soldiers and police officers because of regional conflicts and public security issues. Demand for body protection has expanded from the armed forces and police task forces to prison guards, cash carriers and private individuals. The body armour protects individuals from all kinds of bullets and fragments to stabbing with sharp and pointed objects. Lightweight body armour with improved protection has been studied through research and manufacturing to allow the wearers to perform their duties effectively.

In essence, ballistic body armour absorbs and dissipates the kinetic energy carried by the impacting projectiles so that they lose their ability to harm the body armour wearers by piercing the ballistic panel or by trauma impact. There have been many reports showing the effectiveness of body armour systems in saving lives [1, 2].

There are two types of personal body armour protection used by law enforcement and the military: ‘soft’ and ‘hard’ body armour. The flexible ‘soft’ armour is made from soft ballistic fabric materials and is commonly used when facing a low ballistic threat, while the ‘hard’ armour is a combination of the soft ballistic panel and a hard ballistic panel primarily covering the heart area. It is designed to protect from high energy projectiles [3].

For the soft body armour, the ballistic panels are normally made from multiple layers of a woven or nonwoven structure of high-performance ballistic fibres that have high modules and strength-to-weight ratios. When the fibre is hit with high velocity, a fast-travelling longitudinal strain wave develops and propagates along the fibre as it pulls

the fabric towards the impact area. A slower transverse wave also forms simultaneously [4]. If the projectile hits fabric, the momentum of the projectile will be transferred to the fabric in the vicinity of the impact point [5]. Some authors have reported that woven fabrics with fewer interlacing points show better ballistic performance due to the reduced interference of the strain wave propagating upon ballistic impact, and the major source of kinetic energy absorption is fibre breakage [3]. However, woven fabrics with plain and basket weaves are commonly used for ballistic protection because of the belief that interlacing points in a woven construction facilitate the interaction between warp and weft yarns, causing more yarns in the fabric to absorb energy [6, 7]. In any case, the strain distribution in a woven fabric used for body armour is anisotropic.

The performance of a ballistic fabric can be affected by various factors, such as fibre type, fabric architecture, boundary conditions and friction between yarns. Aramid fibres and ultra-high-molecular-weight polyethylene (UHMWPE) fibres are the most popular materials on the market for ballistic fabrics because of their high tensile strength and modulus and excellent transverse properties. Aramid fibres are well known for their resistance to chemical, mechanical cut and flame, but they are ultraviolet (UV) sensitive [8]. UHMWPE fibres are highly resistant to corrosive chemicals except oxidising acids. Such fibres have extremely low moisture absorption and a very low coefficient of friction due to self-lubricating properties [9]. The use of such fibres has tremendously reduced the weight of the body armour, but the weight is still considered too high, and this continues to be a major concern. A soldier on the battlefield can carry an average load of 40kg; the load generally ranges from 25kg to more than 60kg based on the mission objectives and duration, and 20% (14kg) of this weight comes from the body armour [10]. Clearly, the excessive load is detrimental to

the soldier's performance. There has been demand for the ballistic body armour to become lighter and less bulky while the ballistic performance is retained. There have been extensive efforts to find new technologies for thinner and lighter body armour and to identify new materials along with the existing fibre technology for body armour.

1.2 Aims and objectives

The aim of this research is to enhance the ballistic performance of the soft body armour with reduced weight. Textile techniques will be devised to improve the ballistic performance of the fabric based on the understanding of the influence of inter-yarn friction in fabrics. The research will be done based on experimental and numerical approaches.

The objectives of the research are as follows:

- establish an understanding of the failure mechanisms of ballistic fabrics;
- investigate the influence of inter-yarn friction on the ballistic performance of woven fabrics;
- identify textile techniques that facilitate increased inter-yarn friction in ballistic fabrics;
- evaluate fabrics and panels made from such fabrics for ballistic performance; and
- complete an experimental and numerical analysis of the effectiveness of the devised textile techniques for making ballistic fabrics and panels.

1.3 Thesis layout

Followed by the Chapter 1 Introduction, Chapter 2 presents a review of the literature. Systematic information on the materials comprising the soft body armour, the working mechanism of the ballistic impact, fabric structures, evaluation standards for ballistic

impact, methods for investigating the ballistic fabric, and factors influencing the ballistic performance are covered in Chapter 2.

Chapter 3 presents the primary experimental studies on the created fabrics with extra yarn gripping. The design of the novel fabrics and the production process are discussed. Yarn pull-out tests under a quasi-static condition and ballistic dynamic tests are adopted to investigate the novel fabrics.

Chapter 4 discusses the experimental study conducted on fabric with leno insertion. The selection of the fabric structure is determined to be fabric with a leno insertion based on the V_{50} tests on novel fabrics. The evaluation of a layer arrangement of fabrics was designed and tested by a multilayer penetrating ballistic test. The optimum panel layer arrangement is established.

Chapter 5 presents a theoretical investigation of woven fabrics. The fundamental examination of the inter-yarn friction of novel fabrics is studied by FE analysis to establish the relationship between inter-yarn friction and energy absorption. The FE modelling of the ballistic impact on fabrics was created to study the energy absorption of fabrics, strain distribution on the fabrics, and effect of inter-yarn friction etc. By using FE modelling, detailed information can be obtained that can not be achieved from the experiments.

Chapter 6 presents an extended numerical study of fabrics with leno insertion. Based on the validated model, the optimisation of gap intervals of leno insertion is investigated by ABAQUS® and validated by EV_{50}. The impact locations and energy absorption of fabrics with different layer arrangements are discussed and analysed.

Chapter 7 summarises the research with a conclusion and provides recommendations for future work.

Chapter 2 Literature Review

Together with the advancement in armed weaponry, the design of body armour has been under constant improvement. In order to create advanced body armour, the protective mechanisms of body armour have been under intensive investigation, both theoretically and experimentally. Many experimental and numerical studies to analyse ballistic performance have been done, which has led to essential understanding of the protective mechanisms. Such understanding contributes to the knowledge base, enriching and strengthening the present research methodology.

This chapter presents a review of the literature from six comprehensive aspects: (1) the history of body armour, (2) the working mechanism of soft body armour, (3) factors influencing ballistic performance, (4) ballistic level and standard evaluation, (5) methods for investigating ballistic impact and (6) approaches to modify inter-yarn friction.

2.1 Body armour and requirements

The development of armour began with the human race. Mankind throughout recorded history has used various types of materials to protect itself from injury in combat and other dangerous situations. In the early stages of civilised history, protective clothing and shields were made from animal skins. As civilisations became more advanced, wooden shields and then metal shields came into use [11].

There are generally four types of body armour based on the materials and composition, which are leather, fabric or a combination of both materials, small metal rings linked together (chain mail), and rigid armour made of metal, horn, wood or similar strong materials [12].

Chinese warriors used layered rhinoceros skin as protective armour in the 11th century BC. Ancient Greeks wore thick, multi-layered linen breastplates during the 5th century BC. Densely woven silk was used by the medieval Japanese army. Indians used quilted linen until the 19th century [13]. The hoplites in the main Athenian army were armed with helmets, body armour and equipped with a pike and sword. The Spartan army used body armour consisting of breast and back plates fastened by thongs or straps and buckles. The equipment of the Roman soldier went through a number of changes. During the Punic Wars, they wore a side-covered headpiece and a round buckler three feet in diameter. The warriors carried a scutum consisting of two boards glued together, covered with canvas and skin and incurved into the shape of a half-cylinder [14]. During the 12th and 13th centuries, chain mail was the dominant defence of the protective coat in Western Europe, then it was replaced by plate armour made by steel during the 14th century. The Germans started to use the metal suit with a flexible joint area covering the whole body except for small holes for eyes and for breathing. Plate armour was the main design until the 17th century [15].

The invention of explosive powder changed the dynamics of the battlefield. Mankind became exposed to high-speed projectiles, which are fired from various weapons. The knowledge was limited to the use of steel working as personal protective material. However, this protective armour was incredibly heavy with poor flexibility, and thus could only be used for the protection of large vehicles, not people. In recent years, scientists and researchers have worked on ballistic materials and their interaction with high-speed projectiles [3]. Currently, the primary function of body armour is still to stop high-speed projectile penetration and absorb the impact energy. New requirements of the body armour arise according to modern military operations, technology-driven war tactics and on-street weapons [16].

2.2 Methods for investigating ballistic impact

The ballistic impact in the transverse direction, caused by the high-velocity projectile, is a complicated, dynamic and high-speed physical process. Two main methods have been adopted to investigate this phenomenon in details, i.e. an experimental approach and a theoretical/numerical approach. Both research methods can be used independently or in combination to investigate the ballistic impact in order to enhance the understanding of the mechanisms of failure mode and energy absorption of the protective materials. Each investigation approach has its merits and demerits. For example, the experimental approach is usually time and capital consuming, but it is essential for the validity and effectiveness of analytical models and numerical models. Shen [5] carried out research using combined experimental and theoretical methods to characterise the interaction among bullet, body armour, and human and surrogate targets.

2.2.1 Experimental method

The experimental method is based on experiments using controlled experimental design and equipment provided to test hypotheses. By analysing the data obtained from experiments, the desired information will be found. The experimental method not only provides first-hand information of the design acquirements, but also works to provide necessary validation data for the theoretical hypotheses. It provides a wealth of data and forms the basis for empirical studies. In this research, the experimental method is adopted to investigate fabric response, including energy absorption and other related ballistic performance characteristics of fabrics.

The testing devices used to obtain energy absorption and mechanical properties include the Instron® tensile test machine, ballistic ranges and high-speed photography. Tabiei and Nilakantan [17] reviewed the experimental testing methods in detail

regarding the ballistic impact of the fabric and mechanical properties of the yarn. Photographic and monitoring techniques are commonly adopted by researchers to observe the ballistic event. Susich [18] carried out a microscopic study on the failure mechanism of a penetrated sample constructed by nylon, whilst Wilde [19, 20] conducted a high-speed missile impact upon nylon fabric assisted by the photographic technology. Mitchell [21] used an environmental scanning electron microscope to examine the post failure of innovated body armour. Field [22] systematically reviewed the experimental techniques used for high rate materials deformation and shock studies by dropweight machines, split Hopkinson pressure bars and high-speed photography in association with an optical study. Cork and Foster [23] found through ballistic testing that narrow fabrics absorb more energy than wider fabric panels when undergoing transverse ballistic impact. In general, experimental work can be conducted based on the research aspects of appropriate laboratory instruments. The experimental approach is powerful and useful when a few variables are correlated and the results achieved from the experiments are intuitive and effective. However, the limits of the experimental method are time consuming and costly regarding the material. The accuracy of the achieved data depends on the specific experimental condition and correctness.

2.2.2 Theoretical method

Theoretical methods involve analytical and numerical models, and if used properly, the theoretical methods can be useful to obtain specific data that the experimental methods are not able to detect. A complete and comprehensive study of the ballistic impact process can be achieved through experimental, analytical and numerical approaches separately or in combination.

2.2.2.1 Analytical method

The analytical method is mainly based on a comprehensive mathematical formulation and relies on physical principles.

Several studies were carried out by Smith [24-26] that used analytical methods to investigate the stress-strain relationships in yarns subjected to rapid impact loading from various aspects, such as wave propagation and the velocities of strain waves and shock waves. Analytical modelling of the ballistic impact events on textile fabrics and ballistic impact behaviour has been studied by numerous researchers [4, 27-35] for effective prediction of the process and response of the materials involved. The advantages of the analytical method compared to the experimental method are fewer materials and labour needed during the study. The drawback of the analytical methods is that idealisations of the model have to be made but may cause model inaccuracy [36-38].

2.2.2.2 Numerical method

With the development of information technology, researchers use computer simulation to explore problems and discover data that is highly unlikely to be achieved by experiments and analytical desk calculations. The fundamental concept of the numerical method for analysing the ballistic impact on fabric behaviour is based on the finite element method (FEM) and associated computer software. The FEM's practical application is known as finite element analysis (FEA). The concept of FEA is to divide the integrity to limited small units called mesh and then calculate the components' displacements, strains and stresses under internal and external loads by time step. The commonly used commercial software includes ABAQUS, ANSYS and LS-DYNA.

When it comes to modelling, the first task is the construction of a model for the targeted fabric panel. Three types of models are commonly adopted: the pin-joint model, the 3D continuum finite element model and the unit-cell based model. These models are basically yarn-based.

Pin-joint model

The pin-joint model was developed by Roylance and his colleagues [39, 40]. The fabric panel is first idealised as assemblages of pin-jointed, flexible fibre elements with a mass that makes the areal density of the idealised mesh equal to that of the panel being simulated [40]. The original pin-joint model developed by Roylance is a 2D woven fabric with a 2D truss element net and warp/weft crossover points modelled as simple pin joints. The transverse stiffness of the fabric was not considered. The model created by Roylance was modified by Cuniff and his co-workers [41], and the model is shown in Figure 2-1, where blue bars represent the picks, yellow lines represent the warp ends and green dots denote the crossover points between picks and warp ends. A transverse spring was inserted between a pick and warp end at the crossover point that is used to model the fabric's transverse stiffness. The green dots were modified into torsional spring joints to model the yarn bending stiffness [42].

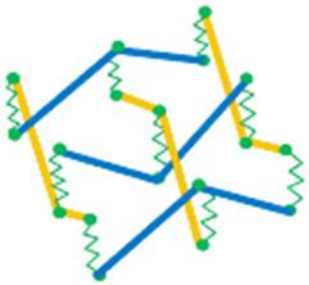

Figure 2-1 Cunniff-Roylance Model [41]

The model was initially established by Roylance and Wang [43] to investigate the ballistic penetration mechanics of textile structures from the aspect of the influence of non-linear viscoelastic relaxation, and they found that non-linear viscoelastic constitutive models can be incorporated into a numerical analysis of textile impact with no real difficulty. Shim *et al.* [44] modelled fabric by pin-joint elements with the consideration of a three-element linear viscoelastic constitutive relationship to represent polymeric material behaviour. Billon and Robinson [33] chose two types of models for the ballistic impact of fabric armour investigation and comparison; one is the pin-jointed finite element method and the other is analytical, and the pin-jointed model shows good agreement with the experiment from the aspect of single and multiple layers made by aramids. Termonia [45] added slippage in at the crossover points on the model and found that the results are in agreement with experimental data, and yarn slippage is responsible for some of the salient features observed in ballistic data. Tan *et al.* [46] introduced crimp in the pin-jointed one-dimensional element model and compared two different ways of incorporating yarn crimp into a fabric model, which include arranging the yarn in a zigzag manner and leaving the yarn elements straight but discounting some element strain that arises from straightening the yarns by the constitutive equations of the elements. Zeng *et al.* [47] used the pin-joint model to investigate the influence of boundary conditions on the ballistic performance, subject to high-strength fabric targets. Novotny and co-workers [48] did an investigation on multi-ply fabric during early stage impact.

The pin-joint method presents a significant advantage on simplifying the problems and effectiveness of predicting ballistic performance under projectile impact. However, because the fabric structure and geometric structure of yarns are oversimplified, the hidden factors such as the yarn cross-section shape, inter-yarn friction and layer-layer

contact are not able to be considered. Therefore, the discrete nature of the model is not capable of obtaining certain data, such as a yarn pull-out mechanism.

3D continuum model

The pin-joint model is capable of presenting fabric responses to ballistic impact, but due to the deficiency of yarn details, some important parameters cannot be investigated. The 3D continuum model is a computational fabric model, constructed based on yarn geometry and properties and weave configuration. The commonly used commercial software packages for 3D continuum are all based on finite element analysis and include DYNA3D by Methods Development Group at Lawrence Livermore National Laboratory; LS-DYNA, developed by the Livermore Software Technology Corporation (LSTC); and ABAQUS by Dassault Systemes. DYNA3D is a general, explicit, finite element programme for static and dynamic structure analysis and uses small time steps to integrate the equations of motion to solve transient dynamic problems. LS-DYNA is more advanced than the original DYNA and DYNA3D. It incorporates all the LLNL codes (DYNA3D, NIKE3D, Topaz and ALE3D) into one code, a fully automated contact analysis capability and a wide range of constitutive models to simulate a whole range of engineering materials. LS-DYNA is far superior on the running time of the model, the efficiency and optimisation compared with DYNA3D. The choice of software depends on the type of simulation.

In the research area, Shockey *et al.* [49, 50] attempted to create a fabric model using LS-DYNA3D to explicitly simulate individual yarn and construct them into a fabric panel to analyse impact tests, as shown in Figure 2-2. Gu [51] adopted a finite element code LS-DYNA incorporated with the Weibull constitutive equations of filament yarns at high strain rate to simulate ballistic impact response, which proved to be

effective in simulating the interaction between the projectile and the multi-layered fabric. Duan *et al.* [36, 38, 52, 53] conducted a series of studies on the role of the friction effect during the ballistic impact of the fabric panel and transverse impact on a ballistic fabric by using LS-DYNA to model the ballistic impact. Zhang *et al.* [54] used the same method to investigate the effect of frame size, type and clamping pressure on the ballistic performance, which is realised by controlling one variable to obtain the required data and effectively acquire the V_{50} results. Rao *et al.* [37, 55] used LS-DYNA to focus on developing a global/local 3D finite element model of plain woven fabric to examine the ballistic impact from a spherical projectile, and on modelling the effect of yarn material properties and friction on the ballistic impact of a plain-weave fabric. The modelling results showed that the 3D finite element method is effective in predicting the fabric's ballistic performance and is a time-saving approach to investigate individual factors. There are more studies [56-60] that have used similar methods to offer in-depth and broad research on the ballistic impact on the fabric panels. More comprehensive structures, including 2D and 3D woven fabrics, can be described by a 3D continuum model. Jin *et al.* [61] created a three-dimensional angle–interlock woven fabric to undergo ballistic impact using ABAQUS/Explicit and found good agreement with the experiment results in terms of impact damage. Chen *et al.* [62] used a constitutive model to investigate the layer arrangement of a hybrid fabric panel.

(a) Single crimped yarn (b) Meshed woven fabric

Figure 2-2 Finite element meshes [49]

The 3D continuum model takes time to run the model package; therefore, structures of the model can be simplified by using a 2D shell element rather than a 3D solid element, using hybrid elements for the fabric panel and coarse mesh for analysis. Grujicic *et al.* [63] and Ha-Minh *et al.* [64] adopted this method to create a membrane-like structure, ignoring the thickness of the yarn. The hybrid materials elements method is from the fabric undergoing ballistic impact subject to different forces; the centre area has more deformation due to the compression, shearing, and bending etc., while the boundary area is less deformed. Barauskas *et al.* [65] applied this hybrid technique to analyse the impact of the multilayer fabric. The coarse mesh means that a number of finite elements will be decreased to achieve increased computer calculation. This method is adopted by Chocron *et al.* [57] and Zhou [66] to study multilayer fabric under ballistic impact.

The 3D finite element model has the advantage of predicting a specific detailed impact mechanism based on the accurate yarn geometry and fabric structure. Therefore, the yarn-yarn frictions, layer-layer contact, pull-out behaviour and mechanics related to the yarn structure and friction can be conveniently investigated. However, this method is time-consuming, and it demands sophisticated computer resources to simulate multi-

layered fabric panels. It is always a consideration in balancing the accuracy of the model and efficiency of the computer software.

Unit-cell based model

The unit-cell based model is a promising method to determine fabrics' mechanical properties [67]. Numerical simulation at the part scale represents a powerful tool to predict the feasibility of a composite part. This scale ensures a good compromise between complexity and accuracy [68]. It has been used extensively to create the equivalent continuum-level material models of textile composites from the knowledge of the meso-scale fibre and yarn properties, fabric architecture and inter-yarn and inter-ply frictional characteristics. The unit-cell is constructed by the smallest unit to enclose the characteristic periodic repeating pattern in the fabric weave as shown in Figure 2-3. The term meso-scale is used to denote yarn-level millimetre-length scale details of the fabric microstructure.

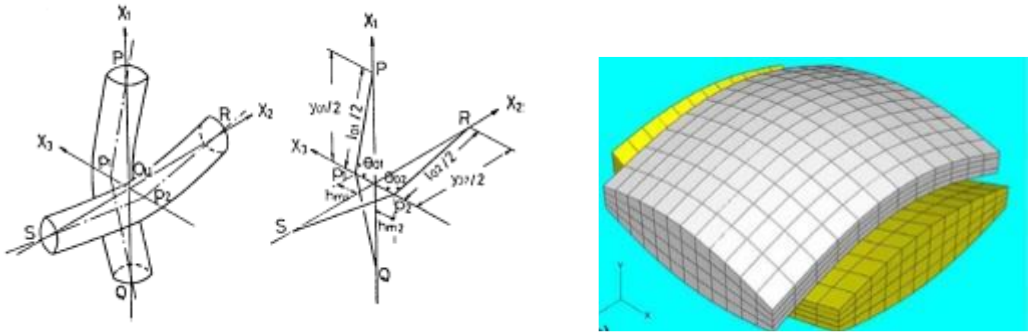

(a) (b)

Figure 2-3 (a) Geometry proposed by Kawabata *et al.* [69] (b) The unit-cell representative of crossover [70]

Unit-cell based approaches were introduced by Kawabata *et al.* [69, 71, 72], who created a simple analytical model to capture the biaxial, uniaxial and shear behaviour of fabrics. Based on the studies of Kawabata, Ivanov and Tabiei [73] developed a micro-mechanical material model that is viscoelastic with a strain rate dependence of the failure, and the model shows reasonably good agreement with the experimental results. Furthermore, King *et al.* [74] proposed a new method for developing a continuum-level material model for fabrics based on the properties of the yarns and fabric structure by using an energy minimisation technique to determine the relationship between the configuration of the fabric structure to the unit cell deformation of fabric components. A new computational approach was developed by Shahkarami and Vaziri [75] to replace the unit cells with orthotropic shell elements that have similar macroscopic mechanical properties as the unit cell, which provided a detailed account of its incorporation into a material model subroutine and can be readily coupled with a commercial dynamic explicit finite element code. Grujicic *et al.* [76] provided an extension work of Shakarami and Vaziri [75] to study a single-ply flexible fabric armour subjected to ballistic impact.

Compared with the pin-joint model, the unit-cell model is able to achieve surface-finish and friction governed by yarn-to-yarn and layer-to-layer contacts. A meso-scale unit-cell model makes it easier to attain computational efficiency when calculating the mechanical response of the multi-ply, fabric-based flexible armour material without significantly sacrificing the key physical properties of fabric configuration and behaviour [76]. However, the main issue of the unit-cell based model is that it requires specific and realistic yarn behaviour when subjected to the force of external impact.

2.3 Working mechanism of soft body armour

The main principle behind the protection provided by body armour is the rapid conversion and dispersal of kinetic energy from a striking projectile to other forms of energy of the ballistic body armour system, including kinetic energy, strain energy and friction dissipation. It is necessary to establish a fundamental understanding of energy absorption mechanisms of fabric panels. The response of a fabric panel is built upon the response of yarn, and yarn is constructed by fibres, thus the mechanics of single fibre impact is the starting point to analyse the behaviour of woven fabric panels under ballistic impact [39].

2.3.1 Response of single fibre and yarn to ballistic impact

The response of a single fibre or yarn under ballistic impact can be divided into five stages. When a projectile hits the fibre, the fibre is considered horizontal and the subject projectile is assumed to be perpendicular to the armour. The wave propagation on the fibre is due to the tensile strain caused by impact, and the material starts inward compression from the area of impact. The projectile impact causes a transverse strain, which moves outward at a speed that depends on the projectile's velocity and the targeted material. The strength is limited by the fibre's tensile strength. All energy that is absorbed after the fibre generates the longitudinal wave decreases the fibre's tensile strength [77].

Wave propagation in the single fibre and yarn attracted much attention from researchers. Smith [24] provided a comprehensive explanation of the longitudinal wave and transverse wave theory, whilst Roylance [39, 78] described detailed calculations of longitudinal wave and transverse wave velocities. Cheeseman and Bogetti [79] confirmed that when a projectile strikes a fibre, two waves, longitudinal and transverse, propagate from the point of impact. The longitudinal tensile wave

travels down the fibre axis at the sound of speed in the material and propagates away from the impact point, which leads to the material behind the wave flowing towards the impact point. In addition to the longitudinal wave, transverse waves are propagated outward from the point of impact. This transverse movement of the fibre is the transverse wave, which is propagated at a velocity lower than that of the material. The response of the single yarn under a projectile impact is shown in Figure 2-4.

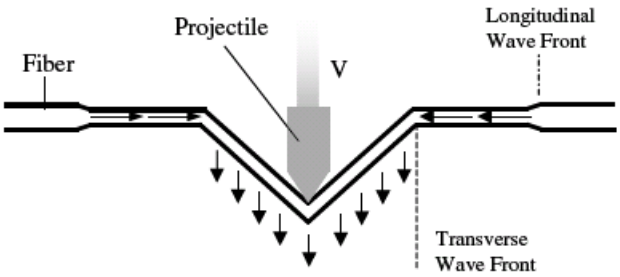

Figure 2-4 Projectile impact into single yarn [79]

The longitudinal wave velocity and transverse wave velocity can be calculated by equations from a theoretical study from Smith [24, 25] as follows:

$$C = \sqrt{\frac{E}{\rho}} \tag{2-1}$$

$$U_{lab} = C\left(\sqrt{\varepsilon_{ins}(1+\varepsilon_{ins})} - \varepsilon_{ins}\right) \tag{2-2}$$

where C is the transmission speed of the strain wave inside the fibre, which is the longitudinal stress wave velocity in yarn; E is Young's modulus of the fibre; ρ is the fibre density (g/cm^3); U_{lab} is the transverse stress wave velocity in the yarn with respect to the laboratory [27]; and $\varepsilon_{ins}$is the fibrous instantaneous strain generated in the yarn at the instance the projectile contacts the yarn.

The theory indicates that the strain developed in a textile filament under transverse impact is dependent on the yarn's properties and impact velocity [27] based on the assumption that the yarn is elastic, and Poisson's ratio is not taken into consideration [28].

2.3.2 Response of fabric when impacted by a projectile

Researchers have noticed that similarities exist between the transverse impact of a panel of fabric and a single fibre. Cunniff [80] found that a similar situation exists when a bullet hits the fabric; the resulting strain wave can be split into a longitudinal wave and a transverse wave. The most involved area is the impact area constructed by principal yarns, and the rest of the yarns in the fabric are considered to be secondary or orthogonal yarns as shown in Figure 2-5. The energy distribution in the fabric has been investigated by Roylance [81], and the projectile kinetic energy will be transferred to the fabric as strain energy and kinetic energy, while the majority of the energy is absorbed by the primary yarns, which is shown clearly in Figure 2-5. One can see the principal yarns are highly stressed, while the secondary yarns are not. Principal yarns interact with the secondary yarns through the intersection, hence, the fabric tends to spread energy over a larger area [77]. The longitudinal wave speed in the fabric is slower than the wave speed in the single fibres by a factor of $\sqrt{2}$, which is attributed to an effective increase in linear density due to the crossovers [39].

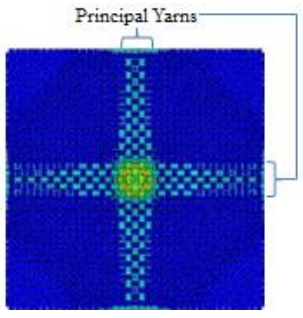

Figure 2-5 Principal yarns under high stress [36]

The essential difference between fibres and fabrics is the extensive and widely distributed wave interactions that are generated by the presence of fibre crossovers. During the event of impact, the crossovers in the fabric facilitate the transfer of the impact stress to the secondary yarns. The yarn-yarn interactions at the crossover points are a function of the friction between the yarns [79]. Crossovers are able to get more yarns involved in absorbing energy; on the other hand, crossovers will lead to excessive elongation of the yarn, which will reduce the efficiency. When the strain waves meet at the crossover point in the fabric, the waves will be reflected back and then meet new coming waves, hence forming a superposition of the reflected wave and the new coming wave. The wave superposition would result in excessive elongation in the corresponding yarn. Freeston and Claus [82] stated that longitudinal wave transmission and reflection at the crossover point do not considerably affect the wave spread away from the impact point. Numerical studies by Roylance [81] showed that crossovers have a great influence on the ballistic response of a panel, and the influence of wave diversion is much stronger than that of reflection.

2.4 Factors influencing ballistic performance

The ballistic performance of a fabric is affected by many factors [17, 79, 83]. There are internal and external design factors that affect ballistic performance, which include the yarn's material properties, fabric architectures, the projectile geometry and velocity, panel boundary conditions and frictions between yarns and projectiles.

2.4.1 Internal factors

The internal factors refer to those related to the target fabric, which include the yarn materials, the fabric configuration and the interaction between the yarns.

2.4.1.1 Yarn Materials

High performance and lightweight are the most important requirements for body armour. The current high-performance ballistic fibres all have certain unique properties because of the manufacturing process and chemical structures. As has been explained previously, a high velocity projectile impact on a woven fabric causes an out-of-plane deformation and an in-plane wave propagation. A greater dissipation of strain will be created, and it will propagate outwards from the impact point with an increased in-plane wave velocity. The propagation velocities of both waves are a function of the tensile modulus as mentioned before. Therefore, the tensile modulus of yarns and tensile strength of yarns are fundamental for ballistic performance [23].

When a projectile hits a fabric, the corresponding yarn experiences a sharp increase in stress, and the magnitude of this stress is proportional to the impact velocity. The 'critical velocity' is the lowest projectile velocity at which the fabric panel can be penetrated. If the impact is less than critical velocity, the initial stress increase is insufficient to break the fibres, allowing the transverse deflection and resultant yarn extension time to propagate, resulting in the absorption of energy by the fabric [44]. It is clear that fibres with high tensile strengths and large failure strains can absorb a substantial amount of energy. The experimental results discovered by Lee [84] showed that fibre strain is the fundamental mechanism of the energy absorption in the penetration failure of ballistic textiles. Results reported by Shim [44] and Cunniff [80] implied that when the velocity of the impacting projectile is over a specific value, the fabric panel will be perforated during the initial stress increase. In other words, a higher speed leads to a shorter time for the fabric stress to rise, which reduces fibre straining, thus reducing the energy absorption of the ballistic fabric. Royland and Wang [43]

numerically illustrated that a material possessing a high modulus E and low density ρ would have a high-wave velocity, so it would be able to transfer the strain wave more rapidly away from the impact point. It is understood that materials as media facilitating higher sound speed are superior in ballistic performance to materials transmitting sound waves with lower velocity.

The ballistic performance of a fabric is determined by the yarn properties' density [85], and Equation (2-3) below explains the relationship between the physical properties of the yarn and the fibre properties, which was used by Cunniff [86].

$$U^* = \frac{\sigma\varepsilon}{2\rho}\sqrt{\frac{E}{\rho}} \tag{2-3}$$

Where U^* represents the fibre ballistic property and is defined as the product of the specific fibre toughness multiplied by its strain wave velocity, σ is the fibre's ultimate tensile strength, ε is the fibre's ultimate tensile strain, E is Young's modulus of the fibre and ρ is the fibre density. It is confirmed repeatedly that armour performance is not defined by these properties, but it is coupled with them.

Another fibre mechanical property that would affect ballistic performance is the shear stress, especially in a situation of high velocity impact with sharp-edged fragments [87]. Under the circumstance of sharp-edged, high impact velocity, the tensile failure could be explained by a cutting mechanism [36, 65, 70, 88]. Ha-Minh *et al.* [89] studied the effects of yarn's transverse properties on the ballistic impact behaviours and found that Poisson's ratio can be negligible in the their impact model. They also confirmed the importance of the shear modulus of a yarn leading to a single yarn breakage affecting the failure of the fabric panel. Apart from the tensile stress and shear stress experienced by the yarn, the strain rate has been found to have a significant

effect on the ballistic performance. Jin *et al.*[61] observed that the projectile would lose more energy when the target materials are subjected to a higher strain rate impact.

Synthetic, high-performance fibres have physical and chemical superiorities, which are distinct from other man-made fibres used for industrial applications. Because of the extreme high-tensile strength and modulus of the fibres to the ratio of mass and lower elongation compared with brittle fibres, such as fibreglass and graphite fibres, high-performance fibres can be easily woven on fabric looms. Such fibres have chemical resistance advantages, such as industrial solvents and lubricants used by the automotive and aerospace industries. Different high-performance ballistic fibres have their own unique property because of the polymer used to manufacture the fibre and the specific spinning process. The structural characteristic at a molecular orientation of the spinning direction determines the tensile properties of the ballistic fibre. The microscopic structure and chain orientation in a ballistic fibre is controlled by the manufacturing process.

Two main types of fibres are used for ballistic protection: the para-aramid synthetic fibre and the ultra-high molecular weight polyethylene (UHMWPE). Kevlar and Twaron® are well-known brand names of para-aramid fibres, and the Dyneema® and Spectra® are reputable brand names of UHMWPE fibres.

Aramid fibres

In the late 1960s, DuPont invented a family of fibres three times as strong as nylon with a far higher modulus [90], and the new fibre was commercialised as Kevlar® in 1971. Kevlar® is a man-made organic fibre with a combination of properties allowing for high strength with low weight, high chemical resistance and high cut resistance.

Kevlar® is also flame resistant; it does not melt, soften or flow, and the fibre is unaffected by immersion in water [91]. These fibres are much tougher and lighter than glass fibres and replaced nylon in flexible and rigid armour used by law enforcement agencies and the military. Kevlar® 29, introduced in the early 1970s, was the first generation of bullet-resistant fibres developed by DuPont, and it helped to make the production of flexible, concealable body armour practical for the first time. In 1988, DuPont introduced the second generation of Kevlar® fibre, known as Kevlar® 129. According to DuPont, this fibre offered increased ballistic protection capabilities against high energy rounds such as the 9mm FMJ. In 1995, Kevlar® Correctional was introduced, which provides puncture resistant technology to both law enforcement and correctional officers against puncture threats. The newest addition to the Kevlar® line is Kevlar® Protera, which DuPont made available in 1996. DuPont contends that Kevlar® Protera is a high-performance fabric that is lighter weight and allows for more flexibility and greater ballistic protection in a vest design due to the molecular structure of the fibre. Its tensile strength and energy-absorbing capabilities have been increased by the development of a new spinning process [91].

Roylance [40] studied the effect of four different fibres: nylon, Kevlar®29, Kevlar® 49 and graphite as indicated in Table 2-1, on the ballistic results when made into fabrics. Graphite has the highest modulus and the lowest fracture strain rate among these four types of fabric. It is evident that the higher the tensile modulus the lower the level of fracture strain. The high tensile modulus is related to high stress wave speed, as discussed earlier.

Table 2-1 Geometric and material properties used in fabric studies [40]

Fibre	*Nylon*	*Kevlar® 29*	*Kevlar® 49*	*Graphite*
Tensile modulus, GPa	7.77	70.4	127	430
Fracture strain, %	14.0	4.0	2.2	1.1
Fabric mass, g	19.53	17.38	25.75	27.09
Yarn denier	1050	1167	1485	1500
Yarns/cm	17	16	16	16

Twaron® is another commercially available para-aramid fibre that is manufactured by Teijing Aramid. Both Kevlar® and Twaron® belong to the aramid family of synthetic fibres, and both contain a large number of elementary constituents (500-1000). It is highly probable that this determines the relatively high level of protective properties of articles made from Kevlar® and Twaron® [92].

Ultra-high-molecular-weight polyethylene (HMPE) fibres

Ultra-high-molecular-weight polyethylene (UHMWPE), also known as high-modulus polyethylene (HMPE) or high-performance polyethylene (HPPE), is a subset of the thermoplastic polyethylene. This type of fibre can be created by gel-spun manufacturing technology. It has extremely long chains, with a molecular weight numbering in the millions, usually between 2 and 6 million. The longer chain serves to transfer a load more effectively to the polymer backbone by strengthening intermolecular interactions. This results in a very tough material, with the highest impact strength of any thermoplastics presently made [93]. It is highly resistant to corrosive chemicals except for oxidising acids. It also has extremely low moisture absorption and a very low coefficient of friction. Because it self-lubricates, it is highly

resistant to abrasion, and in some forms it is 15 times more resistant to abrasion than carbon steel. It is odourless, tasteless and non-toxic [94].

UHMWPE fibres are used in armour, specifically in personal armour and other protective situations. For personal armour, the fibres are, in general, aligned and bonded into sheets, which are then layered at various angles to give the resulting composite material strength in all directions [95, 96]. The main manufacturers of this type of fibre are Honeywell making Spectra® and DSM making Dyneema®.

Poly-p-phenylenebenzobisoxazole (PBO) fibres

Poly-p-phenylenebenzobisoxazole (PBO) forms a strong synthetic polymer fibre. It provides excellent mechanical properties along with extreme thermal stability, which makes PBO the optimum material for applications like lightweight bulletproof vests and fire-resistant suits [97]. PBO is spun from a lyotropic melt in polyphosphoric acid (PPA) under stretching by an adjustable spin-draw ratio (SDR). PPA is removed by coagulation in a water bath, resulting in the as-spun (AS) fibre, which is subsequently heat treated to create the final high modulus (HM) fibre.

In the fatigue property of PBO fibre test conducted by Yamashita *et al.* [98], they observed that the PBO fibre has the best tensile modulus of elasticity in the organic fibre among the high-performance fibres such as Kevlar 49, HMPE, Kevlar 29. However, the compression modulus and the shear modulus are lower than other high strength fibres.

Zylon® is commercialised PBO fibre, which is characterised by high tensile strength (10 times higher than steel), excellent impact energy absorption (twice that of para-aramid) and exceptional thermal stability (limiting oxygen index of 68) [99]. However,

with time, the disadvantage of such fibres is exposed. It has been found that at a temperature of 100℃ or cooler, in ordinary sunlight, the fibre's performance will be decreased [99]. As a result, Zylon® fibre has been banned as ballistic protection in the US.

Nylon

Nylon was the bullet-resistant fibre of choice for many years because of its high strength-to-weight ratio [100]. Nylon fibres' performance is affected by humidity and temperature [101]. It was used as a raw material of body armour for soldiers to provide a degree of protection, but it is bulky and heavy, weighing up to 6 kg. Therefore, nylon was replaced by high-performance synthetic fibres.

Overall, the properties of a material determine the fundamental ballistic performance. Obviously, yarns and fibres with better mechanical properties will improve the ballistic performance.

2.4.1.2 Fabric architecture

Although the yarn property is a fundamental issue for ballistic performance, the response of the fabric constructed by yarn is also pivotal in determining the ballistic performance, as pointed out by Roylance [39]. The material's properties should be combined with effective fabric architectures to produce a fabric response. Woven and nonwoven structures are made into various types of fabric. In addition, yarn's linear density and thread densities in a fabric are also factors affecting the ballistic performance of body armour.

Woven fabrics

A woven fabric is constructed by interlacing warp and weft yarns into a two- or three-dimensional structure. The weave patterns of the two-dimensional woven structure are named by the way the warp and weft yarns are interlaced, such as ‘plain’, ‘twill’ and ‘satin’ weaves. The plain weave has the highest yarn-interlacing density or weave-crimp-density because of a higher number of crossover points, followed by the twill and then satin weave. The three-dimensional woven fabrics can be created based on different types of construction, such as multi-layer, orthogonal and angle interlock. Three-dimensional fabrics can also be created by braiding [102].

Cunniff observed that loosely woven fabrics and fabrics with unbalanced weaves result in inferior ballistic performance [80]. The density of yarns in the fabric, related to the ‘fabric cover factor’, is determined from the width and pitch of the warp and weft yarns and gives an indication of the percentage of the gross area covered by the fabric. The cover factor should range from 0.6 to 0.95 to be effective when utilised in ballistic applications, as noted by Chitrangad [103]. When the cover factor is greater than 0.95, the yarns become crimped, so the efficiency of yarns in resisting ballistic impact is reduced, and when the cover factor falls below 0.6, the fabric is too loose to protect against a piercing projectile. The ‘wedge through’ phenomenon could happen when the fabric is loosely woven. Figure 2-6 illustrates contact between a projectile and a layer of woven fabric. It can be seen that when a projectile strikes a layer of fabric, the fabric deflects transversely and the mesh of yarns is distended, which will result in the enlargement of the spaces between the yarns [79]. Prosser [85] regarded the hole as a ‘trap door’.

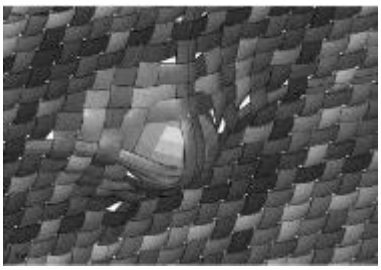

Figure 2-6 Contact between a projectile and a woven fabric [79]

Mechanisms of how the fabric architecture affects the ballistic performance have been studied by Roylance [39], Laible [104], Cunniff [86], Lyons [105] and many others. A crossover in a woven fabric leads to yarn crimp, and crimp has been found to reduce the efficiency of the ballistic performance significantly. Studies indicate that a structure with fewer interlacing yarns has better ballistic performance due to the reduced interference of the strain wave propagation upon ballistic impact [106]. It is conjectured that the various strain waves propagates from the impact point will be partially reflected at the crossover point. Therefore, the crossover density will influence the strain distribution along the yarns involved in energy absorption. It is assumed that reduced crossover density leads to a lighter basis of fabric and more ply panels. Also, lower crossover density will provide a longer duration of stretch prior to local rupture because the strain nearest the impact point is lower [107]. However, a reduction in the number of crossovers in a woven fabric leads to a less stable and less solid fabric, which could also be detrimental to the ballistic performance of the fabric. Wave propagation phenomena occurring at fibre crossovers have a very strong influence on the ballistic response of a panel [81].

Nonwoven

Since the crimp in the woven body armour has a detrimental effect on the energy absorption and fewer interlacing yarns show better ballistic performance, research has been carried out to produce nonwoven ballistic fabrics, and it is reported that nonwoven ballistic fabrics have strong weight advantages over woven fabrics. However, this introduced a significant increase in the bulk of the armour, and unidirectional materials are less flexible than their woven counterparts. It is claimed that nonwoven fabrics allow a great deal of moisture and heat transfer compared to light weaves, which make the ballistic vest more comfortable to wear. On the other hand, moisture degrades ballistic performance; therefore, the packs need to be kept dry by encapsulation [12].

Nonwoven fabrics as ballistic resistant materials have been used in three ways: single fibre components, multiple layers of various single fibres and blended fibre constructions [108]. The experiment was done by Lin *et al.* [77] to test the ballistic performance of nonwoven materials, and the results showed that compound nonwoven fabrics were strong enough to bear the force that is exerted against the chest or the wearer. The compound nonwoven fabric enlarged the impact areas, dispersed the energy and cushioned the ballistic impacts.

A significant factor that has contributed to the soft body armour development is the concept of a hybrid by combining more than one ballistic material in a single armour system [109]. The benefit of such a combination includes utilising the full potential of various ballistic materials. The hybrid materials that are combined with conventional materials and shield-based products have shown significant advantages when used against soft body armour threats.

Yarn linear density and yarn density in a fabric

Previous research has found that fabric constructed of finer yarns performed better than fabric constructed of thicker yarns [102]. This shows that the negative effect of crimp can be diminished by increasing the number of yarns to resist the projectile impact penetration. Basically, the number of fibre breakages on ballistic impact is the mean source of kinetic energy absorption, and it is greater for the fine yarn-based fabric systems than the thick yarn-based systems [110].

In terms of density in a fabric, Lim *et al.* [111] conducted a study on two woven fabrics with different weaving densities, one with higher weft densities than the other; the latter exhibited a higher tensile strength along the warp. Their findings indicate the need for an optimal weave that would minimise damage to both the yarn and fabric. Foster and Cork [23] discovered that square fabrics with the same thread density and yarn linear density in the warp and weft directions show better ballistic resistance performance than others with the same fabric areal density.

2.4.1.3 Influence of friction and inter-yarn friction on ballistic performance

The fibre's friction properties along with the fibre's physical properties play an important role in slowing down the projectile. Friction also helps to strip the jackets from bullets, deform the bullets and ultimately stop the bullets. Controlled friction between fibres is desirable to slow down and deform the bullet. However, when the inter-yarn friction is too high, one fibre will cut another fibre during the bullet penetration and reduce the material's performance. On the other hand, if the friction between fibres is too low, the material will not offer any resistance to the penetrating bullet and the bullet will not slow down or be deformed [112]. In the current armour materials, friction can be adjusted by changing the fibre orientation, which can be done

by applying a coating on the fibre or bonding a film on the ballistic material. Quilting is another technique to increase fibre-to-fibre friction in the woven fabric vests.

Friction is one of the channels to absorb and dissipate energy. The frictional energy dissipated during the impact event is the primary non-linear energy absorption mechanism. Frictional mechanisms usually include frictional dissipation due to the slippage of yarns, interaction of adjacent layers or interaction of the projectile and the target. Many factors will affect the magnitude of the fictional energy dissipated, including the friction coefficient between the contacting yarns and panel boundary conditions allowing or restricting yarn motion. The frictional effect is more obvious at lower impact velocities [113].

Researchers found that yarn pull-out may be directly responsible for absorbing energy during a non-perforating impact event. However, friction between the projectile and the yarns and the yarns themselves may be responsible for how much energy is absorbed during an impact event. The work of Lee [84] observes that increasing the friction between the projectile and the fabric and the yarns themselves will affect the mobility of the yarn and require the projectile to engage and break more yarns, which would result in greater energy absorption. The importance of friction for ballistic impact has been studied by a number of researchers. Briscoe and Motamedi [114] explored the frictional characteristics of three different styles of Kevlar fabric with respect to their ballistic impact performance. Different levels of inter-fibre friction within the Kevlar fabrics were achieved by removing or adding surface lubricants. It was observed that for a given style of fabric, the velocity required to perforate increased while the residual velocity decreased with increasing levels of friction. Fabric with a higher level of friction absorbs larger amounts of energy. Bazhenov [115]

surmised that water served as a lubricant that decreased friction between the bullet and the yarns due to using the wet and dry materials for experiments. They all show that interfacial friction plays a critical role in the ballistic impact of fabrics. Tan and Ching [116] developed a finite element model using bar elements to model the ballistic impact of a rigid sphere onto a plain woven fabric structure made of Twaron CT716 yarns, and the results gained by the experiment and analysis show that the friction helped improve the ballistic performance of the fabric with higher stiffness and higher strength yarns. The friction between the yarns is more important than the friction between the projectile and the fabric [37].

2.4.2 External factors

2.4.2.1 Projectile geometry and impact velocity

Different geometries of projectiles will lead to different penetration abilities. The different geometries of bullets are shown in Figure 2-7. The researchers found that pointed bullets tend to 'wedge through' the fabric, and the velocity will not reduce as quickly as blunt bullets. Montgomery [117] did an experiment to verify this. Tan *et al.* [118] did an experiment on a single ply of Twaron fabric, and they found that fabric creasing and perforation mechanisms were highly dependent on the projectile's shape. Montgomery [117] also found that the effect of the bullet shape decreases as the layers of fabric are applied, which has also been observed by others. Lim [119] investigated two plies of Twaron fabric impacted by four different projectile shapes.

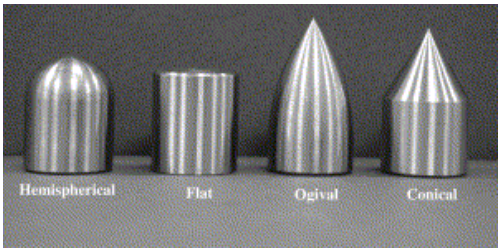

Figure 2-7 Types of projectiles used for experiments [117]

A wedge through perforation and tensile yarn rupture are not the only mechanisms observed in fabric perforation. Researchers [117, 118] have found that projectiles with a sharp edge or travelling at a high velocity penetrate fabrics by shearing yarns across their thickness. Prosser [85] reported that the cutting action is the first action when sharp-edged projectiles penetrate the fabric in the multiple layers of nylon panels.

Besides the effect of projectile geometry, the impact velocity affects the penetration capability at the same time. The energy associated with a bullet is proportional to the square of the velocity of the bullet. If two bullets have the same geometry and weight, but one is travelling at twice the speed of the other bullet, the kinetic energy associated with the bullet with higher velocity will be four times that of the slower bullet [120]. It has been observed that higher velocities and sharper projectiles tend to fail fabrics and multiple plies by shearing across the yarns rather than extending them to failure. Lyons noted that critical velocity was when yarns are struck at an adequate high velocity, they can rupture instantly. Shim [44] used steel spheres with low and high velocity to impact fabric and found differences. When hit by low velocity, the yarn did not rupture during the initial stress increase, therefore, the transverse deflection of the fabric has time to propagate to the edges of the panel, which allows the fabric to absorb more energy. A low-velocity projectile impact gives time for the yarns to extensively crease and stretch, which may contribute to energy dissipation. When the panel is

impacted with high-velocity, the damage is localised and the yarns rupture before significant transverse deflection can develop.

During an impact, the target fabric is a combination of global and local reactions [121]. Strike velocity is considered to be the most significant factor in determining the transition between a locally dominated and globally dominated response. Strictly speaking, the projectile velocity itself does not provide a clear demarcation between the two types of response, but for a given impactor and target system, it may loosely use velocity as a parameter to distinguish between the local and global response. Low velocity allows more time for a global response while high velocity allows no time for energies to spread, which forms a local response. Figure 2-8 illustrates the situation when the projectile impacts the fabric with low and high velocity.

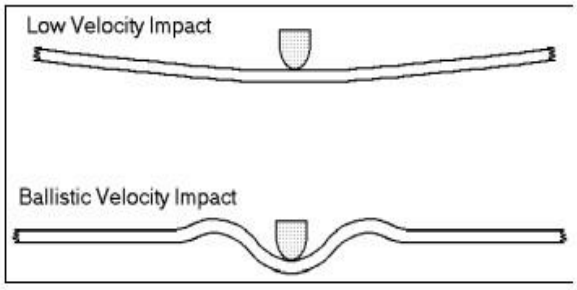

Figure 2-8 Representation of global deformation in low-velocity impact and local deformation in high-velocity impact [122]

Another observation was found on the single yarn by the high-velocity impact. Carr [123] noted the single yarn of ultra-high-molecular-weight polyethene melt, and this situation was found on PBO and Dyneema. This heat degradation of fibres has been observed since the 1950s; the filaments were damaged by softening and melting during ballistic impact experiments of nylon panels.

2.4.2.2 Boundary condition

Ballistic test results can be affected by the size of the specimen and the clamping equipment that is used to fix the fabric. Cunniff [80] tested single plies of Kevlar and Spectra clamped between aluminium plates having different apertures and observed that the ballistic limit of the fabric was strongly dependent on the aperture size. Smaller apertures decreased the ballistic limit. The absorbed impact energy was found to be a function of the clamping pressure; therefore, specialised clamping plates were employed and clamping pressures increased until the absorbed impact energy was found to be independent of the clamping pressure. It is interesting to note that when the insufficient clamping pressure was used and the specimen slipped from the clamps, the energy absorbed was 4.5 times greater than the no-slip cases [84].

Shockey [50] had implemented a number of quasi-static and impact experiments to study the effect of the boundary conditions on absorbed energy. The fragments are 25g blunt and 26g sharp simulators. The velocity of the fragment is between 52 and 113m/s. The results showed that the fabric absorbed more energy when it was gripped on two edges rather than four edges for both fragments. It has also been found that when the fabric was gripped on four edges, the failure of fabric was similar to the failure when the fabric was hit by the high-velocity impact. The two edges gripped absorbed more energy compared with the four edges gripped because of the similarities of the yarn pull-out mechanism observed by Starrat [124] and Shockey [50].

As the yarn pull-out is responsible for some of the energy absorbed during the impact event, the frictional interaction between yarns directly plays a role in the absorption of energy during an impact event. The importance of yarn–yarn friction has also been noted in a numerical study of fabric impact conducted by Parga-Landa and Hernandez-

Olivares [30]. Duan [52] and his colleagues designed simulations on the fabrics with four or two edges clamped in the different inter-yarn friction coefficients, which are 0 and 0.5. The result shows that the boundary conditions significantly affected the fabric deformation, as shown in Figure 2-9.

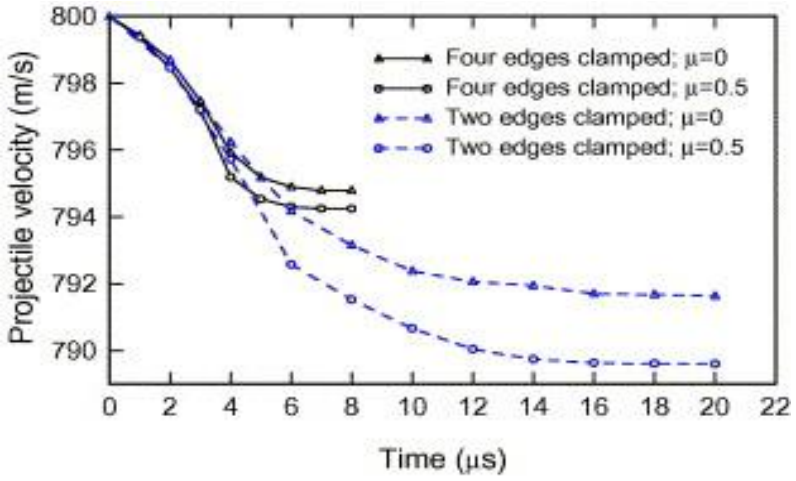

Figure 2-9 Time history of the projectile velocity for the four cases with different boundary and friction conditions [52]

Figure 2-9 shows the time history of the projectile velocity for the four cases. It can be seen from this figure that at equal friction conditions, the fabric with two edges clamped more effectively reduced the residual velocity of the projectile because the time needed for the projectile to perforate the fabric was much less if four edges of the fabric were clamped. Therefore, at equal friction condition, the fabric energy absorption capacity was much higher if only two edges of the fabric were clamped. The boundary condition is a factor that influenced the friction effect as well [52].

2.5 Approaches to modify inter-yarn friction

The frictions between yarns along with other physical properties of fibres play an important role in energy absorption of the ballistic fabric and in decelerating the impact

projectile. Controlled friction between yarns could lead to improved energy absorption and further stress/strain distribution. It has been reported that if the friction between the fibres is too low, the fibre material will not offer sufficient resistance to the impact of the projectile, and as a result, the projectile will not be decelerated or deformed [114]. For a given type of material used for body armour, inter-yarn friction can be adjusted based on different principles, which include the change in the fabric geometry, alteration of the panel construction, fabric surface treatment and so on. Furthermore, quilting is another technique to increase fibre-to-fibre friction in the woven fabric vests [125].

2.5.1 Fundamentals of inter-yarn friction

The friction between the yarns cannot be calculated by the conventional friction formula. Capstan equation 2-4 for strings with rigidity is applied to calculate the friction between the yarns [6, 88, 126]. The illustration of the wrapping angle and tension on the yarn for the capstan equation is shown in Figure 2-10.

$$T = T_0 e^{\mu\theta} \qquad (2\text{-}4)$$

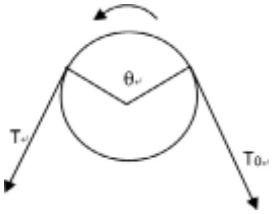

Figure 2-10 Illustration of wrapping angle and tension on the yarn

where T_0 is the hold force of the yarn within the fabric, θ is the wrap angle in radians of weft over the warp (or otherwise), T represents the load force and μ is the frictional coefficient between the yarns.

The inter-yarn friction can be reflected and evaluated through the yarn pull-out test [127, 128]. During the yarn pull-out test, three parameters will affect the pulling tension, which are the holding tension of the yarn, the coefficient of friction between the material and cylindrical surface and the contact wrap angle. Under the same test condition, the holding tension T_0 can be assumed to be the same, and altering either the μ or θ or both will affect the pulling out tension. The higher pull-out force has been shown to perform favourably in an impact test [129]. Therefore, to simplify the question, higher inter-yarn friction can be realised by increasing the contact wrap angle and the friction coefficient. The methods to increase the inter-yarn friction can be divided into two types: one uses purely woven techniques to modify the fabric structure, and the other is to treat the yarn surface to enhance the roughness of the surface.

2.5.2 Method to increase inter-yarn friction through weaving techniques

Fabric inter-yarn friction can be modified through weaving technology. Ballistic fabric is often made by using the plain weave structure to maximise the interaction between warp and weft yarns in the fabric. A further increase of the inter-yarn friction of the plain-woven fabrics, with an aim to achieve improved ballistic performance and to reduce the weight of the body armour, requires something be done on the yarn or fabric. Among many possibilities, textile techniques can be used to enhance inter-yarn gripping. Cork and Foster [23] confirmed that narrow fabrics with the conventional selvedges absorb more impact energy than narrow fabric strips without selvedges in a ballistic event. Sun and Chen [130] and Chen [131] concluded that a good ballistic fabric not only requires a proper level of yarn gripping but also requires material continuity. They engineered different techniques to enhance warp and weft yarn

gripping in plain-woven fabrics. The effectiveness of such techniques was demonstrated in their work.

Zhou *et al.* [88] applied yarn gripping to Dyneema® woven fabric to enhance the inter-yarn friction. The weaving techniques for gripping are double pick insertion from weft direction, leno insertion and cramming insertion. It has been approved that yarn gripping can provide higher inter-yarn friction from the quasi-static yarn pull-out test. However, the energy absorption is not significantly improved through these techniques, and the explanation for this phenomenon is that the degree of gripping force is not high enough to enhance the energy absorption. Sun *et al.* [130, 132] attempted to use leno insertion into plain weave structure made by Kevlar®, and it was found that fabrics with gripping yarns have improved fabric ballistic performance.

The previous study of the gripping insertion techniques implies that body armour can be made lighter without reducing ballistic impact performance by using gripping yarns. More systematic work will be carried out in this thesis to provide a comprehensive understanding of the gripping techniques.

2.5.3 Methods to alter inter-yarn friction through yarn surface modification

Inter-yarn friction can be directly altered by modifying the surface roughness, in other words, increasing the frictional coefficient. Normally, this approach requires other facilitating materials. Early attempts to use conventional chemical finishing to treat yarn surface was done by Hearle *et al.* [133] on Nylon® and Kevlar®, and the research found that this method increased the energy absorption of nylon but did not work on the Kevlar® fabric. The improved performance of Nylon® fabric can be explained by the restricted lateral mobility of yarns at the impact zone, and the reduced energy absorption for Kevlar fabric is due to the high friction level that leads to the over-

restricted fabric structure. Briscoe and Motamedi [114] applied chemicals to treat fabric surfaces and found that increasing inter-yarn friction has a positive effect in improving ballistic performance.

More efforts have been put into finding effective methods to improve inter-yarn friction, such as coating material with natural rubber, applying shear-thickening fluid (STF), sol-gel and plasma treatment etc. Natural rubber (NR) is used to coat the fabric to increase the inter-yarn friction from the research by Ahmad *et al.*[134]. They found that increased inter-yarn friction can improve the ballistic performance but leads to a significant add-on weight. Shear-thickening fluid (STF) behaves like a solid when it encounters mechanical stress or shear. Normally, it moves like a liquid until an object agitates or strikes it forcefully, then it hardens in a few milliseconds [135]. Studies have been carried out by researchers [136-138] to discover the STF effect on the ballistic performance, which indicates that fabric with STF shows promising ability in improving the ballistic resistance compared with neat fabric.

On the other hand, the conditioning situation can affect the friction coefficient. The moisture is found to be a lubricant that can decrease the inter-yarn friction. Bazhenov [96] studied the influence of water on indentation forces and pull out forces and concluded that water substantially changes the friction force during the pull out fibres. During the ballistic test, the wet fabric panel was perforated while the dry one was not. Karahan *et al*. [102] also found supporting evidence that during wet conditions, the average trauma depth is deeper (3.6% increase) than a dry fabric panel and the amount of absorbed and transmitted energies for the dry fabric is 5% higher than the wet fabric.

2.6 Ballistic performance and evaluation

It is necessary to evaluate the ballistic performance. The main reasons for the ballistic test standards can be classified into three aspects [139]: the first is to explore new and higher performance ballistic materials; the second is to have a better understanding of ballistic fibres' behaviour and the third is to provide a better understanding of the ballistic trauma on human organs. In order to assess the ballistic performance, a series of standards and methods are applied for investigation. According to the reasons of standards and requirements of the body armour, the test methods can be generally classified into three types: perforation test, non-perforation test and ballistic limit test, respectively. Results from the different test methods will provide specific data for the ballistic panel.

2.6.1 Penetration test

The aim of the penetration test is to obtain the energy absorption by the experimental specimen when an impact projectile perforates the impact target completely. The energy absorption is calculated by the direct data achieved from the experiment, which is the impact velocity and residual velocity [44, 140-143]. The impact velocity is the velocity when the projectile hits the fabric, and the residual velocity is the velocity when the projectile perforates the impact target. The energy absorption can be calculated by the following equation:

$$\Delta E = \frac{1}{2} m(v_i^2 - v_r^2) \qquad (2\text{-}5)$$

where ΔE is recognised as the kinetic energy loss of the projectile, which is considered to be the energy absorbed by the impact target, m is the mass of the impact projectile, v_i is the impact velocity and v_r is the residual velocity of the projectile. Therefore, the aim of experiments is to obtain the impact velocity and residual velocity. Normally,

the velocity is an average velocity calculated based on time and travel distance. The time will be acquired by sensors or similar equipment and travel distance can be measured easily.

The total energy loss of the projectile can be considered to be transferred to the impact target mainly in the form of kinetic energy, strain energy and frictional dissipation energy, which is without considering the circumstance of any other external force and energy loss by heat, intermolecular friction, air resistance etc. [36, 53, 66, 70, 144, 145]. The penetrating test is a straightforward way to evaluate the direct ballistic performance as well as material saving. However, it is not sufficient to predict the whole ballistic performance, as the ballistic panel will be constructed by layer arrangement and the impact location will affect the results when layering up the fabric, especially if the fabric structure is unbalanced.

2.6.2 Non-penetration test

The non-penetration test is evaluated by the back face signature (BFS) on the clay support behind the impact target fabric panel [146]. It aims to evaluate the ballistic resistance of soft body armour in a real situation. The clay is used as the armour backing material in the frame of the backing material fixture, which is used to simulate the human body. The backing material is Roma Plastilina No. 1 oil-based modelling clay, which should be replaced on an annual basis or more frequently depending on the National Institute of Justice (NIJ) standard 0101.06 [147]. The impact test will leave a pit on the clay surface, which is an indication of the blunt trauma on the human torso. It is known that fabric deflection is a way of dissipating the absorbed energy, but less transverse deflection brings a shallow pit, which means small trauma depth.

As the clay backing material is held in direct contact with the back surface of the armour panel, the back-face signature is an indication of the severity of trauma, which is reflected by the depth of the pit after the impact depression. The BFS shall be measured using a device at least capable of 1mm or better accuracy. When the measured BFS is deeper than 40mm, a second measurement is necessary. All BFS depth measurements should be 44 mm (1.73 in) or less [147]. According to the NIJ standard 0101.06, developed in 2008, it has been widely used as a reference by a number of countries. The ballistic resistance body armour in this standard can be classified into seven levels as shown in Table 2-2 [146]. Type I, IIA, II and IIIA provide increasing levels of protection from handgun threats. Types III and IV armour are used to protect against high-powered rifle rounds in specific tactical situations [146]. The ballistic test set-up is shown in Figure 2-11. The velocities of bullets during the impact procedure will be obtained by two independent sets of chronographs, and an average velocity will be recorded as the velocity of the bullet.

Table 2-2 NIJ standard 0101.04 P-BFS performance test summary [146]

Armor Type	Test Round	Test Bullet	Bullet Weight	Reference Velocity (± 30 ft/s)	Hits Per Armor Part at 0° Angle of Incidence	BFS Depth Maximum	Hits Per Armor Part at 30° Angle of Incidence	Shots Per Panel	Shots Per Sample	Shots Per Threat	Total Shots Req'd
I	1	.22 caliber LR LRN	2.6 g 40 gr.	329 m/s (1080 ft/s)	4	44 mm (1.73 in)	2	6	12	24	48
	2	.380 ACP FMJ RN	6.2 g 95 gr.	322 m/s (1055 ft/s)	4	44mm (1.73 in)	2	6	12	24	
IIA	1	9 mm FMJ RN	8.0 g 124 gr.	341 m/s (1120 ft/s)	4	44 mm (1.73 in)	2	6	12	24	48
	2	40 S&W FMJ	11.7 g 180 gr.	322 m/s (1055 ft/s)	4	44 mm (1.73 in)	2	6	12	24	
II	1	9 mm FMJ RN	8.0 g 124 gr.	367 m/s (1205 ft/s)	4	44 mm (1.73 in)	2	6	12	24	48
	2	357 Mag JSP	10.2 g 158 gr.	436 m/s (1430 ft/s)	4	44 mm (1.73 in)	2	6	12	24	
IIIA	1	9 mm FMJ RN	8.2 g 124 gr.	436 m/s (1430 ft/s)	4	44 mm (1.73 in)	2	6	12	24	48
	2	44 Mag JHP	15.6 g 240 gr.	436 m/s (1430 ft/s)	4	44 mm (1.73 in)	2	6	12	24	
III	1	7.62 mm NATO FMJ	9.6 g 148 gr.	838 m/s (2780 ft/s)	6	44 mm (1.73 in)	0	6	12	12	12
IV	1	.30 caliber M2 AP	10.8 g 166 gr.	869 m/s (2880 ft/s)	1	44 mm (1.73 in)	0	1	2	2	2
Special	*	*	*	*	*	44 mm (1.73 in)	*	*	*	*	*

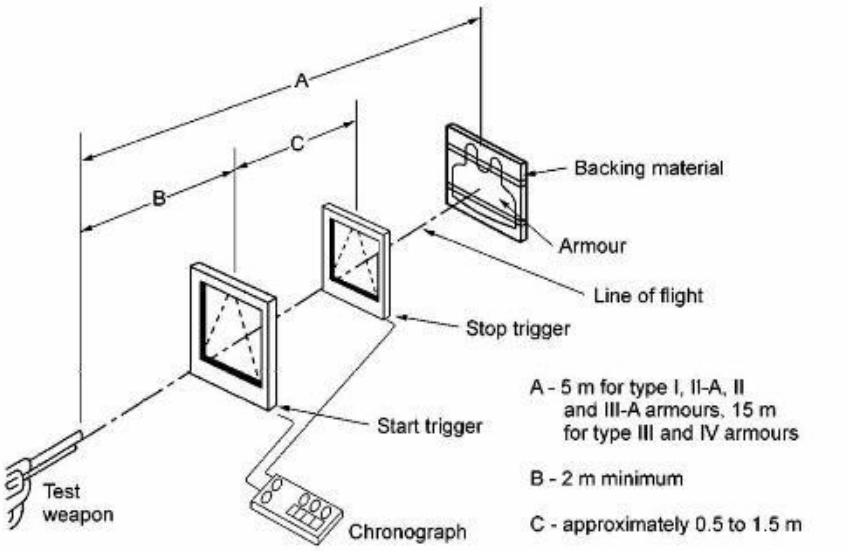

Figure 2-11 Ballistic test set up [146]

In addition, except the NIJ standards, there is another standard, which is the Home Office Scientific Development Branch (HOSDB) ballistic armour standard. HOSDB Body Armour standards are used for UK police and were introduced in 2007 [148], and the body armour system is required to provide sufficient protection to the human torso and against projectile penetration and blunt trauma. The measurement of BFS is similar to the NIJ standard as shown in Figure 2-12. The ballistic test setup is shown in Figure 2-13. In the HOSDB standard, threats can be divided into seven protection levels, which are HG1/A, HG1, HG2, HG3, SG1, RF1 and RF2; the details can be found in Tables 2-3 and 2-4. Types HG1/A and HG1 are for protection against a low-risk situation. Type HG2 is for special duty for use in firearms operations and Type HG3 is for heavy duty armour intended for use in firearms operations. SG1 offers protection from full-length shotguns at close range. Types RF1 and RF2 offer protection against projectiles fired from rifles. The maximum depth allowed from the test shots should be less than 25mm by the specific measurement, except for HG1/A, in which case the maximum depth is 44mm.

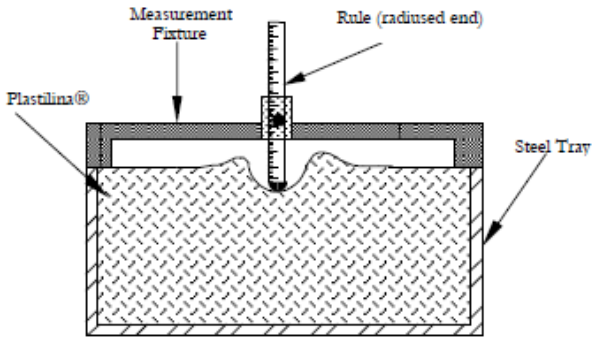

Figure 2-12 Method of measuring back-face signature [148]

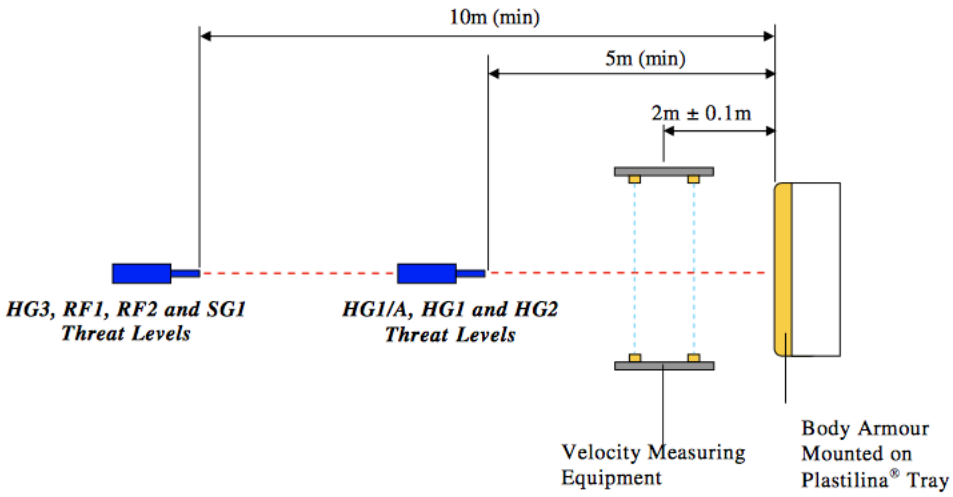

Figure 2-13 Test apparatus for ballistic testing [148]

Table 2-3 HOSDB Ballistic Performance Levels [148]

Performance Level	Calibre	Ammunition Description	Bullet Mass	Range (min) (m)	UPL (mm)	Velocity (m/s)
HG1/A	9mm	9mm FMJ Dynamit Nobel DM11A1B2	8.0g (124 grain)	5	44	365 ± 10
	0.357" Magnum	Soft Point Flat Nose Remington R357M3	10.2g (158 grain)	5		390 ± 10
HG1	9mm Calibre	9mm FMJ Dynamit Nobel DM11A1B2	8.0g (124 grain)	5	25	365 ± 10
	0.357" Magnum	Soft Point Flat Nose Remington R357M3	10.2g (158 grain)	5		390 ± 10
HG2	9mm Calibre	9mm FMJ Dynamit Nobel DM11A1B2	8.0g (124 grain)	5	25	430 ± 10
	0.357" Magnum	Soft Point Flat Nose Remington R357M3	10.2g (158 grain)	5		455 ± 10
HG3	Carbine 5.56x45 NATO 1 in 7" Twist	Federal Tactical Bonded 5.56mm (.223) LE223T3 Law Enforcement Ammunition	4.01g (62 grain)	10	25	750 ± 15

Table 2-4 Continued: HOSDB Ballistic performance Levels [148]

Performance Level	Calibre	Ammunition Description	Bullet Mass	Range (min) (m)	BFS (mm)	Velocity (m/s)
RF1	Rifle 7.62mm Calibre 1 in 12" Twist	BAE Systems Royal Ordnance Defence Radway Green NATO Ball L2 A2	9.3g (144 grain)	10	25	830 ± 15
RF2	Rifle 7.62mm Calibre 1 in 12" Twist	BAE Systems Royal Ordnance Defence Radway Green Nato Ball L40A1 7.62 X 51mm High Power (HP)	9.7g	10	25	850 ± 15
SG1	Shotgun 12 Gauge True Cylinder	Winchester 1 oz. Rifled Lead Slug 12RS15 or 12RSE	28.4g (437 grain)	10	25	435 ± 25

More standards such as MIL-STD-662F, International Standard, ISO/FDIS 14876, STANAG 2920 and PSDB provide methods to classify and evaluate body armours for different protective levels. In general, back face signature (BFS) is the key indication of the blunt trauma of a fabric panel, especially the depth of the pit [134, 136, 149-153]. However, the methods of measuring the depth of the BFS are not sufficient for

evaluating the ballistic resistance performance. Karahan [154] attempted to use the Spline curve fitting method to obtain the volume of BFS, which includes the trauma diameter and trauma depth, however, the volume is based on a single curve turning 360 degrees around the central line, which will create a regular shape. Therefore, the volume shape is always expected to be regular, but the reality is that the BFS is irregularly shaped. As the volume of the BFS is hard to measure, the non-perforation test is still difficult to obtain accurately.

2.6.3 Ballistic limit test

The ballistic limit is the velocity at which a projectile completely penetrates a specific armour when hit at a specified angle of obliquity. It is used to evaluate the fail or pass property of the body armour in a ballistic impact event [146]. The ballistic limit velocity is defined as the incident impact velocity for a specific projectile and target combination that would lead to complete penetration of the target, with a projectile tip reaching the back face of the target with zero velocity [155]. There is an equation proposed by Villanueva and Cantwell [156] to predict the critical impact velocity as shown below:

$$V_b = \frac{\pi\Gamma\sqrt{\rho_t\sigma_e}D^2T}{4m}\left[1+\sqrt{1+\frac{8m}{\pi\Gamma^2\rho_tD^2T}}\right] \quad (2\text{-}6)$$

where V_b is the ballistic limit, m is the projectile mass, Γ is an experimentally determined constant with a value of 1.5 for a hemispherical ended projectile [157], ρ_t is the density of the laminate, σ_e is the static linear elastic compression limit in through the thickness of the laminate, *D* is the diameter of the projectile and *T* is the thickness of the laminate.

The ballistic test is a costly and time consuming operation, and the velocity of the projectile is hard to be manipulated to be the exactly the same, and the complete penetration and partial penetration are not to be clearly identified. Therefore, V_{50} ballistic limit is applied to estimate the ballistic performance rather than V_b. The V_{50} is defined as the average of an equal number of the highest partial penetration velocities and the lowest complete penetration velocity, which occur within a specified velocity range. It can also be understood that it is the velocity at which the probability of penetration of an armour material is 50 percent [146, 155, 158]. A minimum of two partial and two complete penetration velocities are used to complete the ballistic limit, and the frequently used test numbers are four, six and ten [146]. Nilakantan *et al.* [159] attempted to describe the cumulative probability of complete fabric penetration at an impact velocity by the following equation:

$$P = \frac{1}{2}[1 + \mathrm{erf}\left(\frac{V-\eta}{\xi\sqrt{2}}\right) \quad (2\text{-}7)$$

Where P represents the cumulative probability of complete fabric penetration at an impact velocity at V, erf represents the error function, ξ is the standard deviation of the cumulative normal distribution and η is the V_{50} velocity. From equation 2-7, the V_1 *and* V_{99} can be given by:

$$V_1 = \eta - 2.3263\xi \quad (2\text{-}8)$$

$$V_{99} = \eta + 2.3263\xi \quad (2\text{-}9)$$

A substantial amount of research has been done by using a V_{50} ballistic limit to estimate the ballistic performance, which has proven to be the general guidelines for the procedure and to determine the performance of the ballistic armour against projectiles [160-163]

2.7 Summary

In this chapter, a broad view in terms of the ballistic fabric aspects was provided. To have a comprehensive understanding of body armour, it must start with the history of body armour, followed by the working mechanical studies of soft body armour to the methods of how to investigate the ballistic body armour and fabric panel. In the literature review, it was revealed that the ballistic performance can be affected by various factors, from both internal and external aspects. Therefore, it is necessary to find the most effective factors and provide a modification to improve the ballistic performance of the fabric based on the ballistic performance level and standards. At the last part, the summative approaches to modify inter-yarn friction are provided.

According to the previous numerical studies, a 3D continuum FE simulation method is better suited to capture the inter-yarn friction behaviour than the other methods because the yarn geometry will be included, which is essential for yarn to yarn frictional study. Based on the available evaluation of the ballistic performance, the perforation and V_{50} tests will be adopted to assess the ballistic performance of the fabric with a gripping enhancement in terms of the energy absorption and V_{50} velocity comparison.

Through the literature review, previous works provide a basis and guideline for this research to create an improved body armour fabric. It is clear that new material development is far behind the requirement of the ballistic fibre market. The performance of soft ballistic body armour material is decided by the fibre material and the construction of fabric itself. Due to the limitation of new fibre production, the improvement of ballistic fabric relies more on the fabric structure. As inter-yarn friction is one of the key factors determining the performance of woven fabrics, this

research provided a comprehensive study on enhancing the inter-yarn friction using a weaving technique.

The literature review provides an indication of possible methods to modify inter-yarn friction by gripping enhancement in the fabric. Although studies have been carried out by researchers on the gripping methods to increase the inter-yarn friction, the consistency of the results is not strong due to the material and structure effects. There is a lack of studies on the impact location analysis and gripping fabric layer arrangement. In this present research, novel weaving techniques will be incorporated into the plain fabric to create a fabric with higher inter-yarn friction on conventional looms, with an aim to investigate the performance of the novel fabric against the ballistic impact.

Chapter 3 Experimental studies on fabrics with extra yarn gripping

The ultimate goal of this research is to identify a way to develop body armour fabrics with improved ballistic performance based on the use of the weaving techniques. This chapter concentrates mainly on the study of three different yarn gripping methods and their combinations for their ballistic performance. The nature of yarn gripping is the inter-yarn friction. Yarn gripping is created when one yarn wraps over another, which determines the frictional resistance to the relative movement between the two yarns. A yarn pull-out test is popular in evaluating the frictional resistance a yarn experiences when pulled out of the fabric, and ballistic tests can always be used to assess the ballistic performance of the fabric.

This chapter is divided into two parts. The first part is the fabric design and manufacturing with enhanced yarn gripping. The principle for designing the novel fabric is based on the wrapping angle theory and the previous research of narrow fabrics. Three basic weaving techniques are used to provide the enhanced yarn gripping effect in order to increase the inter-yarn friction between the yarns, which are the leno structure, weft cramming in weaving, and double-pick for weft insertion. These techniques are adopted individually or in combinations for fabric engineering.

The second part is the static and dynamic studies on the novel fabrics for ballistic performance. The yarn pull-out test is a quasi-static experiment test, and it serves to evaluate the enhancement in yarn gripping in the newly engineered fabrics. The dynamic study refers to the ballistic penetration test of single-layer fabrics.

3.1 Design of fabrics for extra yarn gripping

In general, the ballistic fabrics are normally created in the form of the plain weave structure because it has the most crossover points compared to other weave structures with the most stable fabric geometry. In a study on plain woven fabrics for ballistic performance, Cork and Foster [23] found that narrow plain woven fabrics with returning selvedge absorbed more energy than fabric stripes with the same widths cut from a wide plain woven fabric when undergoing direct ballistic impact. The plain weave narrow fabric has a higher level of yarn gripping over the fabric stripe, and this enhanced yarn gripping can contribute to improved energy absorption. Inspired by this, plain weave structures combined with enhanced gripping yarns were engineered and are aimed to improve the energy absorption of the ballistic fabrics.

Five fabric structures are designed with the enhancing yarn gripping and material continuity.

3.1.1 Fabric specification

93tex Twaron® yarn used for the fabrics was provided by the Defence Science and Technology Laboratory (Dstl). The plain woven fabric was used as a comparison to the engineered fabrics with extra yarn gripping. The warp and weft densities of the fabric were both 7.8 ends and picks/cm. No twist was added to the yarn to maximise the fabric performance.

Three weaving techniques were applied to create the enhanced gripping effect based on the original plain woven fabric: leno insertion, weft cramming and double-pick weft insertion.

3.1.1.1 Cramming

In weaving a fabric, weft cramming is achieved by not pulling the fabric forward for a certain length of time to create a small length of fabric with high weft density. This can be done by programming the take-up mechanisms of the loom, which stops the take-up motion for a predefined number of picks. This causes an increase of weft density in the crammed area, increasing the gripping of fabric over the warp ends. The wrapping angle of warp ends over the picks in the crammed area is increased, leading to higher inter-yarn friction. The cramming structure is illustrated in Figure 3-1.

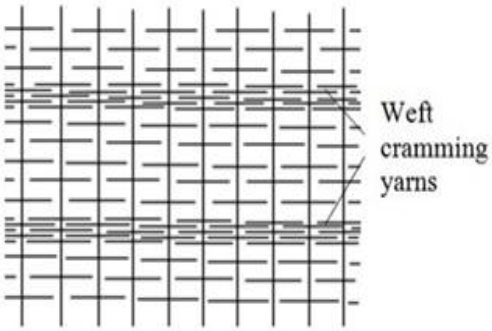

Figure 3-1 Cramming insertion in the weft direction

3.1.1.2 Double-pick weft insertion

A double-pick insertion refers to a situation in which two yarns are inserted into the same shed instead of just one. In the double-pick insertion area, the two yarns occupy one yarn's space. The cross-section of a plain woven fabric with a double-pick weft insertion is depicted in Figure 3-2.

Figure 3-2 Illustration of weft double-pick insertion in the plain woven fabric

3.1.1.3 Leno insertion

Leno fabrics, also termed gauze or doup fabrics, are a known structure that has firmer weft yarn gripping in the fabric and can be produced into broad fabrics. The structure is primarily used to limit yarn movement in order to form open woven fabrics with stable dimensions. Leno fabrics are made with a special attachment (doup) to the normal shedding mechanism and are a structure where a pair of warp yarns are intertwined by embracing a pick of weft yarn in each of the interstices. A fabric having a leno structure would have good dimensional stability and would keep weft yarns from slipping. This feature of the leno fabric was used to increase the gripping of yarns in fabrics compared to a plain woven structure with the same warp and weft density [164]. Leno fabric has the characteristics of low density, thin and lighter fabric with a stable structure and good permeability. Textile fabrics with leno weave are more slip-resistant than fabrics made using plain, twill or satin weaves because the number of crossings within a binding unit is higher and the angle of warp on thread crossings is larger. A structure of leno is shown in Figure 3-3 [165], with (a) and (b) showing the face and cross-section views. The structure involved in the newly engineered fabrics is shown in Figure 3-3 (c).

(a) (b) (c)

Figure 3-3 (a) Leno with standard and crossing ends of the same length (woven from one beam), (b) cross-section of leno with standard and crossing ends of the same length, (c) leno with standard and crossing ends of different length (woven from two beams)

3.1.2 Fabric manufacture

Warping

Warping is an important step in weaving. It is the process of preparing the required number of warp yarn ends with the required warp density associated with the fabric. The machine used for warping in this study was the MS/1800-8 HERGETH Hollingsworth Sample Warper, which consists of a creel, the warping drum, and a beaming device. In the situation of a single end sample warping machine, the creel works to provide a single yarn end and guides the yarn from a yarn cone to the warping machine. The warping drum collects the warp yarn by wrapping the single yarn end the number of times that corresponds to the number of warp ends needed for the fabrics with a fixed length. The required number of rounds of warp yarn has been collected, the looped yarn will be cut and each round will provide a single warp yarn end. The beaming device works to transfer the warp yarn ends from the drum onto the weaver's beam. In this set-up, the warping length was 8 metres, and the warping velocity was

set to 360 m/min. The warp density was controlled to 7.8 ends/cm according to the fabric specification.

During the warping process, the yarn is taken from the yarn cone fixed on the creel. A certain amount of tension will be applied when the yarn end is passed through a thread guide and delivered to the catch bar. Papers are inserted between each circle of warping on the beaming machine to prevent yarn fibrillation.

Weaving

The power loom was a Northrop L16 shaft negative dobby weaving machine. The weaving process contains five main mechanisms, namely warp let-off, shedding, filling insertion, beat-up and fabric take-up.

The beam of warp yarns is taken to the loom to carry out the drawing-in process. The warp yarns are separated into small groups and tied to the fabric beam. Certain tension will be induced on the warp yarn in order to keep them straight to create clear shedding. The weft-filling yarns are stored in the wood-made shuttle ready to be used. The plain fabric is woven on the loom directly, without other facilities.

Fabric with cramming insertion is created when the machine take-up motion is inoperative for a defined period of time. To create a decent cramming gripping effect, five cramming yarns were inserted during the inoperative take-up motion. The shedding motion is not affected during cramming insertion. The beat-up motion will press the yarns in the cramming area tightly to each other to create an enhanced gripping effect.

The designed double-pick insertion increases the wrapping angle by inserting two yarns at one time to occupy one yarn space. However, the power loom cannot achieve

this. The modification of the double-pick structure is created by inserting two yarns combined with one cramming motion to press the two yarns tightly to provide the closest position to the two overlapped yarns.

The leno weaving technique, as previously mentioned, requires a specific heald to create a leno area as shown in Figure 3-4. The leno heald consists of one doup-needle and two legs. The magnet at the bottom of the legs is used to catch the steel needle. The two legs are on separate frames. The yarns to create leno are stored on separate, special, small bobbins. The crossing ends are drawn from the leno bobbins to create a leno structure in the fabric, while the standard ends are on the warp beam as shown in Figure 3-5. The tension of the crossing end yarn can be adjusted on the small leno bobbins and can be measured by a spring tension metre. All the leno tension is tested by hand feel and measured to keep the same tension on each leno line by pulling the leno yarn with slow and constant speed from the leno bobbins.

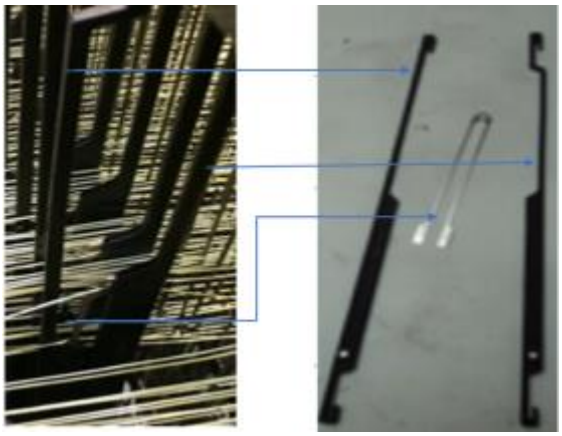

Figure 3-4 Specific heald for the leno weaving technique

§

(a) (b)

Figure 3-5 Warp supply for fabric with leno insertions: (a) Supply of leno warp yarns; (b) Supply of the standard warp yarns

The leno structure was created by the movement of the doup-healds as shown in Figure 3-6. In Figure 3-6 (a), the leno end passes through the doup eye in leno heald D, and the standard end is drawn through the ordinary heald S above the doup-needle. When raising leg L_1, the right-hand shank is disconnected with the magnet on the bottom of leg L_2, which is on the down position as shown in Figure 3-6 (b), and the leno end is on the right-hand side of the standard end and a cross shed is formed. After the weft yarn has been inserted, the doup-needle is moved upwards by L_2 and the left shank is disconnected with L_1 as shown in Figure 3-6 (c). During this movement, the leno yarn transfers to the left hand on the standard end to form a cross shed for weft yarn insertion. The movement of the doup-heald repeats the same process to create the leno structure during weaving.

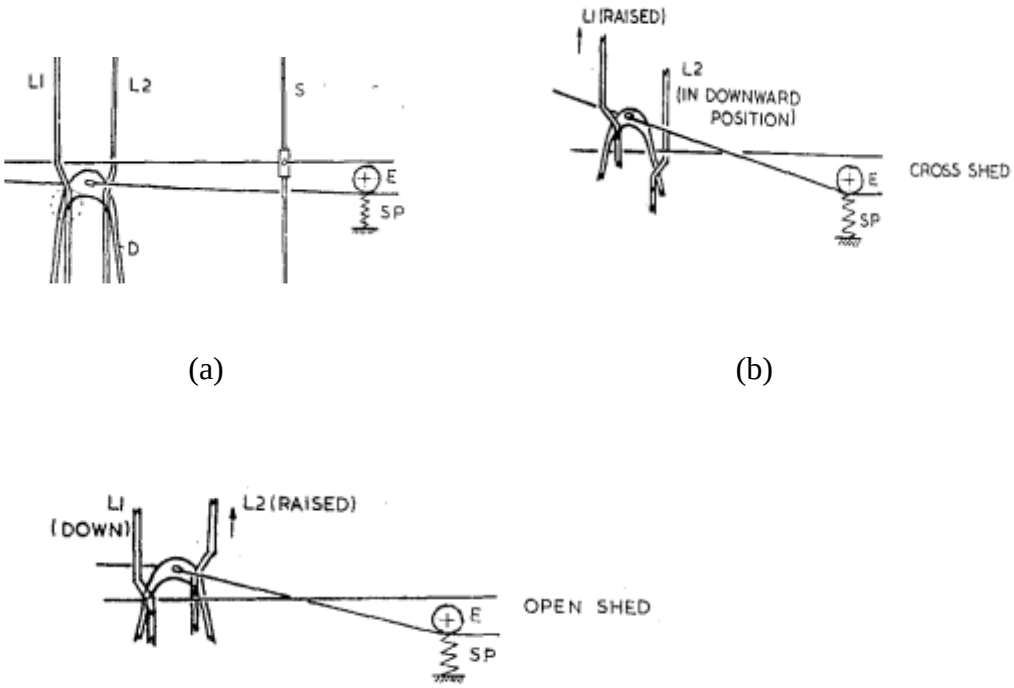

Figure 3-6 Heald movement for creating the leno structure [164]

The tension of the yarns to create a leno woven structure should be controlled to a specific range to enable the leno structure formation, as the leno structure would not be formed with a level of tension that is either too high or too low. In this research, the tension of the leno yarns was set to 250 grammes, and it was measured by a spring tension metre as shown in Figure 3-7.

Figure 3-7 Spring tension metre measures the tension of yarn

3.1.3 Fabric samples

Five types of plain woven fabrics with gripping yarns were created, and the structural details are illustrated in Table 3-1, together with the standard plain fabric structure. All the gripping insertions were set to have the same 2cm interval for the purpose of comparison.

Table 3-1 Fabric specifications

Fabric ID	Fibre type	Fabric density (1/cm)		Yarn counts (tex)		Weave Structure	Remarks
		Warp	Weft	Warp	Weft		
BPL2	Aramid (Twaron ®)	7.8	7.8	93	93	Plain based	Broad plain woven fabric with leno insertions at 2cm interval
BPC2							Broad plain woven fabric with cramming over 5 picks at 2cm interval
BPD2							Broad plain woven fabric with double-pick insertion at 2cm interval
BPL2C							Broad plain woven fabric with leno insertion at 2cm interval and weft cramming at 2cm interval
BPL2D							Broad plain woven fabric with leno insertion at 2cm interval and double pick insertion at 2cm interval
BPW						Plain	Broad plain woven fabric

Photographs of the produced fabrics are shown in Figure 3-8. It needs to be mentioned that the double-pick area was not produced with the same configuration as illustrated in Figure 3-2 because of limitations of the weaving machine. Therefore, the wrapping angle created by double-pick in this situation may be smaller compared with the expected situation.

(a) Plain fabric

(b) Plain fabric with leno insertion

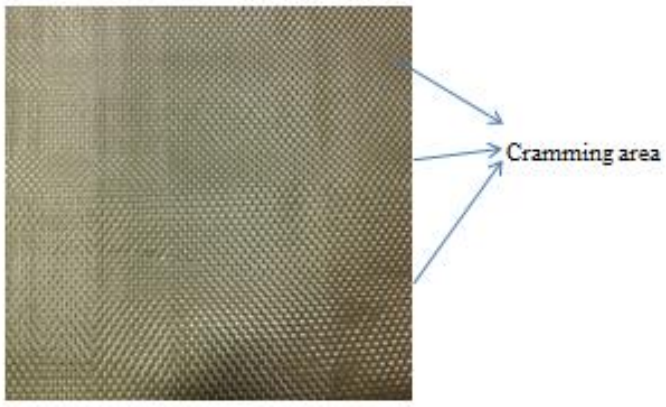

(c) Plain fabric with cramming insertion

(d) Plain fabric with double-pick insertion

(e) Leno and cramming insertion

(f) Leno and double-pick insertion

Figure 3-8 Fabrics made on the weaving loom

3.2 Ballistic range

The ballistic range used for the ballistic tests is shown in Figure 3-9, with the inside sketch map (Figure 3-10) for detailed information. There are two pairs of infrared sensors used to record the time; the time period can be generated by a pair of infrared sensors in minutes. The recorded time period will be shown on the chronograph connected to the sensors. With the distance measured between the paired sensors, the average velocity can be calculated. The paired sensors near the gun are used to record the impact velocity, and the other paired sensors located behind the fabric are applied to record the residual velocity. A high-speed camera with a connected computer is equipped with this ballistic range for the motion capture of the impact process. This ballistic range was used for the single layer penetrating tests in this research.

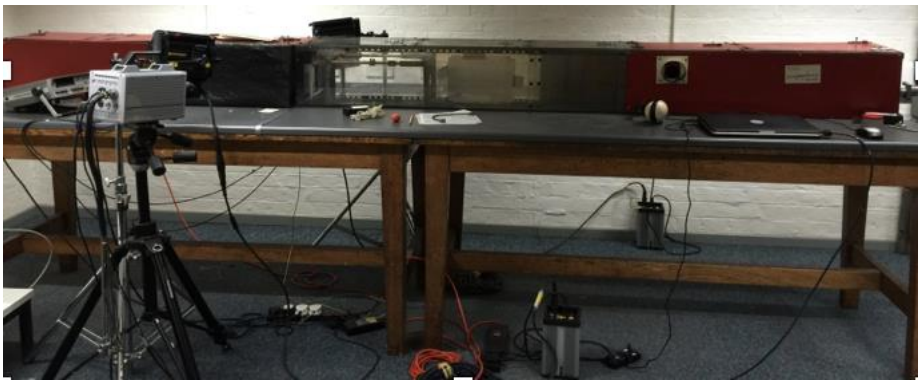

Figure 3-9 Ballistic range for ballistic test

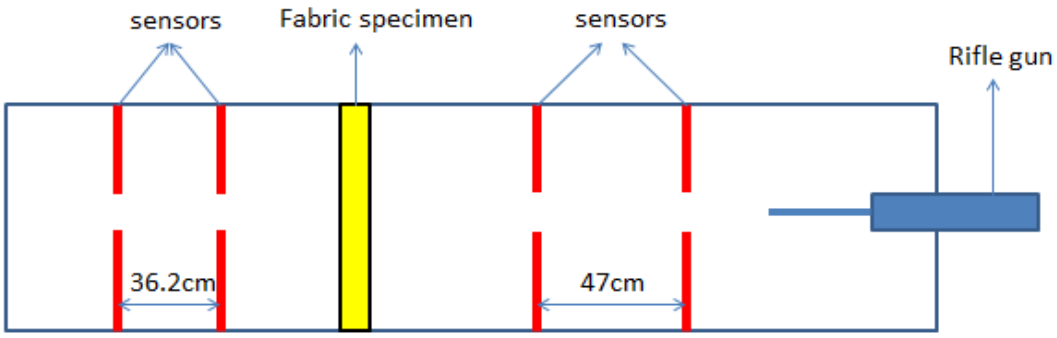

Figure 3-10 Illustration of the ballistic range

A cylindrical steel bearing with a weight of 1 gramme was used as the projectile, which is shown in Figure 3-11. The diameter and the height of the cylindrical projectile were both 5.5 millimetres. In using this device, the projectile would be placed into a plastic sabot before being launched by a blank powder cartridge. The typical velocity of the projectile was 475 m/s.

Figure 3-11 Cylindrical projectile

The fabric specimen was held by the designed clamp, which is displayed in Figure 3-12, and the size of the specimen was cut into a square of 23 × 23cm. In order to grip the fabric specimen firmly, four long steel bars and eight short steel blocks were used to provide enhanced pressure on the edges.

(a)

(b)

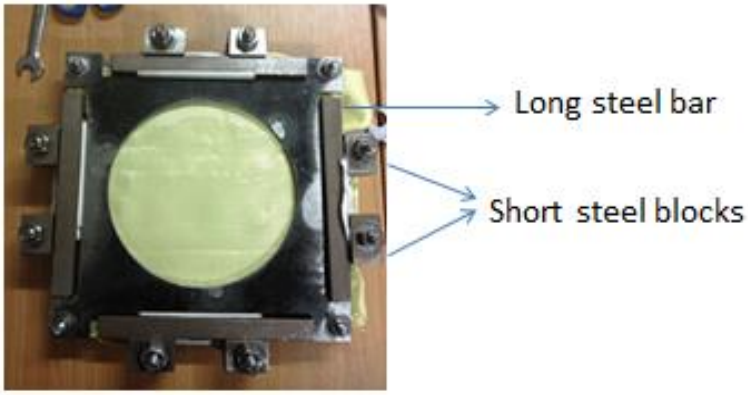

(c)

Figure 3-12 Clamp used for ballistic penetrating test (a) top plate of the clamp; (b) bottom plate of the clamp; (c) fabric clamped between the two plates

3.3 Fabric evaluation

The five structures had extra gripping to some yarns in the fabrics and were to be evaluated for their abilities to absorb energy from the impacting projectile. The fabrics would be subjected to the static yarn pull-out test and the high velocity impact test. In the ballistic tests, single-layer fabrics would be taken as the target panel.

3.3.1 Yarn pull-out test

The yarn pull-out test measures the force that is needed to pull a single yarn out of the fabric, and has been a valid method to evaluate the fabric gripping over its constituent yarns.

3.3.1.1 Method and sample preparation

The fixture for the yarn pull-out test consisted of a plate clamp and a normal clamp on a tensile tester. INSTRON tensile tester (Model No. 4411) was used for this research. The fabric sample was cut into a rectangular shape with a width of 6.5cm and a height of 24cm. An area of 0.5 × 3cm at the bottom centre of the sample was cut out to allow yarn-out. The pull-out speed was set to 100 mm/min. Figure 3-13 (a) shows the sample preparation and (b) the clamping. The yarn pull-out test was carried out in the warp direction for samples BPW, BPC2, BPD2, BPL2C and BPL2D, and in the weft directions for BPW, BPL2, BPL2D, and BPL2C. Each sample was tested 10 times.

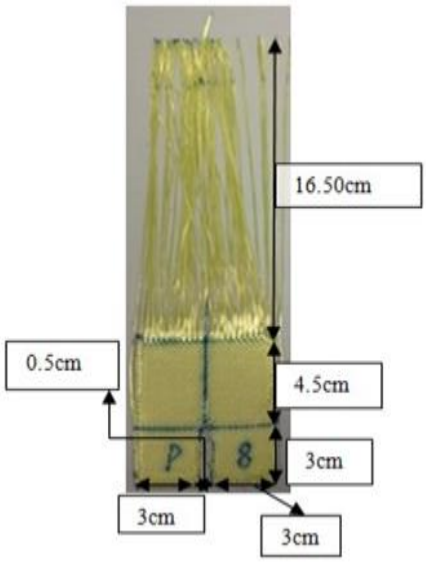

(a)

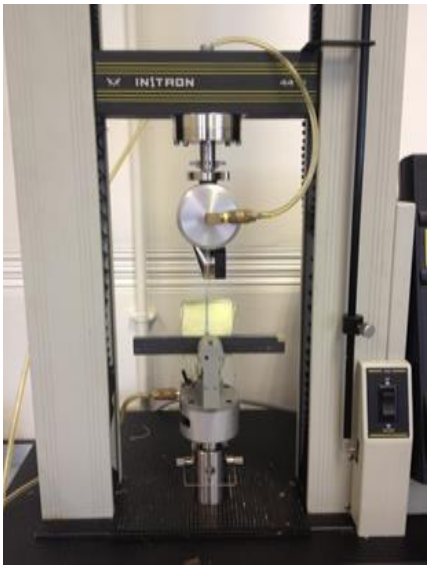

(b)

Figure 3-13 Yarn pull-out test: (a) fabric sample dimensions (b) Experimental test setup

3.3.1.2 Results and Discussion

The purpose of the tests from the warp direction is to evalutate the gripping effect of cramming and double-pick individually or in combination. For the test from warp direction, yarn was pulled out from warp direction from the plain fabric area. Those fabric structures are BPW, BPC2, BPD2, BPL2C and BPL2D.

The purpose of the tests from the weft direction is to evaluate the gripping effect of leno insertion. For the test from the weft direction, the yarn was pulled out from the weft direction from the plain fabric area. The test structures are BPW, BPL2, BPL2D and BPL2C.

The experiment obtained the results from two aspects, load (N) and displacement (mm). When a single yarn is pulled out from a fabric, the peak load is the highest resistance generated from all the frictional contact points on the crossovers along the pull-out yarn. The pull-out force increases because the tension in the yarn accumulates as the strain wave propagates to frictional points along the crossover contacting yarns. When the yarn is fully un-crimped, it reaches the peak load point. After that, the slippage motion dominates the moving behaviour; hence, the pull-out force presents a sudden drop, and a translation region starts. In the translation region, the load fluctuates where peak force and valley force happen one by another due to the load build-up to overcome the coming frictional points followed by the slip behaviour.

The yarn pull-out relationship between load (N) and displacement (mm) in the warp direction: When a single yarn is pulling out from a fabric, the peak load is the highest resistance generated from all the frictional contact points on the crossovers along the

pull-out yarn. Figure 3-14 displays that the cramming and leno insertion gripping create a dramatic, positive effect on increasing inter-yarn friction in the warp direction. The cramming technique increases the inter-yarn friction because the cramming area makes the wrapping angle of the warp yarns bigger, which results in a bigger inter-yarn friction; in other words, the yarns are squeezed tightly in the cramming area, so the inter-yarn friction in that area is increased. BPL2C and BPL2D provide better gripping results than BPC2 and BPD2. The intention of using the leno technique is to grip the yarns in the weft direction because the leno insertion works similar to the selvedge, which provides enhanced gripping to yarns and leads to increased inter-yarn friction. Since the yarns in the weft direction have enhanced the gripping effect, they will transfer the gripping effect onto the warp direction, so the leno assists the yarn gripping in the warp direction as well as in the weft direction. However, double-pick provides an inferior inter-yarn friction compared with a plain weave structure. The double-pick insertion failed to provide more inter-yarn friction because the finished fabric structure is rather loose compared with the designed structure. The designed structure of double-pick area on the fabric is that two weft yarns should occupy one yarn space. However, the finished fabric structure in the lab was that two yarns occupied over one yarn space, which resulted in a small wrapping angle and led to a loose fabric structure.

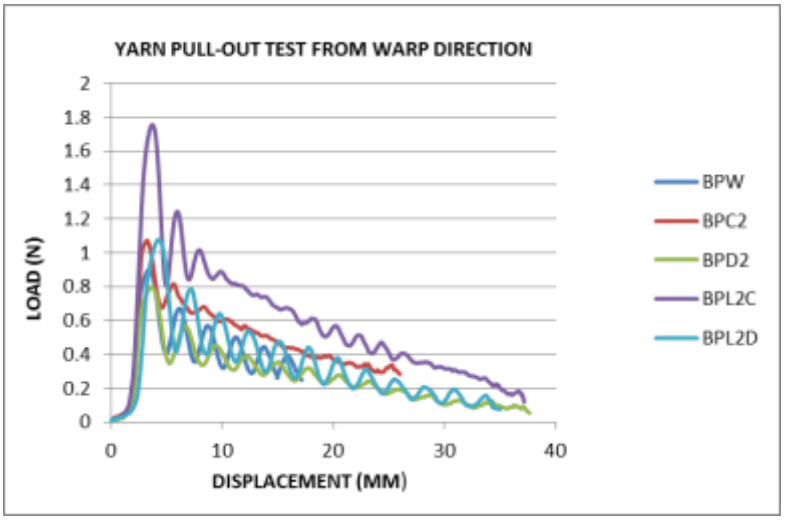

Figure 3-14 Relationship between load and displacement for five types of fabric samples tested from warp direction

The peak loads to pull-out the yarn from fabric are compared in Table 3-2. The data in Table 3-2 clearly shows that for the yarn pull-out quasi-static test, the leno insertion and cramming insertion provide more inter-yarn friction rather than a pure plain weave-based structure and double-pick insertion gripping structure. It can be observed that the leno insertion with weft cramming yarn insertion combination BPL2C has the highest yarn pull-out force, and BPL2D ranks second, followed by BPC2. BPD2 is inferior to BPW. However, even the double-pick insertion did not provide better performance, but combined with the leno insertion, the inter-yarn friction has increased from -11% to 20%. The same situation happens on the cramming insertion, without the leno gripping assistant, purely cramming only increase 20%, but with leno, the result is 96%. It can be concluded that leno plays a great assisting role in performing a significant gripping enhancement in the warp direction.

Table 3-2 Pull-out forces of tests from warp direction

Fabrics (Warp)	*Mean peak load (N)*	*Increasing percentage (%)*
BPW	0.897	0
BPC2	1.072	20
BPD2	0.796	-11
BPL2C	1.754	96
BPL2D	1.077	20

Weft direction yarn pull-out relationship between displacement (mm) and load (N):

From Figure 3-15 and Table 3-3, it can be clearly observed that all the modified fabric structures with extra yarn gripping provide increased inter-yarn friction compared with the plain weave structure. BPL2C shows the best performance amongst all the test results, which increased 128% pull-out force compared with BPW. In terms of the double-pick effect, when comparing BPL2 and BPL2D, again indicates that double-pick insertion gripping does not provide gripping enhancement for increased inter-yarn friction.

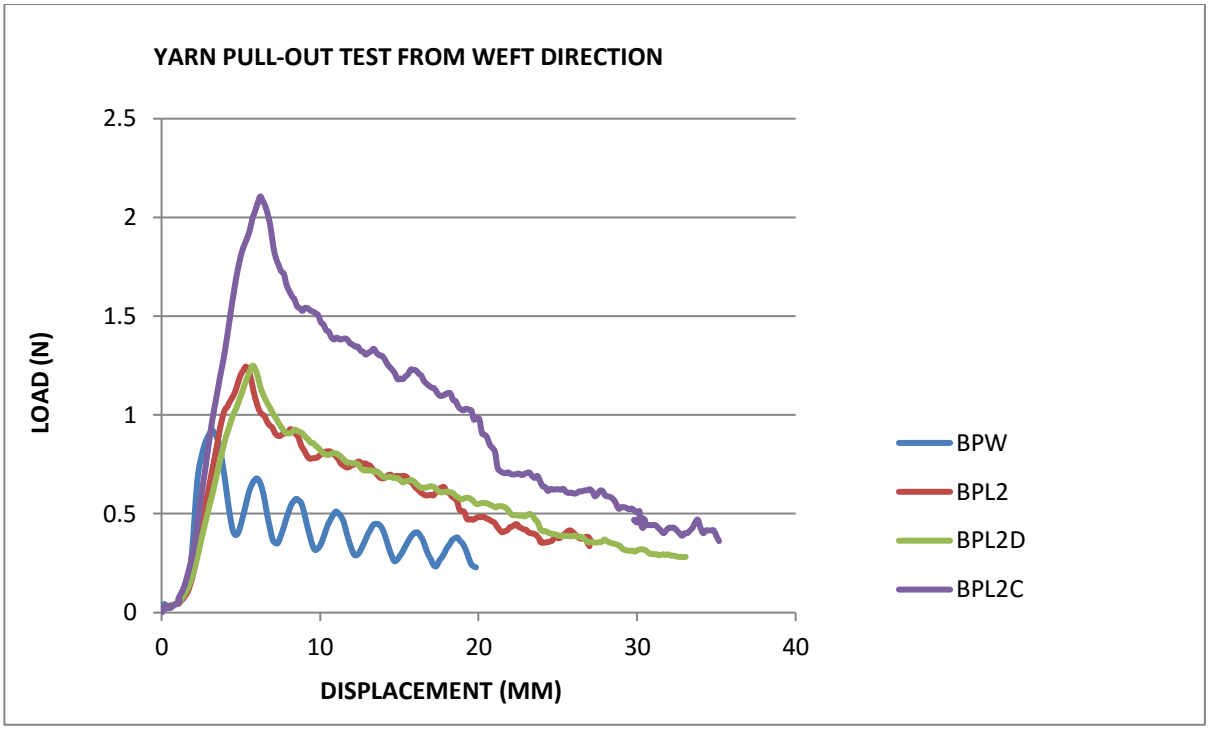

Figure 3-15 Relationship between load and displacement for four types of fabric samples tested from the weft direction

Table 3-3 Pull-out forces of tests from the weft direction

Fabrics (Weft)	*Mean peak load (N)*	*Increasing percentage (%)*
BPW	0.9222	0
BPL2	1.2452	35
BPL2D	1.2497	36
BPL2C	2.1059	128

In general, all the results of the tests from the warp direction and weft direction indicate three general factors. Firstly, leno insertion and cramming insertion make yarn less likely to be pulled out by external force, which has a positive influence on yarn-to-yarn friction; secondly, leno insertion shows more capability in increasing the yarn-to-

yarn friction, which can be observed from Table 3-2 and Table 3-3. Thirdly, the performance of double-pick insertion is inferior to the plain woven structure. The double-pick insertion plain weave-based structure has a relatively loose structure because of the two yarns occupying more than one yarn space at the double-pick insertion location; therefore, the wrapping angle is not big enough to provide more friction in the warp direction. However, double-pick insertion helps, when combined with leno insertion, to improve the inter-yarn friction more than purely leno insertion in the weft direction tests.

3.3.2 Single layer ballistic penetration tests of fabrics with extra yarn gripping

The tests have demonstrated that the gripping weave techniques have a positive effect on increasing the inter-yarn friction from the static test, so it is necessary to investigate the ballistic resistance during the dynamic tests. This section will conduct ballistic penetration tests on the single layer fabric in order to study the gripping effect on the energy absorption ability. Penetrating tests aim to obtain the velocities through the impact process when the projectile penetrates the impact target completely and works out the corresponding kinetic energy loss of projectile, which is an indication of the energy absorption ability of the fabric panel.

3.3.2.1 Ballistic tests on single layer fabrics with extra yarn gripping

For this test, specimens of fabric panels are cut into a square shape of 30cm × 30cm, each subjected to 5 shootings. Three specimens are prepared for each fabric type; hence, 15 shootings occur for each fabric type. The distance between each shot will be 3cm~5cm, and each shot is independent.

For the single-layer penetrating test, the trend of the impact velocity and residual velocity confirms that when the impact velocity is high, the decrease of the velocity

after impacting the fabric is low; therefore, the energy absorption will be low for the high-speed projectile velocity.

The fabric area densities are shown in Table 3-4. The ballistic impact results are shown in Figure 3-16. The results are collected from the original information and normalised to make sure that there is no fabric area density effect on the energy absorption. Unfortunately, the gripping techniques do not provide more significant energy absorption compared to a purely plain structure. Although the plain fabric with cramming insertion BPC2 has a slightly higher figure than BPW, there is a big error bar for the data. The big error bars for the data could be caused by the uneven fabric cut since the fabric is not uniform with one type of structure and there is a limited number of tests. Therefore, the discussion of the effect of impact location is necessary to analyse the energy absorption of the specimens.

Table 3-4 Fabric areal densities of specimens for single layer ballistic tests

Weave structure	**BPL2**	**BPD2**	**BPC2**	**BPL2C**	**BPL2D**	**BPW**
Areal density g/m^2	162.83	161.08	153.66	175.09	171.29	157.89

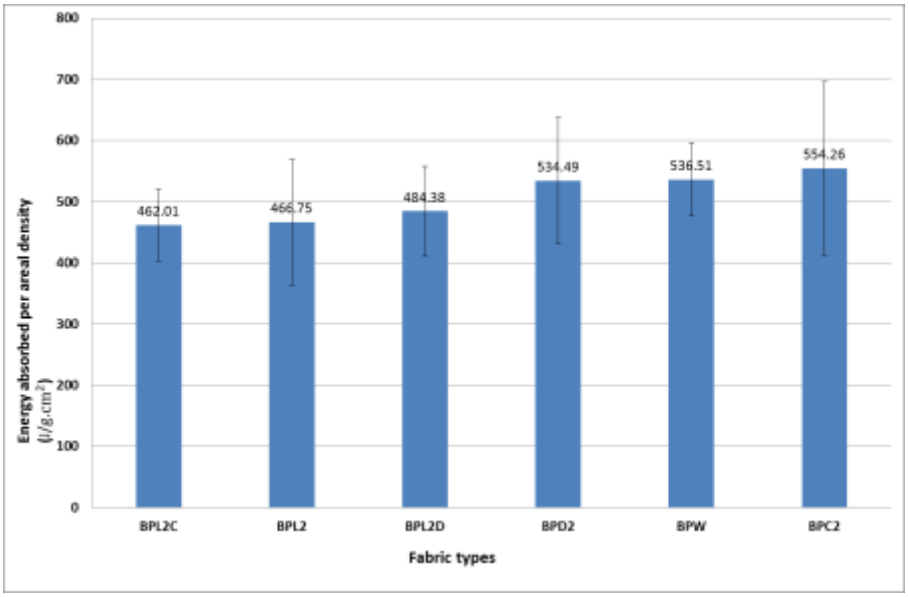

Figure 3-16 Normalised energy absorption for single layer ballistic tests

3.3.2.2 Influence of the impact location on the fabrics with leno insertion

From the appearance of the fabric specimens, large gaps can be found on the leno area on the fabric with leno insertion as shown in Figure 3-17. This has become a concern for the energy absorption of the fabric. In addition, the leno areas possess a much higher inter-yarn friction, which may have different performance compared to the plain area.

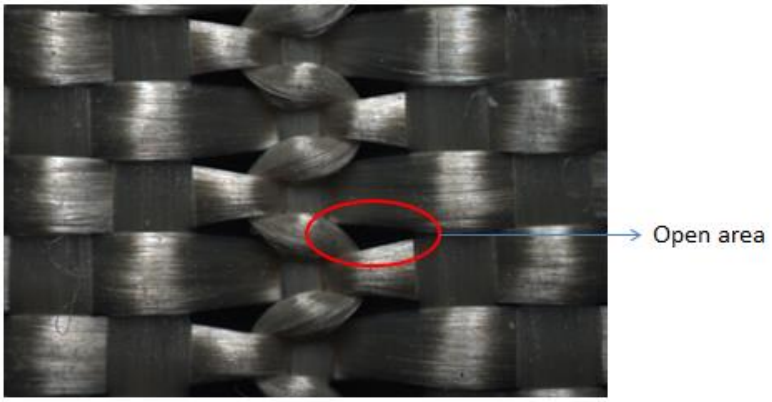

Figure 3-17 Leno line under microscope

For the leno fabric, there are 15 shooting results achieved from tests. One failed because the sensor stopped working for an unknown reason, eight shootings occurred at the plain weave area, and six shootings at the leno area. In general, the chance of impacting a location at the leno area is 43%. Since the leno area has a considerably open structure, a negative effect on energy absorption is assumed. For the total results of leno fabric, the energy absorption is 7.60J, while, for the plain weave structure, it is 8.46J. When the data is classified into two groups for the leno fabric, one is on the leno or involves the leno area, and the energy absorption is 6.71; however, on the plain weave area, the energy absorption is 8.52J. Therefore, it can be concluded that leno insertion does provide a slightly positive effect on the plain weave area for energy absorption. The difference is 0.06J for both structures on the plain area, which is not dramatic due to the limited number of tests. However, it still confirms that higher inter-yarn friction provides a positive effect on energy absorption.

3.4 Summary

In this chapter, the study was carried out from the yarn pull-out test to provide a static investigation on the gripping effect in the developed fabrics. It has been concluded that cramming and leno weave techniques provide a significant increase in the peak load of pull-out force from warp direction and weft direction, and the combination works in both directions. However, the dynamic ballistic penetration test does not show obvious increasing energy absorption in the developed fabrics when compared with a purely plain woven fabric. The reason could be the leno area on the fabric. For the leno insertion, the leno area has a considerably large open area, which provides inferior energy absorption capability compared with the purely plain structure. However, leno insertion does provide an enhanced gripping effect that leads to increased energy absorption in the plain area of the plain fabric with leno insertion.

Chapter 4 Ballistic performance of fabric panels through experimental studies

This chapter investigates the ballistic performance of the multi-layered fabric panels constructed according to the findings from the single layer fabrics. The panels were constructed with a sufficient number of layers of fabrics to stop the impacting projectile. A non-penetration ballistic test and V50 test were used to evaluate the ballistic performance of the panels. FE (finite element) modelling was developed for specific investigations, together with the experimental studies, in order to provide comprehensive understanding, which would be hard to obtain from experiments only.

4.1 V_{50} evaluation of novel fabrics

The V_{50} test is the main method to evaluate the ballistic performance of fabric panels. To identify the V_{50} of a panel, the panel is shot at with different projectile velocities. The velocity at which statistically half of the projectiles penetrate the fabric panel and half do not is defined as V_{50}.

In this study, the fabric panels assessed were made from those used for the single layer ballistic test. The V_{50} tests of the six fabrics were carried out by an independent institution using a 1.1g Chisel Nosed (CN) Fragment Simulating Projectile (FSP). Panels were prepared in a 40 × 40cm square shape, using 19 plies of fabric in all cases, except for the fabric with leno insertions, which used 18 layers. The areal density of all panels was approximately 3 kg/m^2 as shown in Table 4-1. The newly engineered fabrics with extra yarn gripping were all randomly layered to form panels after cutting,

and there was no specific attempt to correlate the gripping area to gripping area, or gripping area to plain weaves.

The V_{50} test was conducted by the Defence Science and Technology Laboratory (DSTL) with a limited number of sample materials. The results of the V_{50} test are very optimistic. The fabrics assessed are the same as those tested during the single layer ballistic test, but 20 FSPs were shot into each sample. The fabric specification and V_{50} results are shown in Table 4-1. In terms of ply number, it can be concluded that all the fabrics with extra gripping provide a positive effect in increasing the V_{50} velocity with the same layer number, and even though the leno has one layer less compared to the rest of the fabric panels, it has a higher V_{50} compared to a purely woven structure. Figure 4-1 depicts the V_{50} results that are normalised by areal density.

Table 4-1 V_{50} results with fabric panel specification

Yarn	*Weave Pattern*	*Plies*	*Measured AD (kg/m^2)*	*$V_{(p)}$ (m/s)*	
				V_{50}	*SD*
	BPL2	18	2.9	488.8	6.0
	BPC2		3.3	522.2	10.5
930 dtex	BPD2		3.1	502.5	10.9
1,000f	BPL2C	19	3.7	492.2	3.8
	BPL2D		3.1	496.5	2.5
	BPW		3.0	487.6	9.0

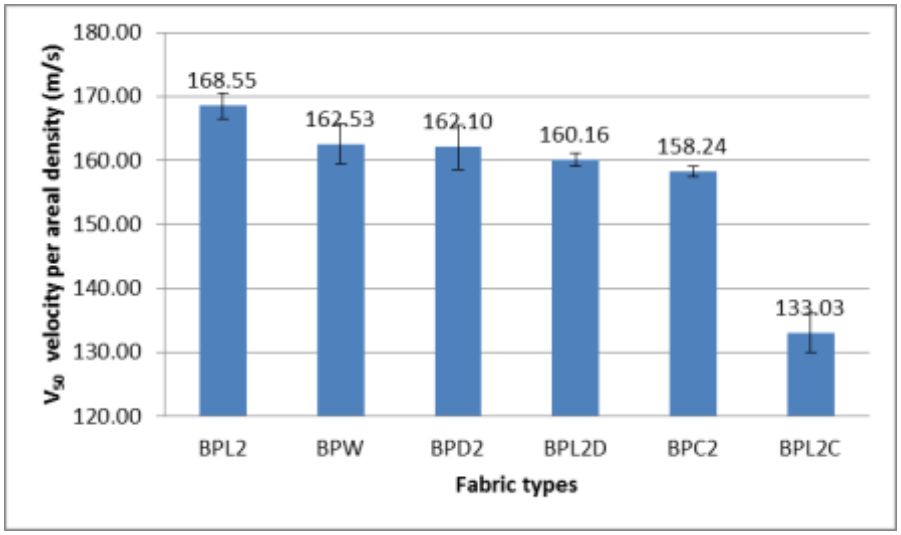

Figure 4-1 Normalised V_{50} results based on areal density

From Table 4-1 and Figure 4-1, it can be seen that all the yarn gripping methods have a positive effect on performance. However, when the V_{50} results are normalised based on the fabric mass, only the leno insertion gripping structure gives a better performance compared to the purely plain weave structure. It can be concluded that the leno insertion gripping structure provides more energy absorption but fewer fabric requirements compared to the plain weave structure.

A higher gripping effect increases the V_{50} results. The V_{50} test has similar results as the quasi-static test (yarn pull-out test), which indicates that the increased inter-yarn friction can improve the energy absorption during the ballistic test. However, there is a difference between the single layer penetration test and V_{50} tests, which shows that the ballistic performance of a single-layer fabric may vary from the performance of multilayer fabrics. The discrepancy between the single-layer penetrating test and the V_{50} multilayer test could be affected by a limited number of trials and increased chances of shots on the open structure area during the penetrating test. Therefore, a

further study of the layer arrangement for the leno fabric will be designed and studied to provide a comprehensive understanding of the ballistic performance of leno fabric.

4.2 Evaluation of the ballistic performance of fabrics and panels made from fabrics with leno insertions

4.2.1 Layer arrangement design for fabrics with leno insertion

It has been found that the layered fabric panels respond differently to the single-layer panel. Moreover, it has also been discovered that the impact location has a noticeable influence on energy absorption. As there is a lack of information on the arrangement for the same fabric type in previous research, it is essential to conduct the fabric panel layer arrangement study. Based on the discoveries, different panel layer arrangements are designed and tested in order to test the energy absorption for different panel arrangements and observe the impact location and the effect of energy absorption.

Three types of fabric layer configurations were used for the layer arrangement, and the layer sequence is based on the leno line direction, namely, a layered leno line for adjacent fabrics by 90 degrees, an aligned sequence for the leno line on the fabric panel and an offset leno line for the fabric panels. The illustration of the layer arrangement is shown in Figure 4-2. The smallest repeated unit for a 90-degree layer arrangement is two layers; therefore, the fabrics are tested in two layers and four layers separately. For each layer type, all the fabrics are cut into 30cm × 30cm, and each panel is subject to five tests. Two specimens were prepared for each fabric type configuration; therefore, 10 tests take place for each fabric layer arrangement type. The ballistic range for this impact test is the same as the single-layer impact test, which was described in detail in Chapter 3. The impact velocity is the same as the experiment for

the single-layer penetrating test. The method used to evaluate the fabrics' ballistic performance is based on the kinetic energy loss of the projectile.

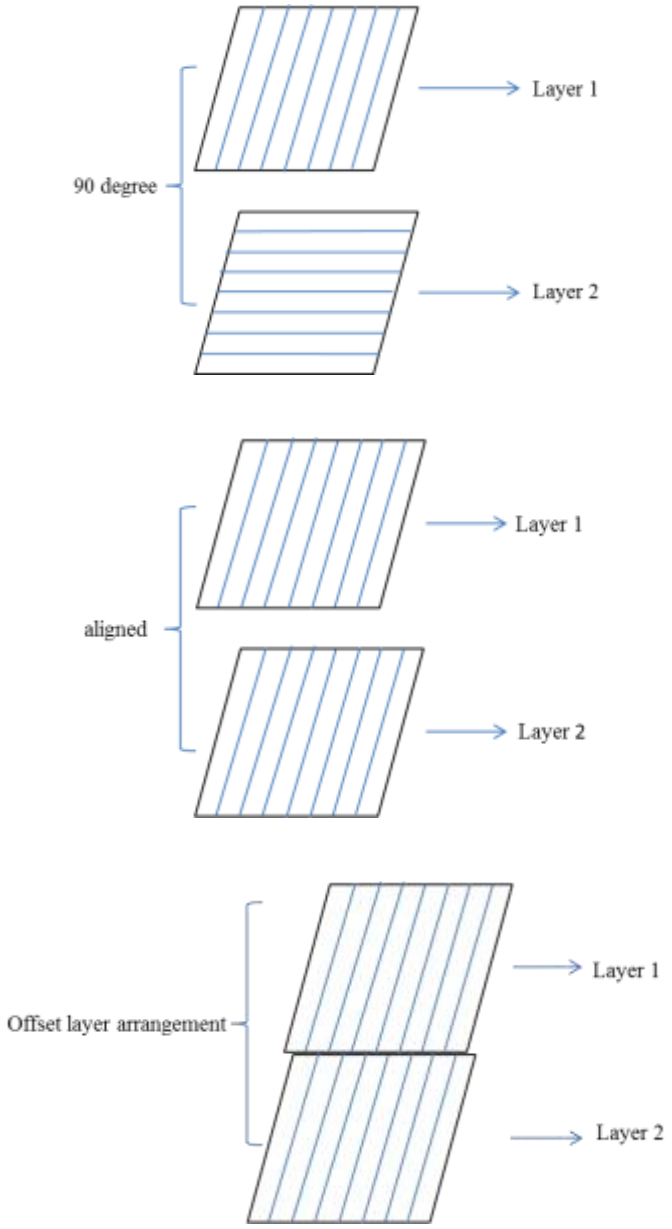

Figure 4-2 Illustration of layer arrangement

4.2.2 Ballistic test results and discussion

The results for two layers and four layers of different layer configurations are shown in Table 4-2 and Table 4-3. In Table 4-2, except for the 90-degree layer, the layer configurations provide higher energy absorption as compared with the plain fabric layer arrangement. The reason the 90-degree layer arrangement failed to provide higher energy absorption may have been caused by the cross point of the leno lines created by more stressed yarns compared to the plain weave area. The two-layered offset fabric layer arrangement provides the highest energy absorption; the reason could be that this approach effectively avoids just the leno line being subjected to projectile impact directly. The aligned leno line layer arrangement shows better performance than the 90-degree layer arrangement, which could be explained by the probability that the impact location affects the final average results. In terms of the four-layer tests, the offset layer arrangement exceeds the rest of the fabric specimens, which indicates that it is the optimum layer arrangement for leno fabric.

From the layer arrangement tests, it can be observed from both the two-layer tests and four-layer tests that the offset layer arrangement shows the best energy absorption ability. This approach maximises the use of the gripping effect of leno line as well as avoids the disadvantages of leno line.

Table 4-2 Ballistic results for two-layer construction with different layer arrangements

Type of layer arrangement (two layers)	*Areal density (kg/m^2)*	*Average energy absorption (J)*	*Normalised energy absorption ($J/kg.m^2$)*
Plain	0.3022	14.23	47.74
90-degree layer (leno)	0.3256	14.66	45.57
Offset leno line	0.3256	15.70	48.82
Aligned leno line	0.3256	15.53	48.30

Table 4-3 Ballistic results for four-layer construction with different layer arrangement

Type of layer arrangement (Four layers)	*Areal density (kg/m^2)*	*Average energy absorption (J)*	*Normalised energy absorption ($J/kg.m^2$)*
Plain	0.6043	24.68	41.39
90-degree layer (leno)	0.6511	26.98	39.40
Offset leno line	0.6511	28.77	44.73
Aligned leno line	0.6511	26.71	41.54

4.3 Summary

This chapter presents the experimental results from the V_{50} tests for conventional layer fabrics and multi-layer penetrating tests for designed layer arrangement. V_{50} shows promising energy absorption results of the designed fabrics with gripping insertion.

All the fabrics with gripping enhancement with similar layers require higher V_{50} velocity compared with purely plain fabric panels, which indicates increased ballistic performance. To achieve the same level of V_{50}, less fabric is needed for fabric with leno insertion than plain fabric. When the results are normalised by the fabric areal density, only the fabric with leno insertion needs a higher V_{50} velocity than the plain fabric. All in all, leno gripping in the fabric is the most effective method for improving the V_{50} velocity among all the gripping techniques. For the designed layer arrangements, the approach of the offset layer arrangement provides the highest energy absorption in both two-layer tests and four-layer tests rather than the rest of the structures. The different performances of energy absorption for layer fabric panels in the two-layer situation and four-layer situation may have been caused by the impact location probability and the weakness of the leno line exposed directly to the subjected projectile impact.

Chapter 5 Numerical studies of the influence of inter-yarn friction on fabric against ballistic impact

As mentioned previously, one of the main aims of this research is to study the influence of inter-yarn friction on the ballistic performance of fabrics and panels. It is difficult to achieve different levels of friction between the yarns through experiments; therefore, the finite element method was adopted to analyse the effect of inter-yarn friction on the ballistic response of the fabrics and panels engineered for this research. Using the FE method, comprehensive information can be obtained from the validated FE models.

This chapter reports the establishment of the FE model for ballistic fabrics and the FE results from the simulation. The fabric geometric model with different levels of inter-yarn friction, subjected to ballistic impact under the same ballistic impact conditions, was to be studied from different aspects to complement an improved understanding of the ballistic behaviour of the fabrics and panels.

5.1 Finite element modelling of ballistic impact on fabrics and panels

5.1.1 Brief introduction to ABAQUS

ABAQUS® is commercial software for Finite Element Analysis (FEA) developed by ABAQUS Inc. In this research, ABAQUS® software was chosen to model the ballistic impact event as an extension of the experiments. ABAQUS® supports the creation of the geometric models of fabrics, and it works with a substantial list of material models to simulate the behaviour of most types of engineering materials, including metals, rubber, polymers, composites, and so on [107]. Among the ABAQUS®/standard and

ABAQUS®/explicit, ABAQUS®/explicit was used for the simulation and analysis of ballistic impact events.

The creation of a complete ABAQUS® finite element model comprises three stages: model creation, jobs submission and monitoring, and results' evaluation. The three stages can also be described as pre-processing, simulation and post-processing.

Model creation in the interactive environment includes creating the part geometry, assigning the materials' properties to the part created, parts assembly, interaction defined and load and boundary condition applied. The model parts can be either sketched in the ABAQUS®/CAE or imported from other external software. Material properties need to be assigned to the specific part to define the model for the part. All parts are able to be positioned to create an assembly structure. The interaction defines the behaviour of two different surfaces. In the load module, boundary conditions and predefined fields are applied for analysis. To request an output, a sequence of steps will need to be defined to analyse and capture the change in the model. The output results can be selected, which lead to a faster computer running time. To discretise the whole model into finite elements, a mesh module is applied, and different units of geometric elements will lead to different analysis results.

This section of the thesis describes the use of finite element modelling to analyse the process of a projectile impacting a ballistic fabric.

5.1.2 Geometrical model creation

The fabric structure to model is the plain woven fabric used for the earlier experimental study, with warp and weft densities of 7.8 threads/cm. The linear

density of the yarn used for warp and weft is 93 tex. The areal density of the fabric is 157.89 g/m^2.

5.1.2.1 Projectile

The ballistic impact event involves the yarn-based geometric structure and a projectile. The projectile to model is a cylindrical steel object with 5.5 mm in both height and diameter, as shown in Figure 5-1. The mass of the cylindrical object is around 1.06 grams, and it is considered a rigid body, which means there is no deformation because of high velocity impact against the soft fabric. The projectile was defined as solid with the density of steel, which is 7800kg/m^3.

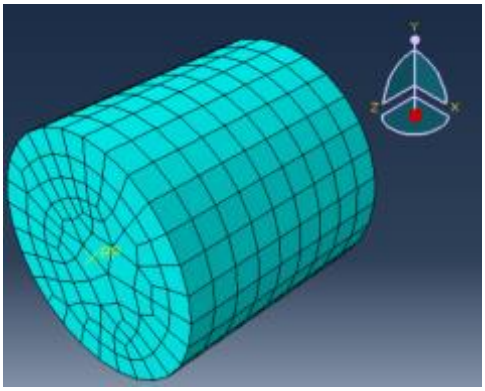

Figure 5-1 Model of projectile with mesh

5.1.2.2 Yarn cross-section and yarn path

When it comes to analysing yarns, the yarn cross-section needs to be considered. The yarn cross-section shape is modified from circular geometry to racetrack shape to lenticular figure in the previous research.

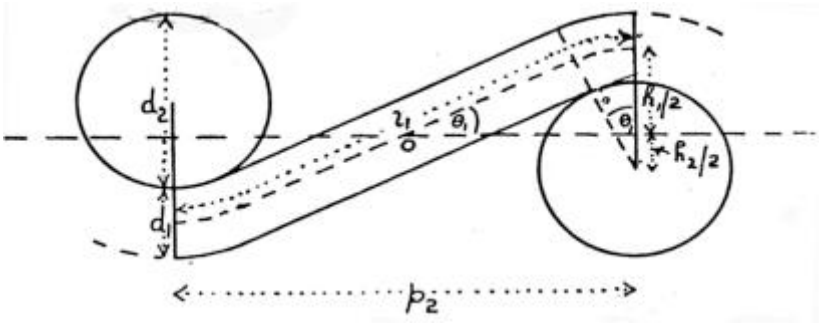

Figure 5-2 Peirce's model [166]

Peirce [166] first assumed the yarn cross-section as a circular shape and did an intensive analysis of the woven fabric structure based on the cross-section. In his model, he assumed that the cross-sectional shapes of woven threads were circular and that the yarn path in the fabric consisted of a circular arc in which the yarn was in contact with the thread at right angles, with a straight portion between contacts. These assumptions indicated that the yarn was rigid enough to give no distortion when subjected to the internal stress caused by a collision with the woven fabric; the yarns were completely flexible and had elastic recovery properties.

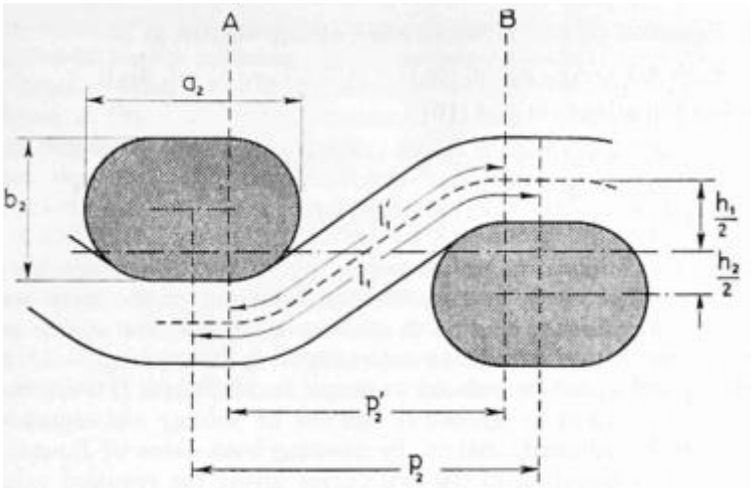

Figure 5-3 Racetrack model

Kemp [167] has modified the shape of the yarn cross-section from a circular to a racetrack section as displayed in Figure 5-3 to reflect that yarns are flattened in most woven fabrics. The racetrack shape consists of a rectangle between semi-circular ends.

The most-used yarn cross-section model in simulating fabric is lenticular, which was suggested by Hearle and Shanahan in 1978 [139]. This is particularly true for fabrics made from continuous filament yarns. A cross-section is presented in Figure 5-4.

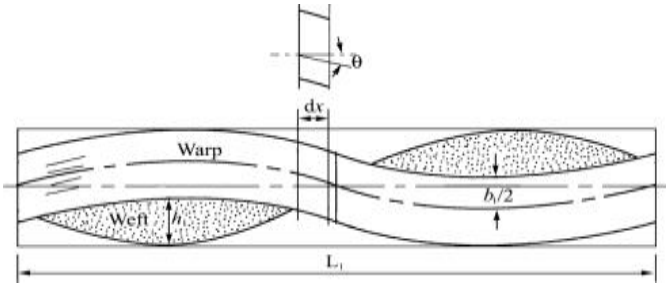

Figure 5-4 Lenticular model [168]

For convenience, Hearle [169] developed two yarn paths for fabric-forming yarns. One is the elastic form for a yarn profile with inconstant elliptic curvatures; the other is the modified constant curvature. The yarn path formed by arcs of circles is the most commonly used model in fabric simulation.

In order to observe the cross-section of the fabric under an optical microscope, a sample of fabric specimen is prepared. A small fabric sample is cut into a small piece to be placed into a small container vertically. To help the fabric stand vertically, a mixture of resin and hardener with a 10 to 1 ratio is used to fix and solidify the fabric piece. After the solidification process, the sample with the resin is taken out. In order to observe the cross-section of the fabric, the sample with resin needs to be polished on the side of the required cross-section by sandpaper fastened to the grinding machine

to achieve a smooth, flat and clear surface [170]. The image from the optical microscope is shown in Figure 5-5.

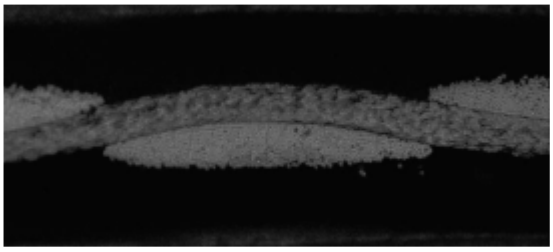

Figure 5-5 The cross-section of the yarn in the plain fabric [170]

It can be clearly seen that the cross-section of yarns in the fabric is more like a lenticular structure. The yarn path can be constructed by two lenticular arcs as the smallest repeat unit. Other data required are the width of the cross-section, weave length of the cross-section and the thickness of the fabric. In this study, the width of the cross-section and the weave length of the cross-section were obtained using SEM, since the differences between these two are very small, and this is shown in Figure 5-6.

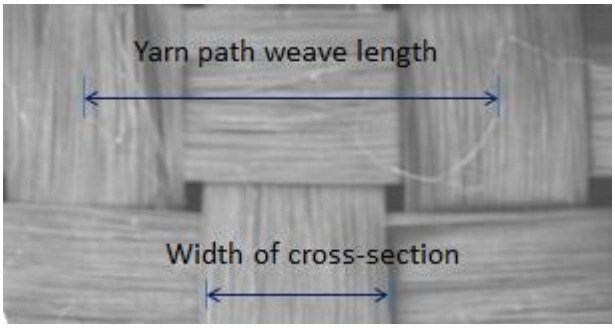

Figure 5-6 SEM observation of the woven fabric

The average wave length of the yarn path was 2.556 mm based on multiple measurements from different areas. The average width of the yarn cross-section was

1.134 mm using the same measuring methods. The thickness of the fabric was measured as 0.210 mm by a vernier caliper. The model with real dimensions was simulated in ABAQUS®/CAE as shown in Figure 5-7.

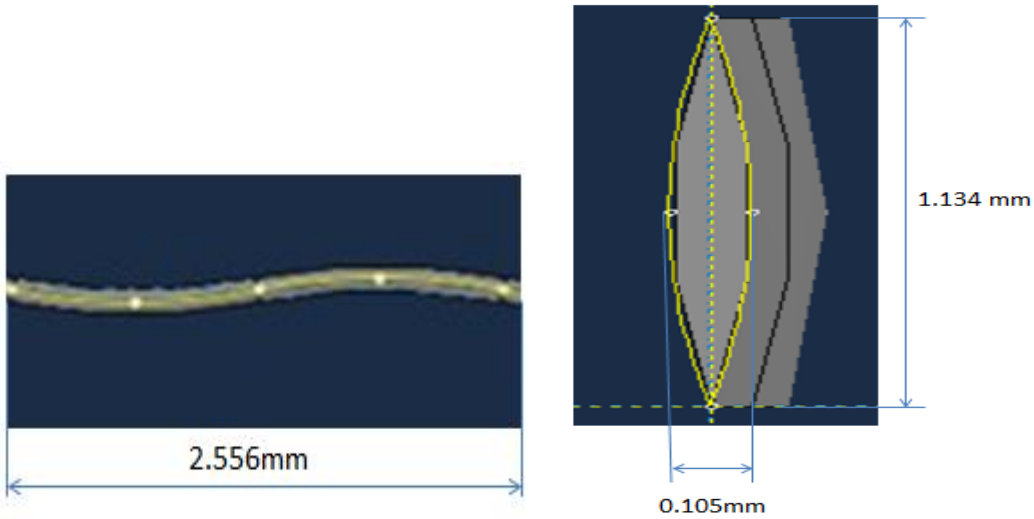

Figure 5-7 Model with real dimensions

5.1.2.3 Construction of fabric model and the mesh scheme

Fabric

A square, 15 × 15cm fabric was considered for the simulation. Due to fabric symmetry, only a quarter of this fabric was simulated in the numerical analysis. Accordingly, a quarter of the projectile was used to impact the fabric. Figure 5-8 shows this quarter of the model.

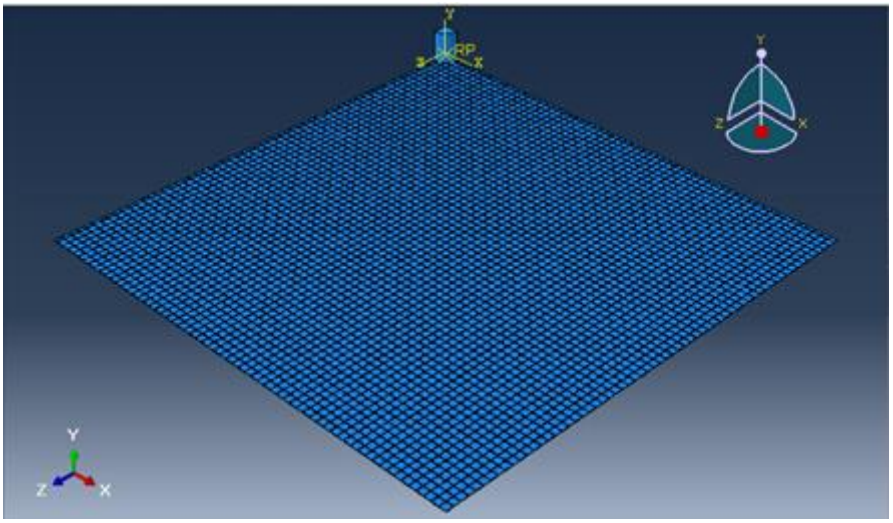

Figure 5-8 Quarter fabric model

Mesh scheme

The parts should be meshed to carry out the finite element analysis. A C3D8R element was selected for meshing, which is a general purpose linear brick element representing a continuum, 3D, 8-node, with reduced integration. Figure 5-9 illustrates this element, and Figure 5-10 presents the meshed fabric and projectile models.

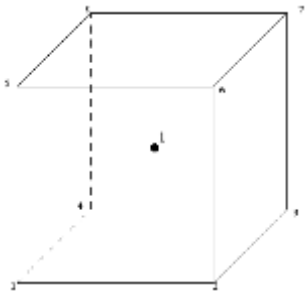

Figure 5-9 C3D8R element with integration point

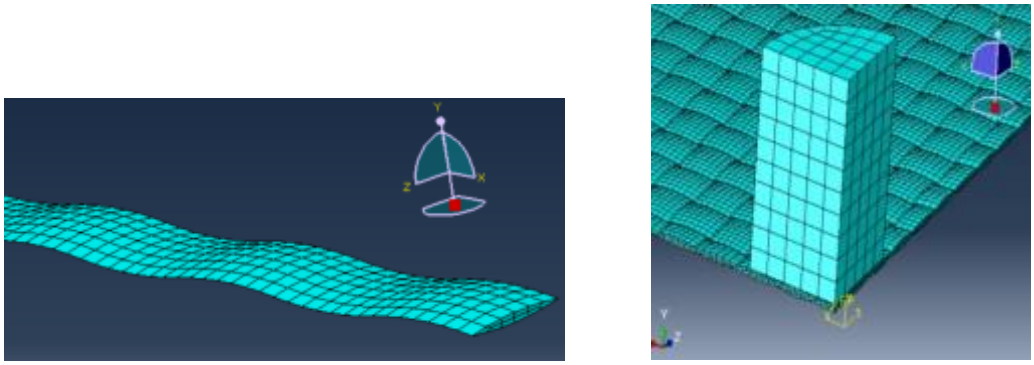

(a) (b)

Figure 5-10 (a) Mesh for the single yarn and (b) mesh of the whole model

Boundary conditions

Because of the symmetry of the fabric, only a quarter of the fabric is necessary, which minimises the time for calculation. The two adjacent original edges of the fabric were fully constrained, and the two edges representing symmetrical lines were constrained to reflect material continuity. The full model size was 15 × 15cm, and the quarter fabric was 7.5 × 7.5cm, as shown in Figure 5-11.

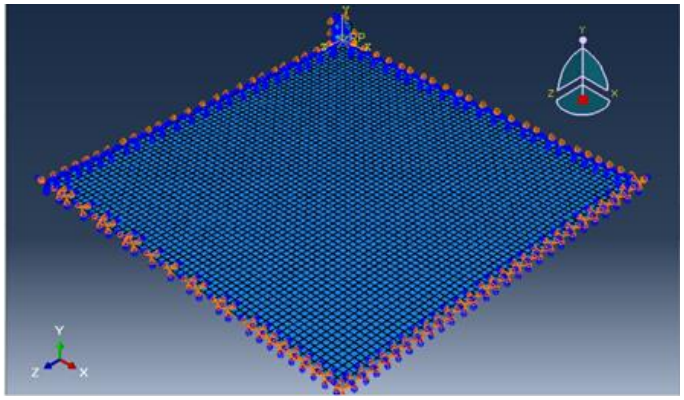

Figure 5-11 Fabric model with boundary condition applied

The projectile was constrained to be able to move in the Y direction while the fabric model was placed in the X-Z plane.

Materials' properties and failure criteria

In a real situation, a single yarn is composed of hundreds or thousands of bundled filaments with orthotropic properties. However, it was impossible to take fibres into account explicitly creating a yarn model. During the ballistic impact event, the mechanical property of the material of the yarn is mainly dominated by the longitudinal tensile properties. In common practice, the model for the yarns can be assumed to be homogeneous and isotropic [36-38, 53]. Previous studies [30, 109, 171] have shown that the homogeneity and isotropic assumptions of the yarn provide acceptable results with few inaccuracies, approximately 2.4%, in energy absorption. This research assumed that the yarns were homogeneous and isotropic. The Young's modulus of the yarn was set to be around 72 GPa according to the Young's modulus of Twaron® materials. The stain rate is 1000/s, with the Young's modulus of 72 GPa for Twaron® yarn based on the research results of Zeng *et al.* [144]. The fracture strain and the yield stress were set to be 4.28% and 2.9 GPa, respectively, according to the test results and estimates from previous research [172]. The density of the yarn was set to be 1296 kg/m^3, assuming the fibre packing density in the yarn is 0.9. The mass density of yarn is smaller than the mass density of fibre, which is around 1440kg/m^3 [37]. The Poisson ratio was set to be 0.3 according to the previous data [56][145]. The projectile is steel with a density of 7850 kg/m^3. As fabric response is the focal point of the investigation and the projectile is much stiffer than fabric, the projectile was defined as the rigid body without deformability.

ABAQUS®/explicit offers a general capability to model progressive damage, which reflects the materials' property degradation to indicate the fracture of the material

[107]. The failure of the material is normally either a brittle failure or a ductile failure. In the case of yarn in a fabric, the stress-based ductile damage criterion was used to define the failure mode, and these failure criteria were applied in the simulation analysis by the researchers for the investigation of yarns [109, 173].

Interaction

For a ballistic impact event, the interaction in the simulation is mainly based on the contact definition. Two different types of contacts were there for the ballistic impact, i.e. the yarn-to-yarn contact and the yarn-to-projectile contact. The coefficient of projectile-to-fabric friction was set to be 0.18 [37], and that of yarn-to-yarn friction was set to be 0.2 [37, 114].

As there was a large number of possible contact pairs in the geometric structure, the general contact method was used to define the contact interaction for the simulation. With general contact, ABAQUS® can automatically detect the contacts among the elements and surfaces involved in the simulation. If there is more than one interaction property, the individual property assignments will allow specified pairs and contact property. It needs to be noted, when assignments overlap, that the more recent assignments override earlier assignments as well as the global assignment.

5.1.3 Validation of the plain fabric model

The validation of the FE model was based on the comparison of residual velocities from both experiments and FE numerical simulations, respectively. There are differences in tensile properties under high strain rate and low strain rate [174]; high strain rate was adopted in the simulation. When the impact velocity increases from 248 m/s to 550m/s, the strain rate is found to range from 800/s to 1200/s. As the impact

velocity is around 475 m/s, it is reasonable to assume that the strain rate is around 1000/s [61, 172]. Under the condition of strain rate of 1000/s, the Young's modulus was set to be 72GPa and the failure strain is 4.28% in the model, based on the research by Zeng *et al.* [144].

During the ballistic impact test, the impact and the residual velocities were measured and recorded. These two velocities were also read after the FE simulation. The comparison of velocity results between experimental and FE modelling is shown in Figure 5-12 (a). Figure 5-12 (b) shows the residual velocities from the FE model and experiments.

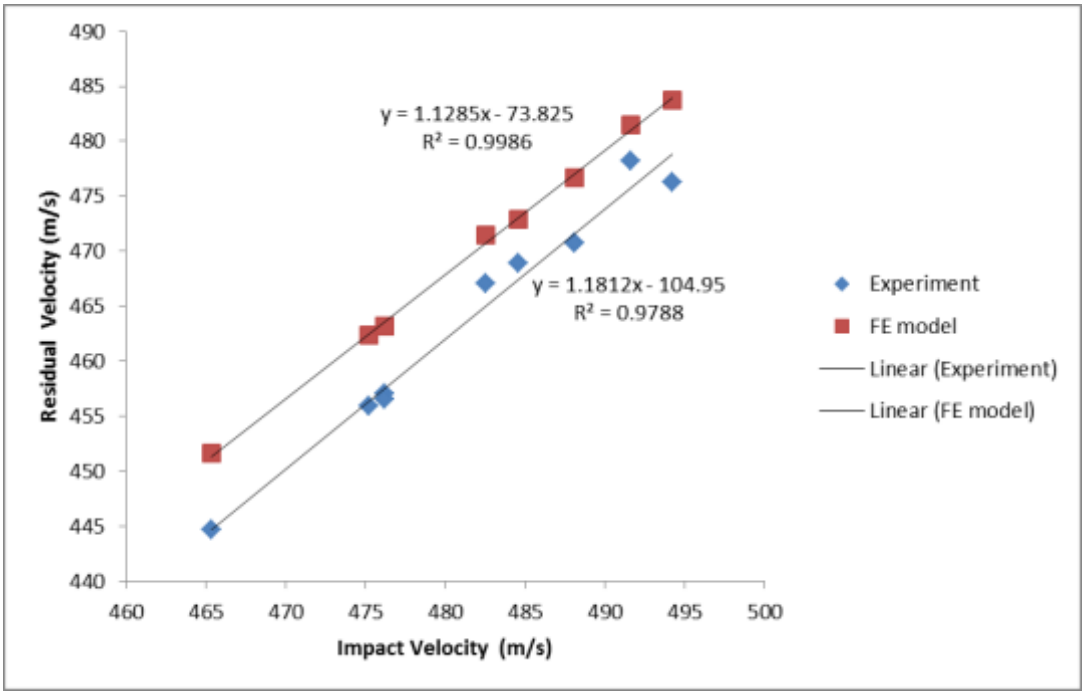

(a)

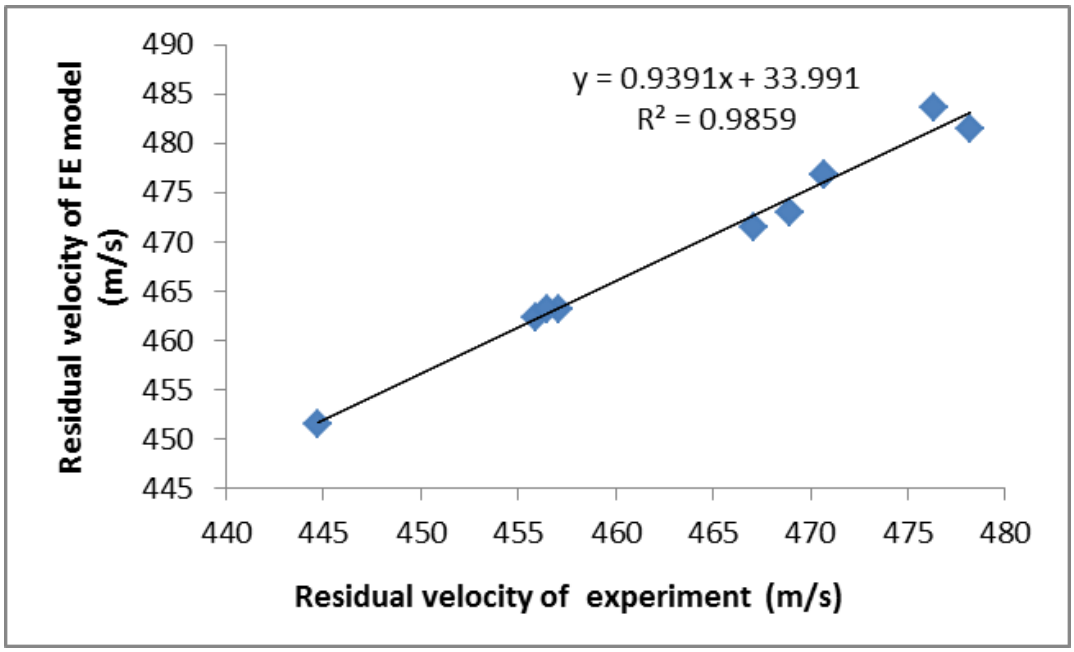

(b)

Figure 5-12 Impact velocities and residual velocities from experiment and model

In Figure 5-12 (a), the regression lines for impact velocity and residual velocity from the FE modelling and experiment are parallel to one another, meaning that the FE modelled result reflected the same trend as that from the experiment. It can be noticed that the residual velocities from the FE modelling were all higher than the residual velocities from the experiment, and this can be attributed to the size difference between the model and the real specimen. This can also be explained by the air resistance to the projectile, which exists in the experiment but does not in FE modelling. Figure 5-12 (b) displays the agreement of the residual velocities between the model and the experiment, with a significant correlation coefficient of 0.9859, indicating that the data from the FE model agreed well with the data from the experiment. The comparison results in Figure 5-12 confirm that the FE model created to evaluate the ballistic performance of woven fabrics is valid.

5.1.4 Investigation on energy absorption of ballistic impact in the FE model

After validation, the FE model was used to simulate wider issues related to the ballistic performance of the fabric. FE modelling provides the deformation and stress-strain distribution. Figure 5-13 depicts the contour maps of the fabric from the side and top views of the fabric deformation at various time points under the impact velocity of 475m/s.

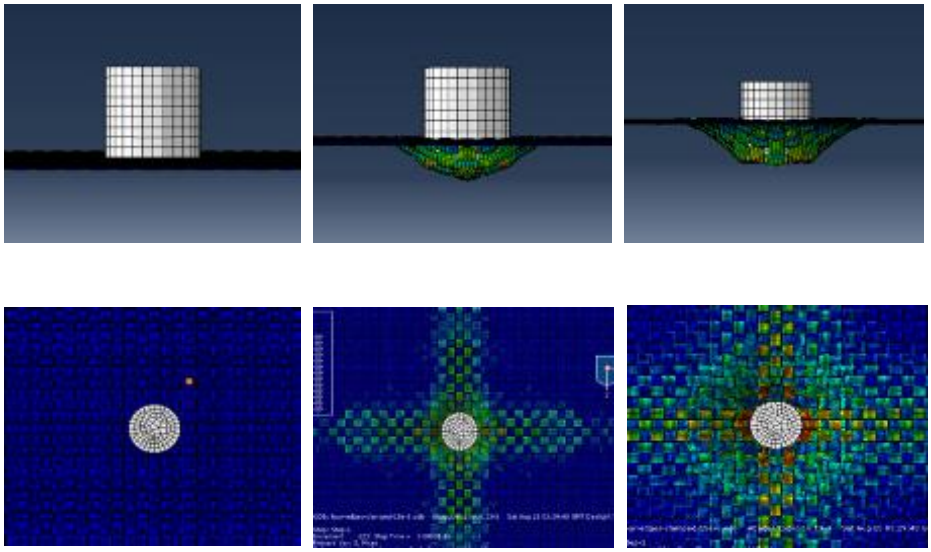

Figure 5-13 Top and side view of the fabric deformation at specific times (V=475m/s, four fabric edges clamped)

Figure 5-13 implies that the projectile momentum was transferred to the fabric panel. With the time increment, the fabric in the impact zone moved together with the projectile, and the longitudinal wave and transverse wave propagated away from the impact zone. At 3μs, the principal yarns started to be involved in the longitudinal stress

wave propagation. More yarn-yarn interaction occurred, causing secondary yarns to be involved in propagating stress and strain, as can be witnessed at the moment of 6μs. The front of the transverse deformation on the back of the fabric basically developed in a rough diamond shape between 3μm and 12μs.

As time went on, the kinetic energy carried by the projectile was gradually transferred to the fabric panel in various forms during ballistic impact. In practical situations, the air resistance to the projectile is usually ignored, therefore, the energy loss from the projectile was taken as the energy absorption of the ballistic panel. In FE modelling, the air resistance to the projectile was not considered. Figure 5-14 presents the changes in velocity of the projectile and energy absorption against impact time. From Figure 5-14 (a), it can be seen that the velocity of the projectile rapidly decreased within the first 0.6 μs, then the rate of decrease slowed down, but velocity continued to decrease. The velocity levelled after 14 μs, indicating the penetration of the projectile through the fabric. Related to the decrease of the projectile velocity, the energy absorption of fabric panel increased correspondingly. As shown in Figure 5-14 (b), the energy absorption started immediately after the ballistic impact, and the energy absorption was sharply increased to 1.5 J within the first 0.6 μs. Since the impact happened so quickly, the fabric sessions beyond the impact zone were not affected at the beginning. As the impact process continued, more yarns became involved in absorbing energy. This is in agreement with the findings of previous studies by Duan *et al.* [53].

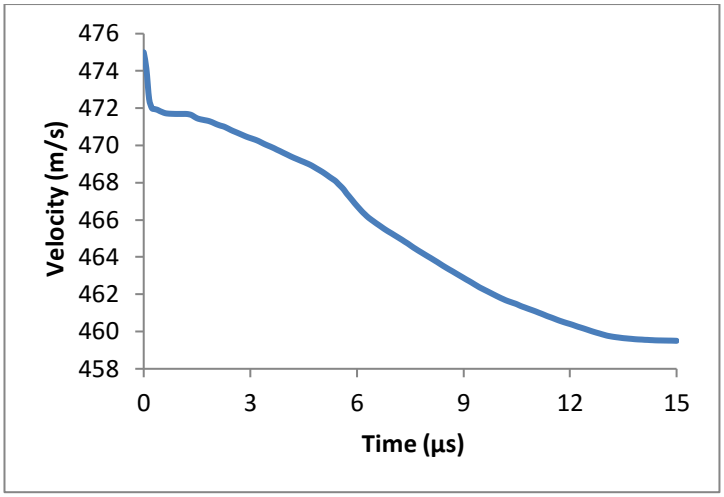

(a)

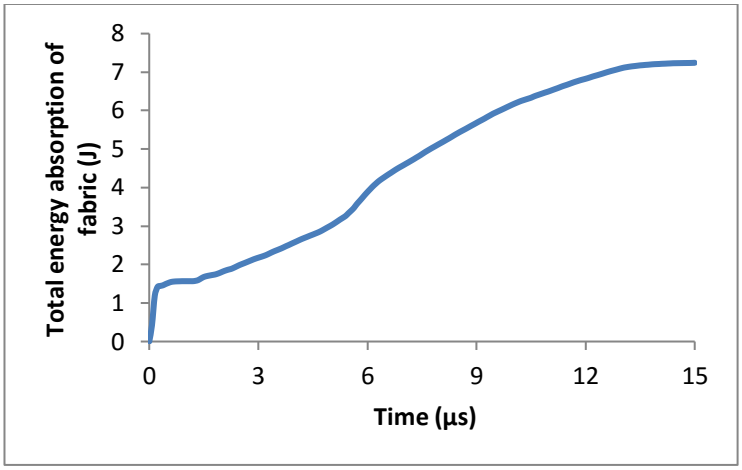

(b)

Figure 5-14 Time history of (a) projectile velocity decreasing and (b) total energy absorption of fabric panel

The kinetic energy transferred to the fabric panel is in the forms of strain energy, kinetic energy, frictional dissipation energy and other forms, as mentioned earlier. Figure 5-15 shows the time history of the energy transfer between the projectile and the fabric from the FE modelling.

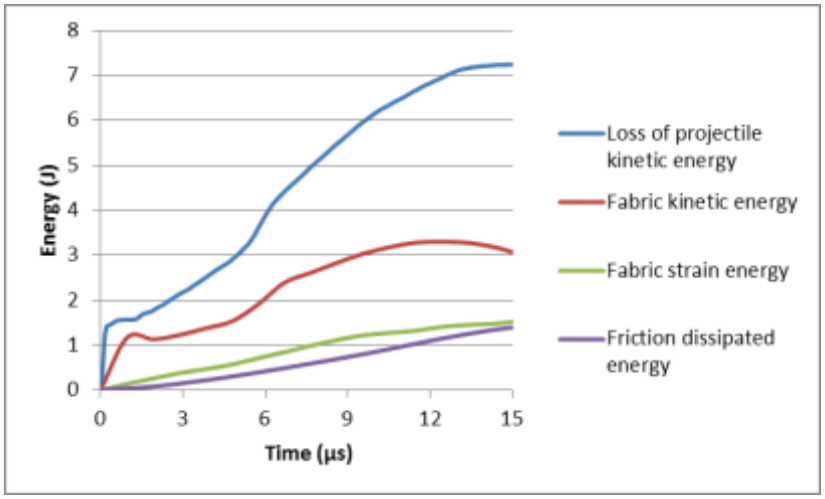

Figure 5-15 Time history of energy transfer between the projectile and the fabric

Figure 5-15 demonstrates that as time went on, more kinetic energy carried by the projectile got lost, and the major forms of energy absorption by the fabric panel kept increasing. It is clear that most of the energy lost from the projectile was converted to kinetic energy of the fabric panel, followed by strain energy, friction dissipation and other forms of energy. The details of the energy conversion are illustrated as a pie chart in Figure 5-16.

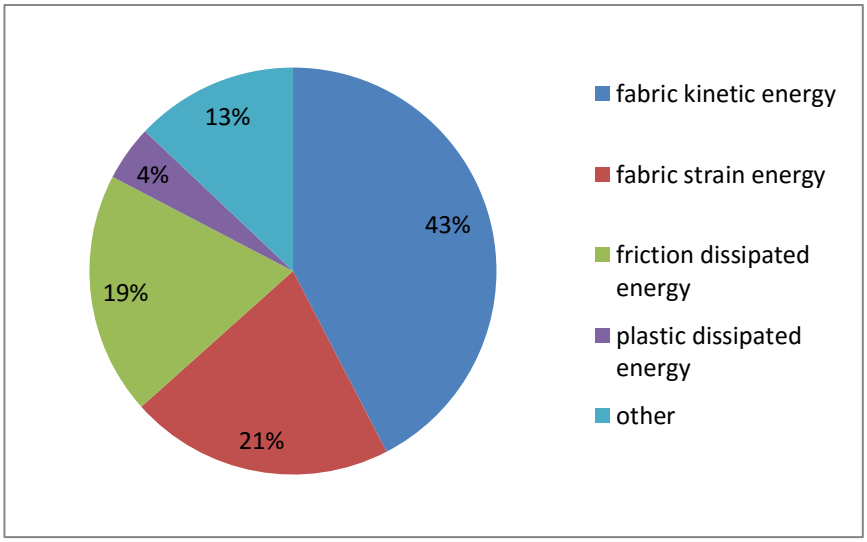

Figure 5-16 Contribution parts for total energy absorption of fabric

As can be seen in Figure 5-16, the fabric kinetic energy contributeed 43% of the total energy absorption, with fabric strain energy and friction dissipated energy of 21% and 19%, respectively. It needs to be mentioned that the friction dissipated energy included the friction between the yarns and the friction between the yarn and projectile. The plastic dissipated energy accounted for only 4%. Other forms of energy absorption could be energy dissipated by viscoelasticity, 'artificial' strain energy, energy dissipated by damage and so on.

5.1.5 Factors influencing ballistic performance

5.1.5.1 Impact velocity

By using the FE model, it is easy to obtain the energy absorption of the fabric by changing the impact velocity to verify the effect on the energy absorption of sample fabric. Figure 5-17 provides (a) residual velocities against various impact velocities and (b) energy absorption of fabric under various impact velocities.

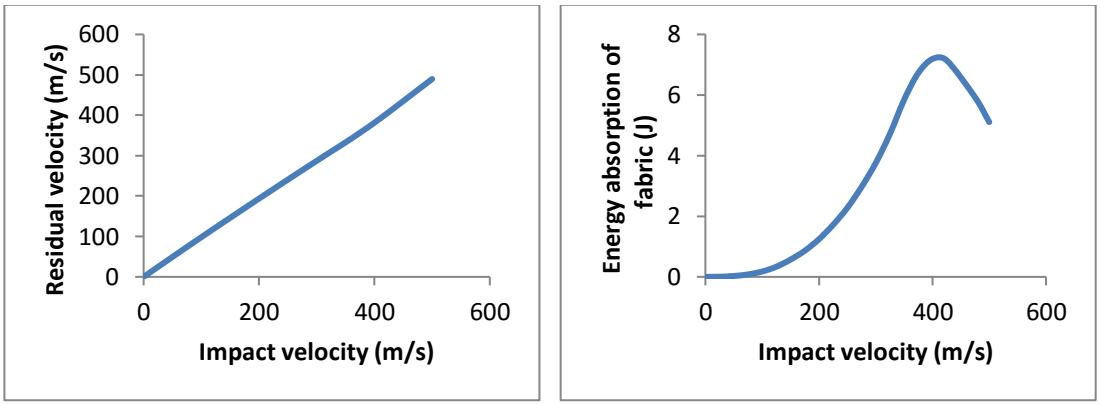

(a) (b)

Figure 5-17 (a) Impact velocity vs residual velocity (b) Energy absorption as a function of impact velocity (period of impact time is 15 μs)

It can be seen that a higher impact velocity would lead to a higher residual velocity. However, an impact velocity that gives the maximum energy absorption exists. In this simulation, when the impact velocity was around 400 m/s, the energy absorption reached its peak. When the impact velocity was higher than 400 m/s, the energy absorption started to drop. Low impact velocity leads to low energy absorption, but when the projectile impacts the fabric panel above a certain velocity, it leads to reduced energy absorption.

5.1.5.2 Boundary conditions of the fabric

Three cases with different boundary conditions were modelled to investigate the effect of boundary conditions, which were the opposite-side clamped, four-side clamping and free boundaries. The data for comparison were the velocity before and after impacting the fabric panel and the corresponding energy absorption of the fabric after impact. It was found that there are almost no differences in the velocity changing with the time increment for the three types of boundary conditions when the impact velocity is 475m/s and when the fabric size is 15cm×15cm, which can be explained in the energy dissipation and fabric penetration happen so quickly that yarns far from the impact zone are not even affected by the wave transportation during the high impact velocity, when the fabric size is too large to explore the boundary condition effect. The impact area is localised. When the model size was reduced to a 5cm×5cm square fabric, the boundary condition affected the projectile velocity significantly. Figure 5-18 depicts the projectile velocity as a function of time for the three cases that were impacted by the same velocity of 475m/s. It can be noted that at the beginning of the impact process under 7μs, the projectile velocity is the same for all three cases, which means the boundary condition does not play a decelerating role at that time. After that, the projectile experiences the most deceleration with the four edges clamped boundary

condition. The projectile penetrates through first in the condition with four fabric edges clamped compared with the other two situations. Generally speaking, the less the clamped boundary condition, the more the projectile velocity decelerated. When the longitudinal wave arrived at the free end of the yarn, it reflected back towards the impact zone. The yarn tensile strength faded away and the interaction between the yarns created bowings along the fabric edges. When the longitudinal wave arrived at the clamped edge, it was reflected and propagated towards the impact zone, but the tensile strength was doubled, hence, the stress in the clamped yarns was much larger than the stress in the unclamped yarns. The energy loss of the projectile within 40μs is shown in Figure 5-19 and reflected that the less clamped edges result in high projectile energy loss.

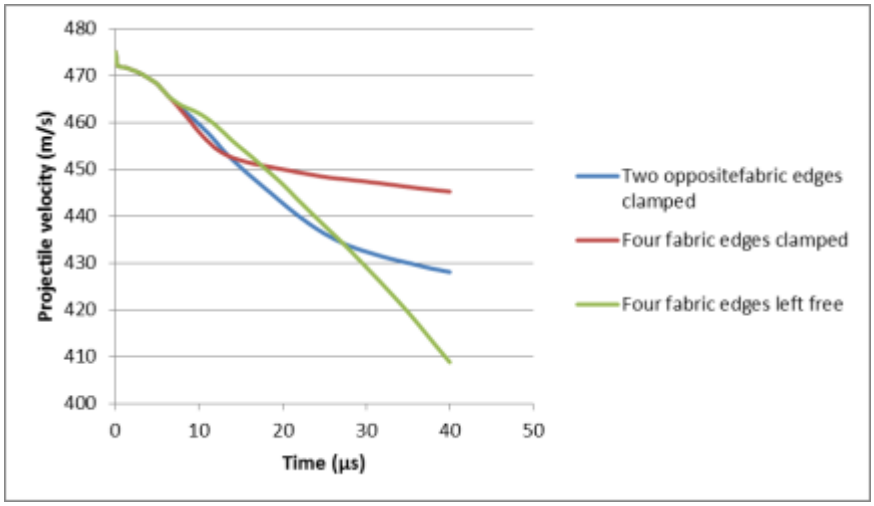

Figure 5-18 The projectile velocity as a function of time for the three types of boundary conditions that have the same impact velocity of 475m/s

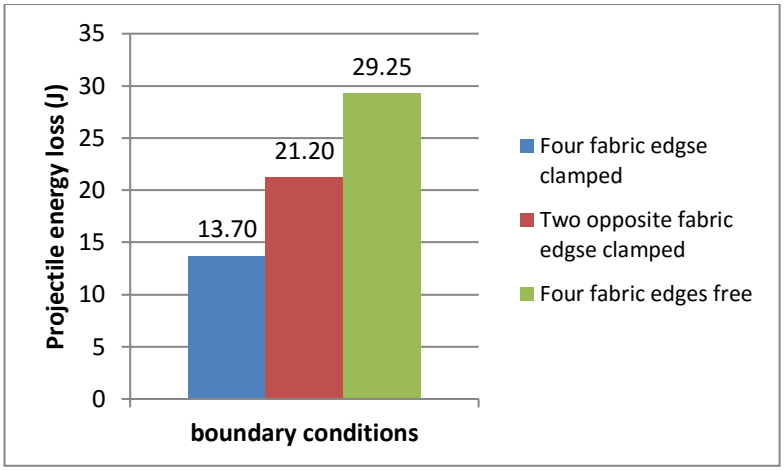

Figure 5-19 Projectile energy loss for the three types of fabric boundary conditions

Figure 5-20 provides contour plots for the three situations at 21µs at the impact zone. It can be noticed in case (a) that the main stress is distributed around the ballistic bottom edge when the four edges are clamped and the fabric is deeply stretched out. In case (b), the main stress is distributed along the direction of the opposite clamped yarns. In case (c), no obvious stress is noticed around the ballistic edges. The contour plot confirmed that the clamped edges lea to higher tensile stress on the yarn and led to early failure of the fabric.

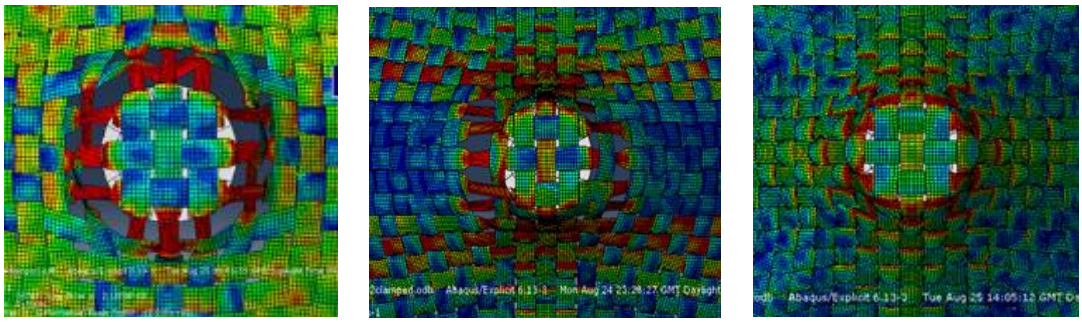

(a) (b) (c)

Figure 5-20 Contour plot of the (a) four edges clamped fabric (b) two opposite edges clamped (c) four edges left free at the time of 21µs

5.1.5.3 Impact location

Two impact locations were considered in this investigation. One is that the projectile impacted exactly on the yarn, and the other is that the projectile impacted between two adjacent yarns. Figure 5-21(a) illustrates a situation in which the projectile landed on the centre of the cross-over point (the point of RP) of the warp and weft yarns, and (b) that the projectile impacted (the point of RP) between the adjacent yarns. The difference in energy absorption at the different impact locations is shown in Figure 5-22. Fabric absorbs 7.4 J under the condition of case (a) while it absorbs 7.9 J when impact location is case (b). It can be seen that in case (b) in Figure 5-22, the number of yarns involved in contact with the projectile surface is higher than in case (a), so the yarns in the fabric in case (b) were working more efficiently to absorb the energy from the impact projectile.

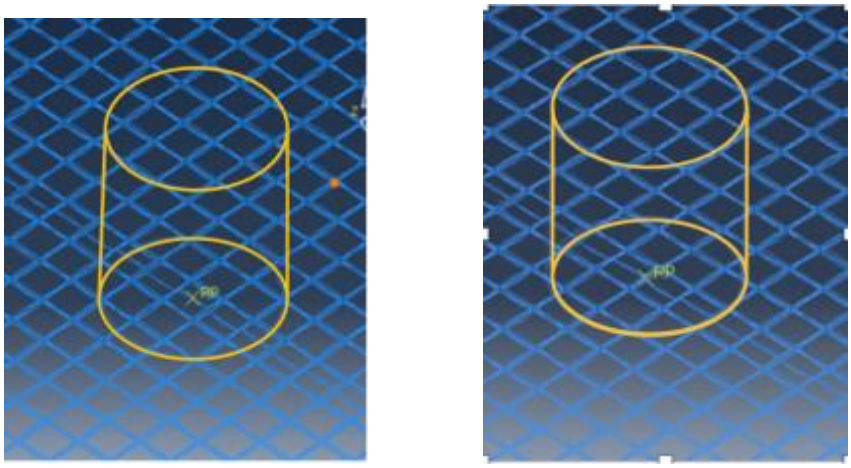

(a) (b)

Figure 5-21 Impact location illustration

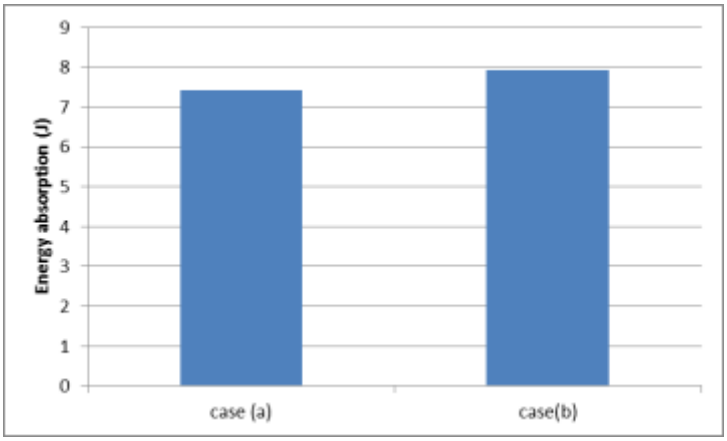

Figure 5-22 Energy absorption of the fabric for different impact locations

5.2 Effect of inter-yarn friction in plain fabrics

5.2.1 Influence of inter-yarn friction on the total energy absorption of the woven fabric

The total energy absorption by the fabric is assumed to be the projectile's kinetic energy loss. In this investigation, different frictional coefficients between 0 and 2.0 were assumed between the warp and weft yarns. Figure 5-23 shows the plot of the projectile's kinetic energy loss as a function of the inter-yarn frictional coefficient. It can be seen that the total energy absorption reached the highest value, 7.5 J, at μ=1.0, and the lowest energy absorption (5.7 J) was shown when μ=0.1. There was a constant increase of energy absorption when the frictional coefficient increased from 0.1 to 1. After μ=1, the energy absorption started to drop slightly and remained at almost the same level up to the situation when μ=2.0. A slight decrease of energy absorption was also noticed when the coefficient changed from 0 to 0.1. In the realistic aramid fabric, the frictional coefficient is around μ=0.2 [144] . This exercise clearly indicated that an increase of the frictional coefficient would enhance the energy absorption of the fabric.

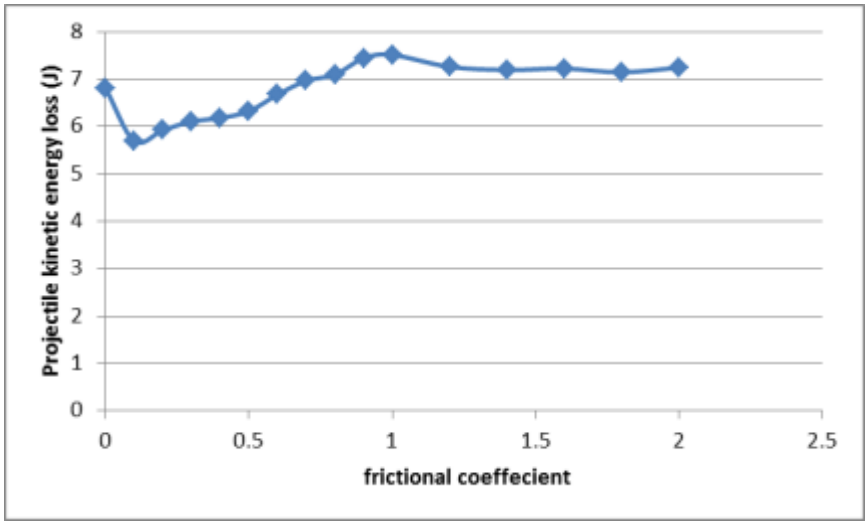

Figure 5-23 Projectile kinetic energy loss as a function of the coefficient of inter-yarn friction

The investigation also revealed that a fabric with higher inter-yarn friction would take a longer time to be penetrated, as shown in Figure 5-24. At 9μs, the fabric with μ=0.1 failed, whereas for the fabric with μ=1, the yarns just stated to crack at the same time.

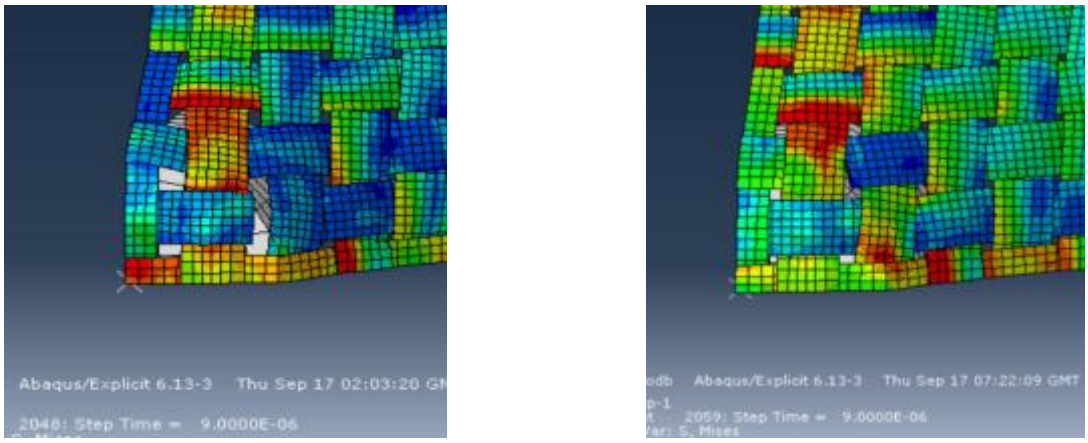

(a) μ=0.1 (b) μ=1

Figure 5-24 Single-layer fabric model under ballistic impact at 9 μs

5.2.2 Effect of inter-yarn friction on energy absorption in different forms

As mentioned previously, fabric absorbs energy mainly in the form of friction dissipation, kinetic energy and strain energy. Figure 5-25 shows the relationship between the friction coefficient and energy absorption of fabric due to friction dissipation. It can be observed that friction dissipation increased sharply with the change in the frictional coefficient μ when it is smaller than 0.25. Energy absorption in the form of friction dissipation started to decrease afterwards. It can be explained that under μ=0.3, the frictional coefficient effectively prevents yarn slippage to enhance the integrity of the weave and enables more yarns to be involved in absorbing the energy. However, when the inter-yarn friction is high enough, μ over 0.3, it starts to restrain relative slippage between yarns, leading to less frictional dissipation energy.

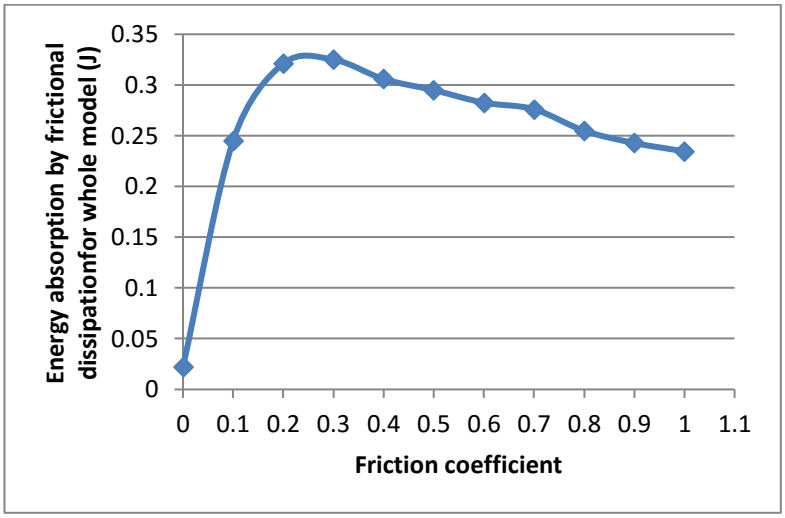

Figure 5-25 Friction dissipation energy as a function of the coefficient of inter-yarn friction

In investigating the kinetic energy absorption and strain energy absorption mechanisms, three cases, μ=0.1, μ=0.5 and μ=1.0 were selected to represent different levels of friction for comparison. Figure 5-26 demonstrates that the kinetic energy of

fabric increased with an increasing friction coefficient. The kinetic energy of the fabric sharply increased at the early impact time because yarns require time to respond. When the yarns started to respond to the projectile impact, the increase rate maintained a stable growth rate until the fabric was penetrated by a projectile. The highest kinetic energy appeared around 10 μs when the fabric was penetrated. As the inter-yarn friction contributes to the integrity of the weave structure, a higher frictional coefficient provides better integrity, which leads to more yarns involved to move in the same direction of the impact projectile. A similar trend can be observed from the strain energy absorption in Figure 5-27; the strain energy increased with the increased frictional coefficient, which can be explained as the same process that happens in kinetic energy absorption.

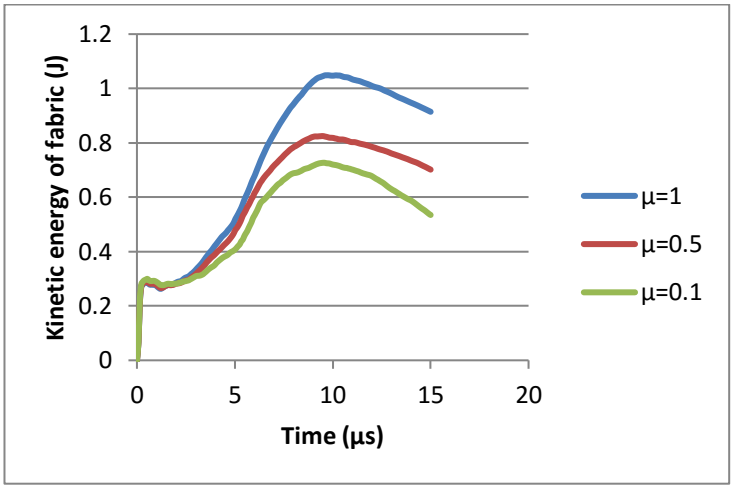

Figure 5-26 Time history of fabric kinetic energy with three levels of inter-yarn friction

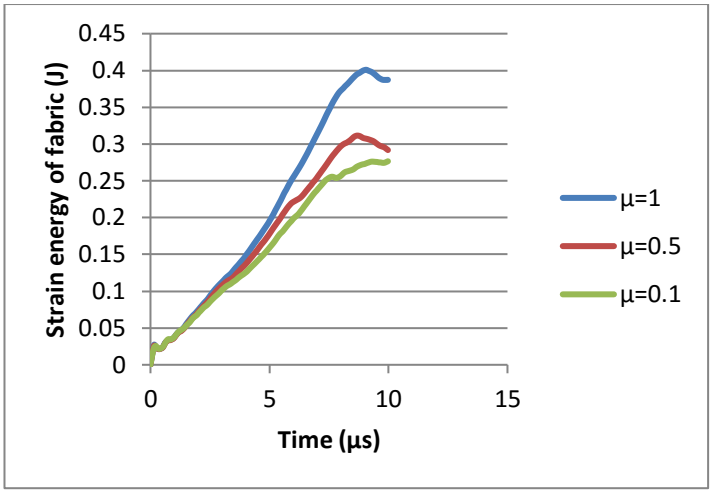

Figure 5-27 Time history of fabric strain energy with three levels of inter-yarn friction

Stress distribution can be noticeably affected by inter-yarn friction. The contour plots of ballistic impact on the fabric model with three different inter-yarn friction levels are shown in Figure 5-28, and Von Mises Stress was adopted as an indicator of the fabric stress distribution against ballistic impact. The coloured area indicates that the stress is distributed on the yarns. From Figure 5-28, it can be seen that with increasing time, the stress distribution area is increased, and the increase of inter-yarn friction leads to more involved yarns in the impact centre rather than along the principal yarns. The larger area in the vicinity of the impact point is developed because of the friction between the yarns. The higher inter-yarn friction helps more secondary yarns become involved in energy absorption as well as hinders the stress propagation along the primary yarns. When the stress is not concentrated along the primary yarns but distributed on more secondary yarns, it becomes more difficult for the fabric to be penetrated by a projectile.

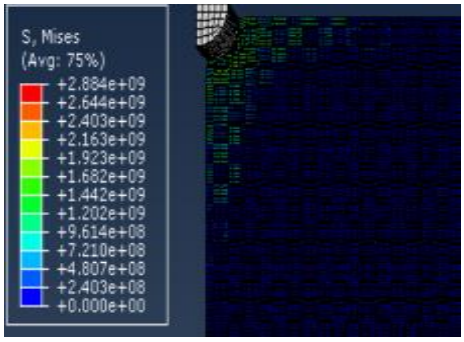

μ=0.1

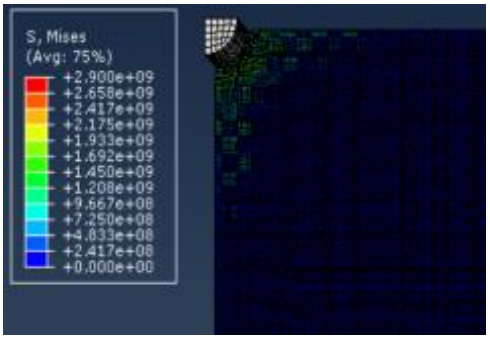

μ=0.5

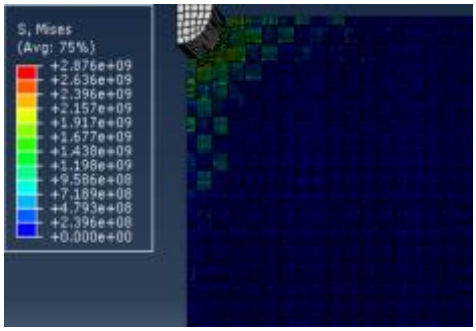

μ=1

(a) Impact time at 1.5 μs

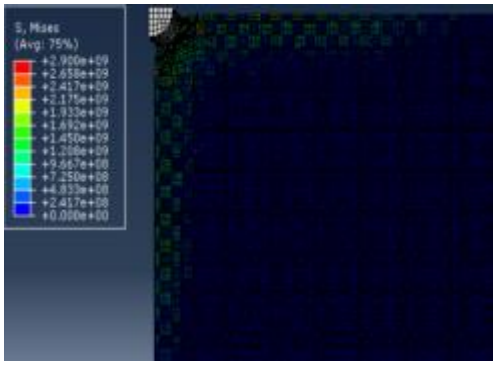

μ=0.1

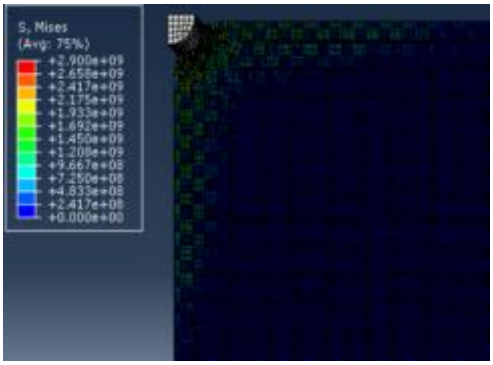

μ=0.5

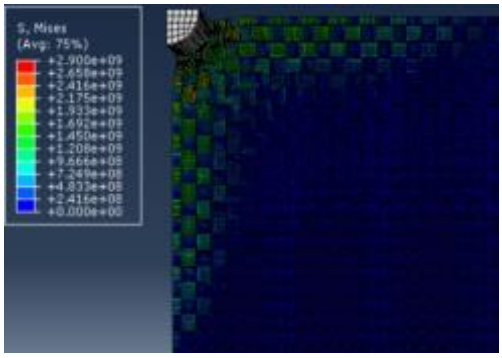

μ=1

(b) Impact time at 4.5 μs

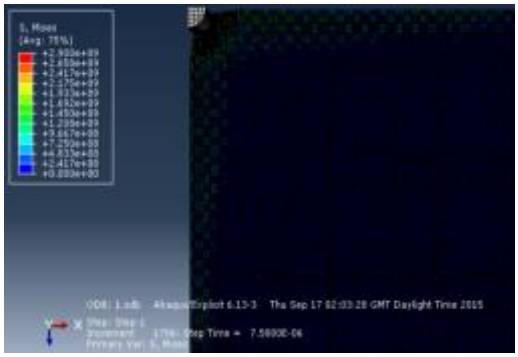

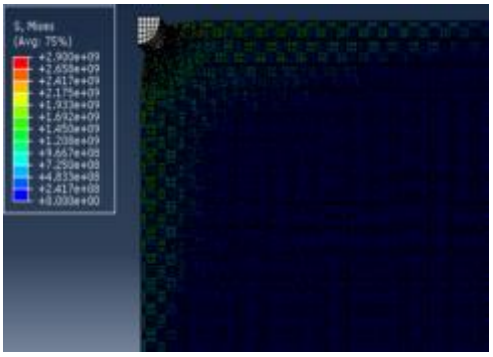

μ=0.1 μ=0.5

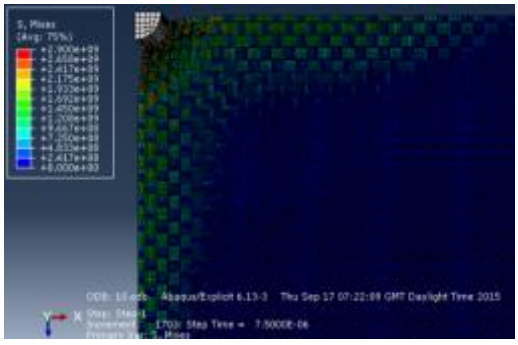

μ=1

(c) Impact time at 7.5 μs

Figure 5-28 Contour plots for fabrics at specific times under impact

5.2.3 Influence of inter-yarn friction on the energy absorption of principal yarns and secondary yarns

Figures 5-29 and 5-30 show the kinetic energy absorption on the primary yarns and secondary yarns, respectively, for the three friction coefficients, μ=0.1, μ=0.5 and μ=1.0. It is clear that the principal yarns respond directly and dramatically and increase the kinetic energy absorption. At the same time, the secondary yarns gradually increase the energy absorption with time. The higher inter-yarn friction enables the case of μ=1.0 to have more kinetic energy absorbed in both impact areas on the fabrics, and in the friction coefficient ranging from 0.1 to 1, the kinetic energy on both primary yarns and secondary yarns increases with added inter-yarn friction. This indicates that the frictional coefficient, in other words, inter-yarn friction, has a positive influence on the kinetic energy absorption in the fabrics. In terms of strain energy absorption on primary yarns and secondary yarns, a similar tendency can be observed in Figure 5-31 and Figure 5-32. The enhanced coupling effect due to increased inter-yarn friction enables more stress to be distributed on the secondary yarns.

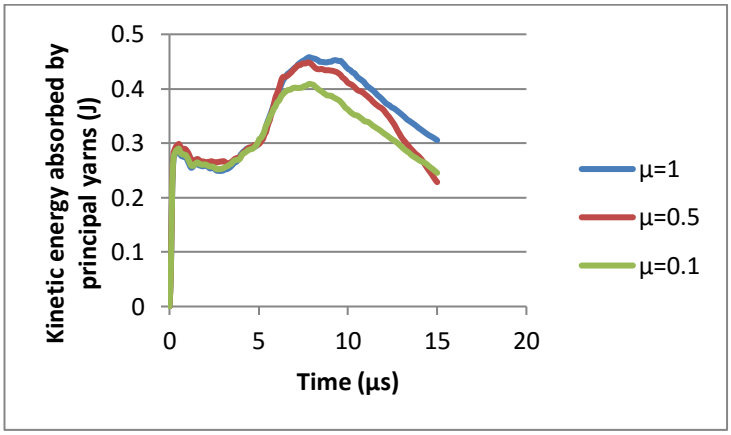

Figure 5-29 Time history of kinetic energy on the primary yarns

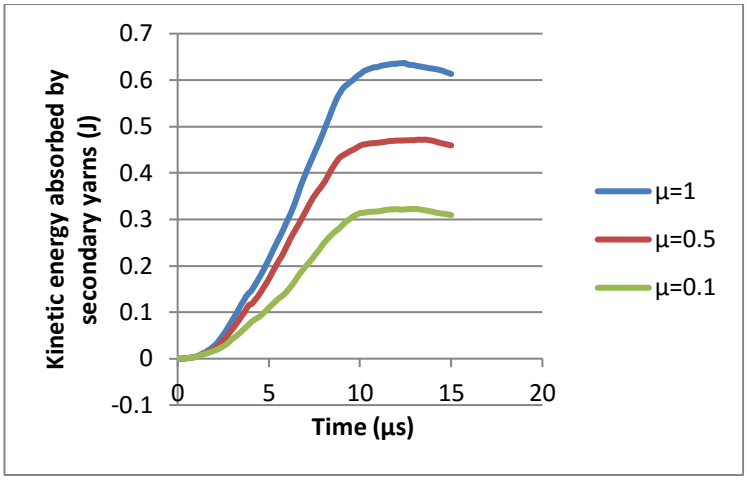

Figure 5-30 Time history of kinetic energy on the secondary yarns

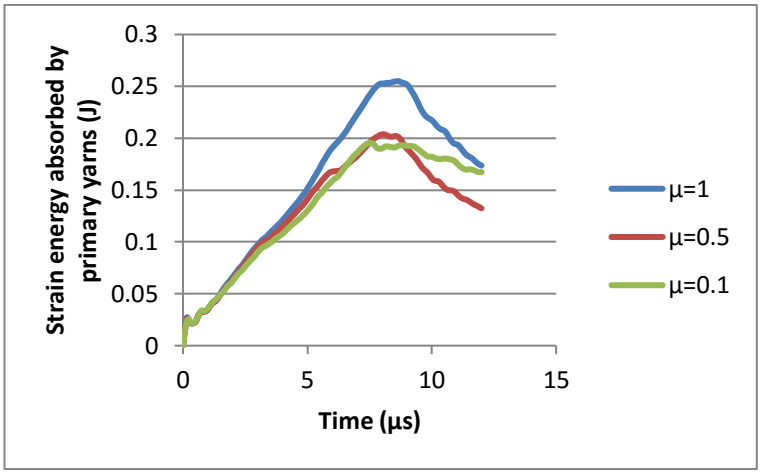

Figure 5-31 Time history of strain energy on the primary yarns

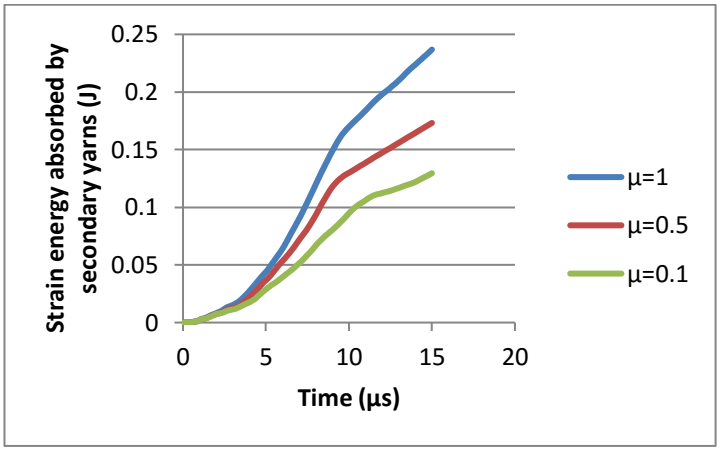

Figure 5-32 Time history of strain energy on the secondary yarns

5.2.4 Stress distribution along the principal yarns and secondary yarns

Stress distribution on the primary yarns

A single yarn is selected to represent the primary yarn and is used to reflect the stress distribution along the selected primary yarn as shown in Figure 5-33. To provide a plot of stress as a function of the distance from the impact point, specific nodes along the yarns have been selected to reflect the stress magnitude at the area of the node. The nodes are selected with the same distance interval along the yarn.

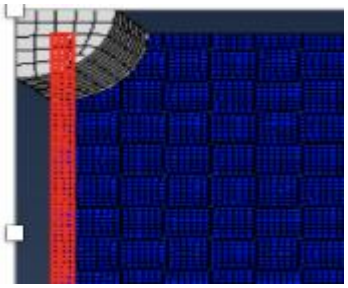

Figure 5-33 Primary yarn selection for analysing stress distribution

Figure 5-34 displays the stress distribution on the selected yarn at 1.5 μs, 4.5 μs and 7.5 μs. Three levels of μ=0.1, μ=0.5 and μ=1 are chosen to represent different inter-yarn frictions in the fabric. It has been noticed that with increasing time, the distance from impact point for selected primary yarn to distribute stress is not affected by inter-yarn friction. In other words, the speed of the longitudinal wave is not influenced by the inter-yarn friction. However, the stress distributions are different under varying inter-yarn friction situations. It can also be found in Figure 5-34 (b) and (c) that higher inter-yarn friction may bear a higher load compared to relatively lower inter-yarn friction at 4.5 μs, but when the time increases, there is time to include more yarns to bear the stress load, hence the pick load for stress distribution is almost the same at the impact zone. One thing that needs to be noted is overly high inter-yarn friction will restrict the movement of the yarns and lead to a local stress concentration.

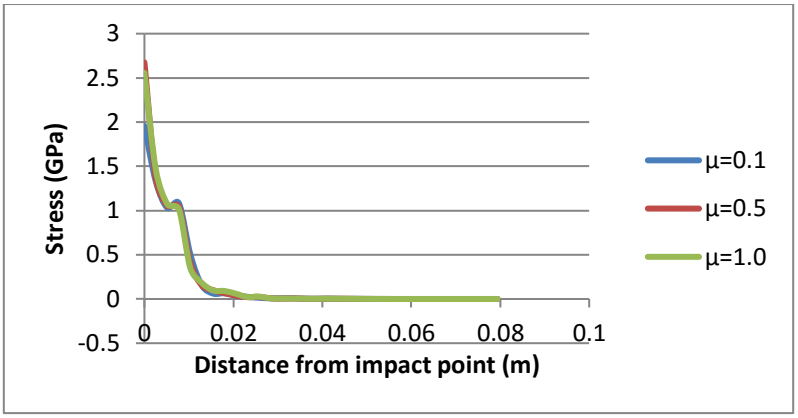

(a) 1.5 μs

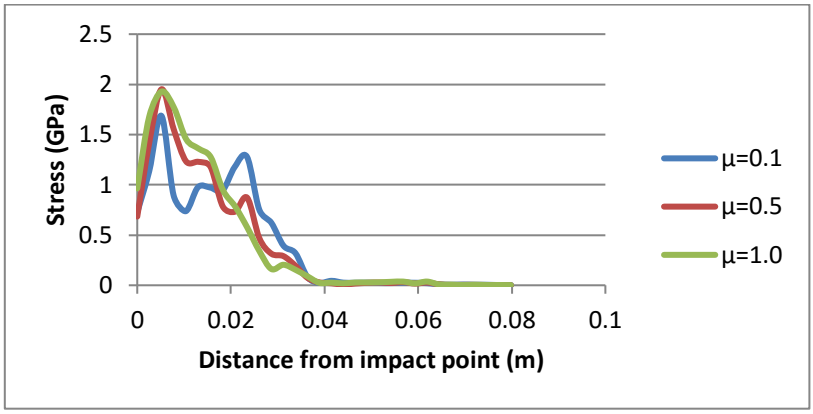

(b) 4.5 μs

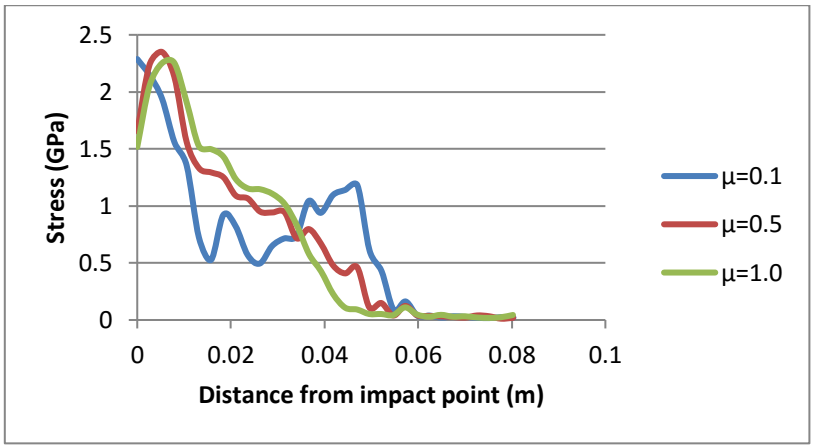

(c) 7.5 μs

Figure 5-34 Stress distribution for selected primary yarn with three different levels of friction coefficient at specific times

Stress distribution on the secondary yarns

A secondary yarn near the impact zone is selected to investigate the stress distribution on the secondary yarn, as shown in Figure 5-35. The nodes on the edge of the selected yarn are picked to represent the yarn. The results can be found in Figure 5-36, and it can be confirmed that the inter-yarn friction enables the secondary yarn to have more stress distributed in the area near the impact point; therefore, the stress is not concentrated in the local area. Increased inter-yarn friction provides a smoother stress distribution than lower inter-yarn friction, which shows a fluctuated stress distribution along the yarn that can be observed in Figure 5-36 (c). The enhanced inter-yarn friction enables better integrity of the weave and enhances the interplay between yarns.

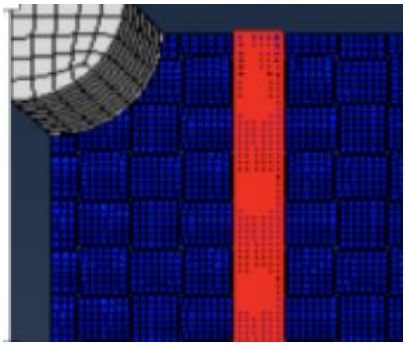

Figure 5-35 Secondary yarn selection for analysing stress distribution

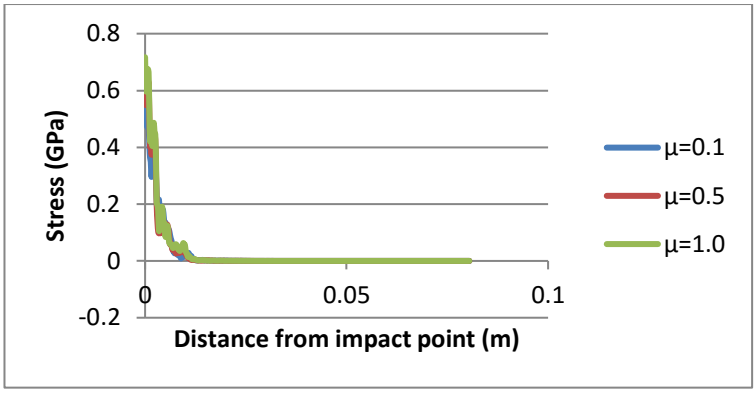

(a) 1.5 μs

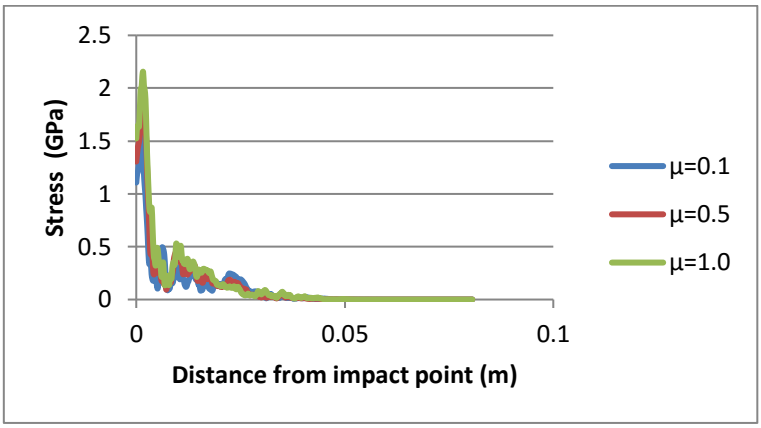

(b) 4.5 μs

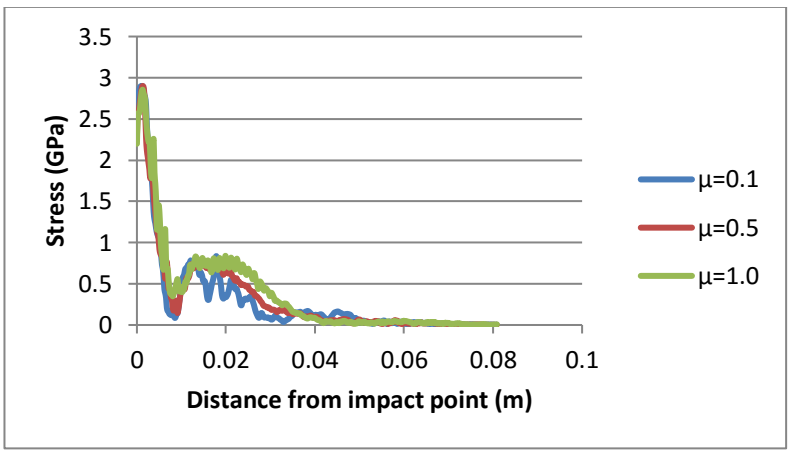

(c) 7.5 μs

Figure 5-36 Stress distribution on selected secondary yarn with three different levels of friction coefficient at specific times

5.3 Summary

This chapter provides the theoretical methodology adopted for the investigation of the problems to achieve the targets and objectives in this research. The methodology was mainly based on the ballistic range provided and the development of the finite element model by ABAQUS. The present study is focused on the development of the ballistic fabric structure. A basic plain woven fabric model was created, and its effectiveness has been clearly demonstrated by the FE model. It has been found that under a lower impact velocity range (under 400 m/s), the energy absorption increased with the increase of impact velocity; when the fabric is subjected to higher impact velocity, the energy absorption decreased with the increasing impact velocity because of the localised impact area involved in absorbing the energy. The kinetic energy of the projectile is mainly absorbed by the fabric in the form of kinetic energy, which occupies 43% of the total energy absorption of the fabric panel. Meanwhile, friction dissipation energy and strain energy are the other two main forms of energy absorption.

External factors such as impact velocity, fabric boundary conditions and impact location are studied for the effect on the ballistic performance. In the aspect of boundary condition, it has been found that energy absorption can be affected significantly when the fabric sample size is small (5cm×5cm) under low impact velocity because the larger the fabric, the longer the wave transfer will take. However, fabric boundary conditions do not affect the energy absorption dramatically when the fabric sample size is big enough or the impact velocity is high. The impact location will affect the energy absorption of the fabric panel slightly because of the different location determining the number of direct contact yarns.

One of the objectives of this research is to investigate the influence of inter-yarn friction on ballistic performance of woven fabrics. In this chapter, FE models provide a feasible and effective method to conduct an investigation of the effect of inter-yarn friction on energy absorption. It has been proven that the highest energy abortion for the fabric is under the condition of μ=1 among conditions of the three specific frictional coefficients (μ=0.1, 0.5 and 1). Regarding boundary condition, it has been found that energy absorption can be affected significantly when the fabric sample size is small (5cm×5cm) under low impact velocity because the larger the fabric, the longer time the wave transfer will take. By separating the energy absorption behaviour into groups, it has been found that higher inter-yarn friction leads to increased kinetic energy and strain energy absorption for the whole fabric. As the inter-yarn friction contributes to the integrity of the weave structure, a higher frictional coefficient provides better integrity and leads to more yarns being involved to move in the same direction of the impact projectile. However, frictional dissipation of energy starts to decrease when μ is over 0.3 as shown in Figure 5-25. The higher μ (μ>0.3) starts to restrain relative slippage between yarns, which leads to less frictional dissipation energy. The same situation occurred for primary yarn and secondary yarn in terms of kinetic energy and strain energy absorption with increased friction coefficient. It has been found that the inter-yarn friction does not affect the longitudinal wave velocity. A higher stress load is distributed onto the secondary yarn due to the higher inter-yarn friction, which can avoid stress concentration on the primary yarn.

Chapter 6 Extended numerical study of fabrics with leno insertions

Since the leno fabric shows excellent results among all the gripping methods, increasing the yarn pull-out force and energy absorption in experimental studies, it is important to evaluate the leno fabric by FE methods to provide a more comprehensive understanding. As the gripping idea is to increase the wrapping angle in the fabric to increase the inter-yarn friction and to simplify the structure, it is possible to use a plain weave structure at the leno line area but introducing higher inter-yarn friction along the leno line to mimic a leno gripping effect.

Based on the results of the selection of effective gripping methods from an experimental study, leno gripping is proven to have a positive effect on the fabric energy absorption. This chapter focuses on the optimisation of the leno gripping structure rather than a selection of the valid gripping method. The experimental method is adopted to validate the numerical results.

6.1 Model creation and validation

For the fabric structure to simulate the fabric with leno gripping, it was decided to use plain woven fabric instead of the real geometrical structure of the leno line. The pull-out test has been conducted by pulling out the standard yarn from warp direction on the leno area and comparing it with the pull-out force on the corresponding plain fabric. The peak load for pulling out the standard yarn in the leno structure is around 6.5 times higher than pulling out in the plain woven fabric. The coefficient friction for plain fabric is 0.2, and the inter-yarn friction is set to be 1, which is realistically the largest friction coefficient that can be achieved on the leno area. In addition, during the investigation of the friction coefficient study in plain weave structure, $\mu=1$ has been

tested and confirmed to enable energy absorption at a maximum degree within the practical friction coefficient range. The interaction for the model is general contact with individual property assignment. This contact assignment is much quicker to define and easier than ‘surface to surface contact’ in the ABAQUS software system, and time will be saved by selecting individual surfaces. The selected line to work as leno gripping is shown in Figure 6-1.

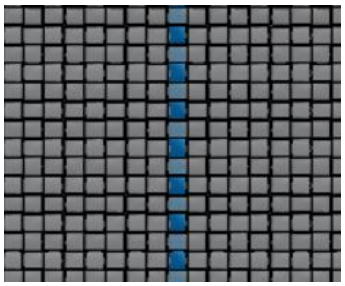

Figure 6-1 The coloured area is the individually assigned inter-yarn friction coefficient

Figure 6-2 describes the model validation for two situations with different impact locations, one impacting the leno line and the other impacting the plain structure area in the plain woven fabric with leno insertions. The linear regressions show that the gradients of the regression lines for impacting the leno line and the plain area are 0.9341 and 1.0512, respectively, and the correlation coefficients are 0.945 and 0.820, respectively. These results imply that the FE models for impacting different locations were validated.

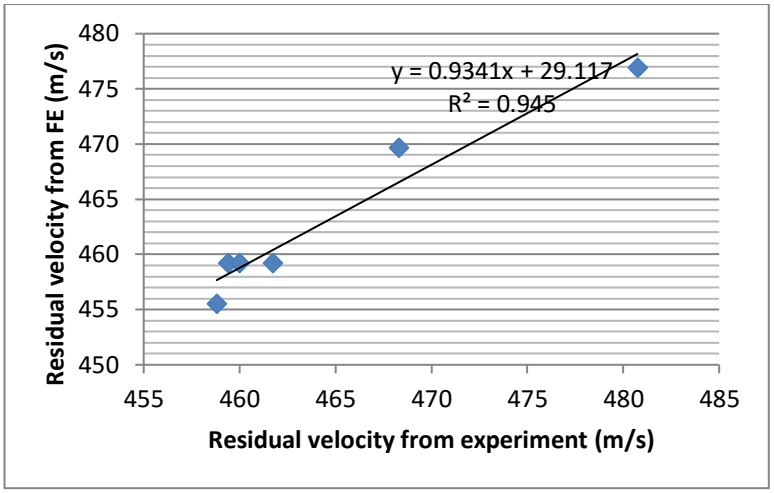

(a) Impact on the leno line

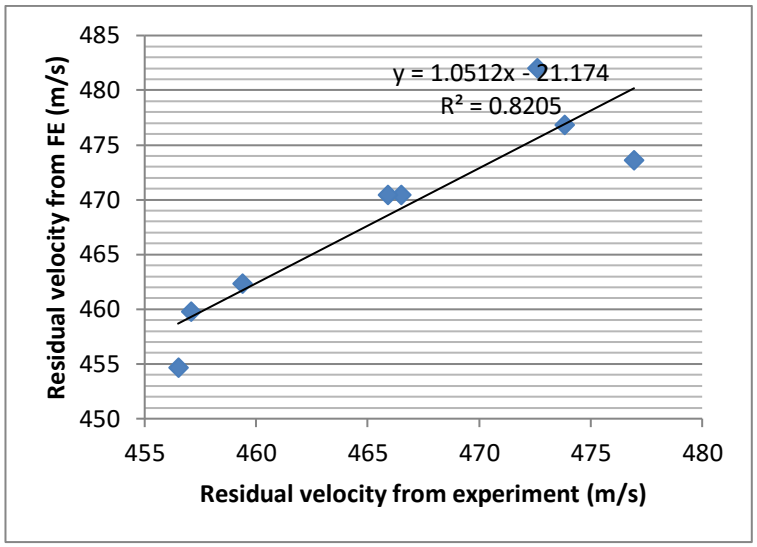

(b) Impact on the plain area

Figure 6-2 Model validation for different impact location conditions

6.2 Optimisation of gap size between leno lines for ballistic performance

6.2.1 Total energy absorption

The main difference between fabric with leno insertion and plain fabric is the introduction of the leno line. The gap between leno lines in the fabric can affect the energy absorption since it works as a convert method to alter the boundary condition

and affect the gripping effect. The results are based on the condition when the impact velocity is 475 m/s and the residual velocity is obtained from the model. Figure 6-3 reveals the energy absorption for the fabrics with leno insertion. It can be found that the plain area absorbs more energy than the leno area. It can be explained that a limited area with higher inter-yarn friction leads to a localised impact area, and the yarn is over constrained compared to the corresponding plain area. The optimum distance between the leno lines is 4cm; a distance under 4cm and over 4cm shows inferior ability of energy absorption. If the leno lines are too close to each other, the narrow area between leno lines shows inferior energy absorption because of the overly constrained yarns. On the other hand, when the distance between leno lines gets wider, the fabric tends to be a broad fabric that loses the gripping effect and leads to less energy absorption. This study shows a good agreement with the results achieved by Sun [6].

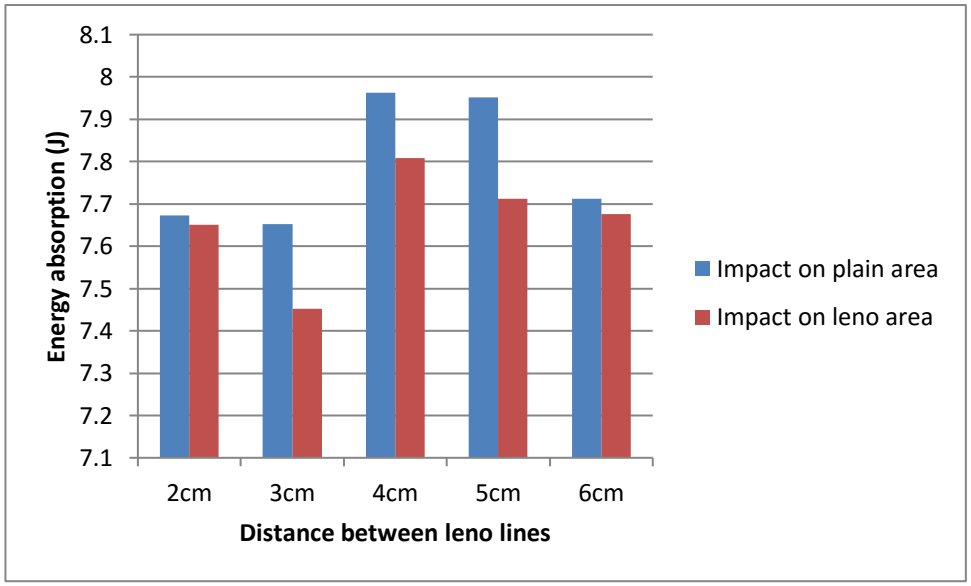

Figure 6-3 Energy absorption for fabric with different leno gap distances

6.2.2 EV_{50} evaluation of fabric panels with and without leno insertion

Estimated ballistic limits (EV_{50}) are adopted to validate the numerical data and evaluate the fabric panels without consuming a great amount of fabric for the V_{50} ballistic test. The EV_{50} has been compared to the experimental ballistic limit by Sabet and his colleagues, who found that the estimated ballistic limit values are at the same level as corresponding experimental results [172]. EV_{50} is calculated by using the initial and residual impact velocity according to the following relationships for perforated panels:

$$½mVr^2 = ½mVi^2 - ½m(EV_{50})^2 \quad (6\text{-}1)$$

$$EV_{50} = (Vi^2 - Vr^2)^{1/2} \text{ for } Vr > 0 \quad (6\text{-}2)$$

where *Vi* is the initial impact velocity, *Vr* is the projectile residual velocity and *m* is the mass of the projectile. The above equations assume a non-deformable projectile and conservation of energy.

By using EV_{50} to evaluate the effectiveness of the leno line to increase the ballistic limit, the impact velocity, which is also known as initial velocity, and residual velocity are required for calculation. This section aims to evaluate the fabric panels with and without leno insertion; in other words, plain fabric and plain fabric with a leno line are chosen for comparison. The purely plain fabric and plain fabric with a 2 cm leno insertion have been used to identify the effectiveness of energy absorption of the leno gripping effect as well as EV_{50} velocity comparison. Two layers and four layers of fabric panels are chosen for EV_{50} evaluation. The results in Table 6-1 are obtained from the average results of 10 ballistic tests, and the detailed impact velocities and residual velocities are shown in the appendix

Table 6-1 High-velocity impact test results

Fabric Type	*No. of layers*	*Fabric Areal density (kg/m$^{2)}$*	*EV_{50} (m/s)*	*SD of EV_{50} (m/s)*	*Normalised EV_{50} (m/s)*
Plain	2	0.29812	167	12	559
	4	0.59624	219	28	367
Plain+Leno	2	0.3216	180	23	561
	4	0.6432	238	30	370

It can be seen that ballistic panels made from fabric with leno insertions demonstrated increased EV_{50}. The normalised results confirmed that leno provide positive effects on EV_{50}.

6.2.3 EV_{50} evaluation of fabric panels with different leno intervals

As has been predicted by the numerical evaluation, a 4cm gap between the adjacent leno lines in the plain woven fabric with leno insertions gave the best energy absorption results. It would be of great interest to find what the EV_{50} would be for body armour made from this new material.

As reported in Chapter 4, the V_{50} tests confirmed that the fabric with leno insertions with a 2cm gap between adjacent leno lines increased the V_{50} velocity over its plain woven counterpart. The comparison puts the focus on leno fabric with a 2cm gap and 4cm gap by using the EV_{50} method. Table 6-2 shows the comparison between the fabrics with different leno intervals, 2cm and 4cm. The results shown in Table 6-2 are average results obtained from five high-velocity impact tests.

Table 6-2 High-velocity impact test results for leno fabric with 2cm and 4cm gap intervals

Fabric Type	*No.of layers*	*Fabric Areal density (kg/m$^{2)}$*	*EV_{50} (m/s)*	*SD of EV_{50} (m/s)*	*Normalised EV_{50} (m/s)*
Leno with 2cm interval	2	0.3216	180	23	561
	4	0.6432	238	30	370
Leno with 4cm interval	2	0.28924	175	8	605
	4	0.57848	236	32	407

Normalised EV_{50}, defined by the average EV_{50} for a specimen divided by its areal density, shows an increase in normalised EV_{50} with a 4cm gap, as compared with 2cm in both two layers and four layers of fabric panels, as demonstrated in Figure 6-4. This result implies that a body armour panel made from plain woven fabric with 4cm leno lines would offer better protection.

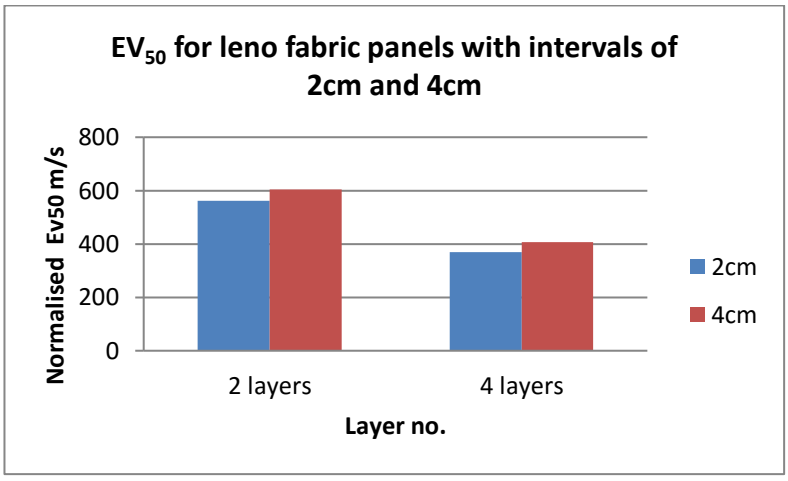

Figure 6-4 EV_{50} for leno fabric panels with different leno gaps

6.3 FE analysis of impact location in fabrics and panels with leno insertion

As previously mentioned, the performance of the leno line and plain area shows different energy absorption ability, and the layer arrangement is taken into consideration. Through experiments, there is an indication of the existence of optimum layer arrangement for leno fabric, which is an offset leno line to layer the fabric discussed in Chapter 4. The energy absorption results are due to the probability of the impact location and the variation on the impact location. Since it is difficult to achieve a certain amount of data from experiments on specific impact areas, the FE model was created to discover the energy absorption on different impact locations for different layer arrangements. As the smallest repeat unit for the construction of the 90-degree layer arrangement, two layers of fabric models are created to investigate all layer arrangements. The impact locations are specified in Table 6-3.

Table 6-3 Impact location specification

Name of impact location	Remarks
90-L-L	Leno line layer by 90° layering, impacting the leno lines of the first layer and second layer
90-L-P	Leno line layer by 90° layering, impacting the leno lines of the first layer and the plain area of the second layer
90-P-P	Leno line fabric 90° layering, impacting the plain area of the first and second layer
90-P-L	Leno line fabric 90° layering, impacting the plain area of the first layer and the leno line of the second layer

offset-L-P	Leno line fabric offset layering, impacting the leno line of the first layer and plain area of the second layer
offset-P-P	Leno line fabric offset layering, impacting the plain area of the first and second layer
offset-P-L	Leno line fabric offset layering, impacting the plain area of the first layer and on the leno line of the second layer
aligned-P-P	Leno line fabric aligned layering, impacting the plain area of the first and second layer
aligned-L-L	Leno line fabric aligned layering, impacting the leno line of the first layer and second layer

FE simulations were carried out according to the models described in Table 6-3. The energy absorptions of the different panels are illustrated in Figure 6-5. It is clear that panels with an L-L fabric arrangement absorbed the least amount of energy for both the 90° and aligned arrangements. For a two-layer panel, the L-P and P-L layer arrangement did not make a significant difference in energy absorption, although the P-L arrangement showed slightly higher energy absorption for both the 90° arrangement (0.5%) and the offset (1%), as compared to the L-P arrangement. In the case of P-P arrangement, the panels achieved the highest energy absorption, with the aligned model relating to the lowest energy absorption. In practical situations, projectiles may impact the ballistic panel randomly. This investigation suggests that the offset arrangement of the plain woven fabrics with leno insertions is optimal to achieve the best ballistic performance, which indicates that the higher gripping effect created by leno insertion led to better fabric integrity, and the evenly distributed leno line created a larger transfer of impact energy to an interaction of more individual

yarns. The offset layer arrangement can maximise utilising the gripping results to get more yarns involved in efficient energy absorption.

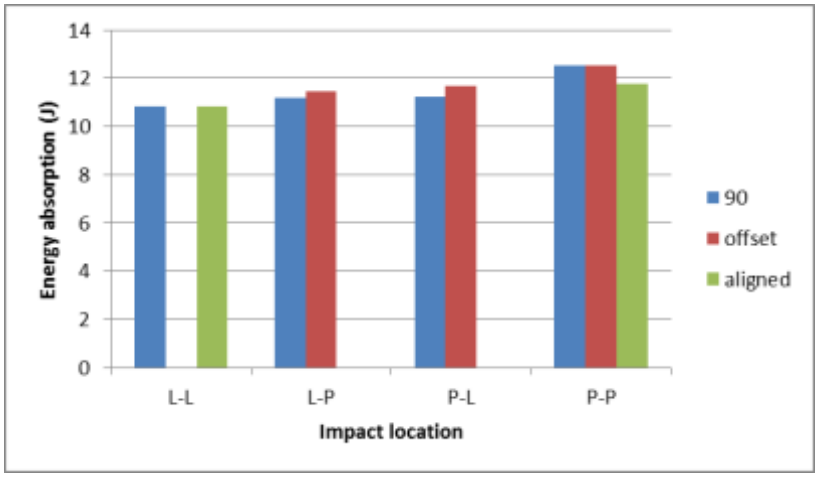

Figure 6-5 Energy absorption at different impact locations for different layer arrangements

6.4 Summary

This chapter focused on the optimisation of the leno fabric by using the numerical method and experimental EV_{50} method for validation.

Since the fabric with leno gripping is the most effective method among algripping methods, it is worthwhile to investigate the leno gap. The leno fabric model has been created and validated by EV_{50} ballistic tests.

Leno fabric has been studied, and 4cm is found to be the most suitable gap between the leno lines for energy absorption, as a smaller gap leads to over-constrained weft yarns, and a larger gap reduces the gripping effect on the weft yarns. The impact location studies have been conducted with different layer arrangements and different impact locations. It has been found that the offset layer arrangement offers higher

energy absorption at all impact location areas in the numerical model, which is strong evidence for explaining the superior energy absorption results during multilayer ballistic tests in Chapter 4. The results from the numerical model have been validated by EV_{50}, which confirms the superior ballistic limit for leno fabric with a 4cm gap rather than a 2cm gap.

Chapter 7 Conclusions and Future work

7.1 Conclusions

The aim of this research was to improve the ballistic performance of soft body armour with reduced weight by using weaving techniques. For this purpose, novel woven fabrics were engineered to offer enhanced inter-yarn gripping to maximise the ballistic performance. In order to achieve the aim of this research, objectives were designed to include the following: (1) establish an understanding of the failure mechanisms of ballistic fabrics; (2) investigate the influence of inter-yarn friction on ballistic performance; (3) identify textile techniques that facilitate increased inter-yarn friction in ballistic fabrics; (4) evaluate fabrics and panels made by designed fabrics with enhanced yarn gripping insertion; (5) analyse the effectiveness of the selected design gripping methods and find the optimisation of the leno gap.

The achievements from the research are as follows:

(a) Fabric innovation and evaluation

Based on the findings of the ballistic fabrics with enhanced inter-yarn friction for improved ballistic performance, five inter-yarn gripping methods were devised associated with the use of textile technology: weft cramming, double weft insertion, involvement of leno lines, combination of leno lines and weft cramming, and combination of leno lines with double weft insertion. Quasi-static yarn pull-out tests confirmed that the plain woven fabric with leno insertion was the most efficient for extra yarn gripping, leading to an almost 36% increase in yarn pull-out resistance. The results from the ballistic impact experiments demonstrated that the innovative fabric structures made the fabrics more energy absorbent. The independent V_{50} tests reassured the efficiency of the yarn gripping techniques used for the new fabric innovations.

(b) Improved understanding of the panel formation from the innovative fabrics

It has been found that the panels may behave differently from a single layer on energy absorption, and the impact location was noticed to influence the ballistic performance. Therefore, three types of fabric layer configuration were used for the layer arrangement, and the layer sequence was based on the leno line direction, namely a layered leno line for adjacent fabrics by 90 degrees, an aligned sequence for the leno line on the fabric panel and an offset leno line for the fabric panels. During the experimental tests, the energy increase for fabric panels with offset layer arrangement was 8% compared to the plain woven fabric structure. This investigation suggests that the offset arrangement of the plain woven fabrics with leno insertions is optimal to achieve the best ballistic performance, which indicates that a higher gripping effect created by leno insertion led to better fabric integrity, and the evenly distributed leno line created a larger transfer of impact energy to the interaction of more individual yarns. An offset layer arrangement can maximise the gripping results to get more yarns involved in efficient energy absorption, which indicates that the optimum layer arrangement for leno fabric exists.

For the designed layer arrangements, an offset layer arrangement provides the highest energy absorption in both the two-layer test and four-layer test rather than all other structures. The different performances of energy absorption for the layered fabric panels in the two-layer situation and four-layer situation may have been caused by the impact location probability and the weakness of the leno line exposed directly to the subjected projectile impact.

(c) Influence of inter-yarn friction on energy dissipation

It has been proven that the highest energy absorption for the fabric is under the condition of $\mu=1$. A further increase does not help increase the energy absorption,

which may bring over-constrained yarns with limited movement. It has also been noticed that more time is required to penetrate the fabric for relatively high inter-yarn friction. It has been established and confirmed that increasing the inter-yarn friction can improve the ballistic performance. To classify the energy absorption mechanisms into groups, the following results have been achieved:

(1) The increased inter-yarn friction leads to increased kinetic energy and strain energy absorption for the whole fabric. As the inter-yarn friction contributes to the integrity of the weave structure, a higher frictional coefficient provides better integrity, which leads to more yarns being involved to move in the same direction of the impact projectile.

(2) Frictional dissipation energy is increased by increasing the inter-yarn friction and then starts to decrease when μ is over 0.3. The higher inter-yarn friction restrains the relative slippage between yarns, which leads to less frictional dissipation energy.

(3) Inter-yarn friction has a positive effect on improving the kinetic and strain energy absorption for both principal yarns and secondary yarns.

(4) It has been found that the inter-yarn friction does not affect the longitudinal weave velocity. Higher stress load is distributed onto the secondary yarn due to the higher inter-yarn friction, which can avoid stress concentration on the primary yarn.

(d) Optimised interval size of leno lines in fabric using EV_{50} and FE

In a further study conducted on leno fabric by FE and EV_{50}, 4cm was found to be the most suitable gap between leno lines for energy absorption and EV_{50}. It has been established that the optimal interval exists, and it can be explained that if the leno gap is too small, it can lead to over-constrained weft yarns and increase the probability of

shooting on the leno line, which results in lower ballistic energy absorption. When the distance between the leno line becomes larger, the gripping effect will get weaker and even disappear, as the small gap leads to over-constrained weft yarns and a large gap reduces the gripping effect on the weft yarns. The leno structures with different intervals were created by ABAQUS® and used to find the gap effect on the energy absorption of the fabric. The results were validated and confirmed by EV_{50}.

(e) Investigation of impact location for designed layer arrangement

The landing position will affect the energy absorption of the fabric for single-layer fabric while, for a multilayer fabric panel, the influence of the impact location will be diminished when the number of layers increases. *Single layer*: Leno fabric on the plain area is increased almost 1%, but on the leno area is decreased by 20% as compared with plain fabric. *Multilay*er: The weak point of the leno area can be averaged out, which can be proved by V_{50} results. When the leno lines were offset during layer arrangement, the results were better.

The impact location studies have been conducted on two-layer fabrics with three (90-degree, offset and aligned) designed layer arrangements with a specific landing area (L-L, L-P, P-P and P-L). It has been found that the offset layer arrangement offers higher energy absorption at all the impact location areas. In the case of P-P arrangement, the panels achieved the highest energy absorption.

7.2 Future work

The theoretical analysis and experimental results provide strong evidence that the gripping insertion does affect the ballistic performance. However, fabric uniformity is hard to maintain due to the gripping insertion. From the aspect of leno insertion, the leno area leads to a rather loose structure, which can contribute to poor results when

the impact is on the leno area. Modified warp and weft densities are required to fill the open area, and such fabrics need to be evaluated. The tension on the leno line needs to be studied for the energy absorption of the fabrics.

In terms of the fabric structure modification, there are two alternative methods that are suggested to modify the double-pick weft insertion. One is inserting two yarns at the same time with an overlapped position, and the other is changing the double-pick yarns into a thicker yarn, ideally with a higher frictional coefficient.

The single-layer shooting experiment did not reflect the results notably between each fabric energy absorption structure. The trauma areas affect the fabric more than the influence of the weave structure insertion in the fabric. It is recommended to conduct a non-penetrating test on the modified fabrics. For the ballistic tests, non-penetration tests work as a complementary method to provide a further understanding of the energy absorption ability.

As FE has proved to be a feasible method to analyse the ballistic impact performance, it is highly recommended to conduct the work on the geometrical model simulation. The more precise the geometrical model, the better simulation can be achieved. In order to make use of the fabric advantages on energy absorption, it is desirable to use different fabric structures in the fabric layer construction. FE models and ballistic experiments can be carried out to study and analyse the ballistic performance.

Reference

1. Guide, N., *Selection and Application Guide to Personal Body Armor*.
2. Mabry, R.L., Holcomb, J.B., Baker, A.M., Cloonan, C.C., Uhorchak, J.M., Perkins, D.E., Canfield, A.J., and Hagmann, J.H., *United States Army Rangers in Somalia: an analysis of combat casualties on an urban battlefield.* Journal of Trauma and Acute Care Surgery, 2000. **49**(3): p. 515-529.
3. Wagner, L., *Introduction*, in *Lightweight Ballistic Composites Military and law-enforcement application*, Bhatnagar, A., Editor. 2006, Woodhead Publishing Limited: Abington Hall. p. 1.
4. Vinson, J.R. and Zukas, J.A., *On the Ballistic Impact of Textile Body Armor*. Journal of Applied Mechanics, 1975. **42**(2): p. 263-268.
5. Shen, W., Niu, Y., Bykanova, L., Laurence, P., and Link, N., *Characterizing the Interaction Among Bullet, Body Armor, and Human and Surrogate Targets.* Journal of Biomechanical Engineering, 2010. **132**(12): p. 121001-121001.
6. Chen, X., Sun, D& Wells, G, *Effect of inter-yarn friction on ballistic performance of woven fabrics*, in *Polymeric Protective Technical Textiles*, In B.J. McCarthy (Ed.), Editor. 2013, Smithers Papra.
7. Bhatnagar, A., *Lightweight ballistic composites*, in *Fabrics and composites for ballistic protection of personnel*, Song, J.W., Editor. 2006, Woodhead Publishing Limited Cambridge. p. 212-215.
8. Horrocks, A.R. and Anand, S.C., *Handbook of technical textiles*. 2000: Elsevier.
9. Tong, J., Ma, Y., and Jiang, M., *Effects of the wollastonite fiber modification on the sliding wear behavior of the UHMWPE composites.* Wear, 2003. **255**(1–6): p. 734-741.
10. Larsen, B., Netto, K., and Aisbett, B., *The effect of body armor on performance, thermal stress, and exertion: a critical review.* Military medicine, 2011. **176**(11): p. 1265-1273.
11. Carothers, J.P., *Body Armor: A Historical Perspective; USMC CSC*. 1988.
12. Chen, X. and Chaudhry, I., *19 - Ballistic protection*, in *Textiles for Protection*, Scott, R.A., Editor. 2005, Woodhead Publishing. p. 529-556.

13. Saxtorph, M.N., *Warriors and Weapons of Early Times*. 1972, NY: Macmilan Co.
14. *Body Armor History*. 2011; Available from: http://www.globalsecurity.org.military.systems.ground.body-armor2.htm.
15. Wilkinson, F., *Battle Dress*. 1969, Garden city , NY: Doubleday & Co., Inc. pp.64-71.
16. Scales, R.H., *Clausewitz and World War IV.* Military Psychology, 2009. **21**(S1): p. S23.
17. Tabiei, A. and Nilakantan, G., *Ballistic impact of dry woven fabric composites: a review.* Applied Mechanics Reviews, 2008. **61**(1): p. 010801.
18. Susich, G., Doglitti, L.M. and Wrigley, A.S., *Microscopic Study of Multi-Layer Nylon Body Panel Armor After Impact.* Textile Research Journal, 1958. **28**: p. 5.
19. Wilde, A.F., Roylance, D.K., and Rogers, J.P.M., *Photographic Investigation of High-Speed Missile Impact upon Nylon Fabric Part I: Energy Absorption and Cone Radial Velocity in Fabric.* Textile Research Journal, 1973. **43**(12): p. 753-761.
20. Wilde, A.F., *Photographic Investigation of High-Speed Missile Impact upon Nylon Fabric Part II: Retarding Force on Missile and Transverse Critical Velocity.* Textile Research Journal, 1974. **44**(10): p. 772-778.
21. Mitchell, C. and Carr, D., *Post Failure Examination of a New Body Armor Textile by Use of an Environmental Scanning Electron Microscope.* Electron Microsc Anal, 1999. **161**(3): p. 103-106.
22. Field, J.E., Walley, S.M., Proud, W.G., Goldrein, H.T., and Siviour, C.R., *Review of experimental techniques for high rate deformation and shock studies.* International Journal of Impact Engineering, 2004. **30**(7): p. 725-775.
23. Cork, C. and Foster, P., *The ballistic performance of narrow fabrics.* International Journal of Impact Engineering, 2007. **34**(3): p. 495-508.
24. Smith, J.C., McCrackin, F.L., and Schiefer, H.F., *Stress-Strain Relationships in Yarns Subjected to Rapid Impact Loading Part V: Wave Propagation in Long Textile Yarns Impacted Transversely.* Textile Research Journal, 1958. **28**(4): p. 288-302.
25. Smith, J.C., Blandford, J.M., and Towne, K.M., *Stress-Strain Relationships in Yarns Subjected to Rapid Impact Loading Part VIII: Shock Waves, Limiting*

Breaking Velocities, and Critical Velocities. Textile Research Journal, 1962. **32**(1): p. 67-76.

26. Smith, J.C., Blandford, J.M., and Schiefer, H.F., *Stress-Strain Relationships. in Yarns Subjected to Rapid Impact Loading Part VI: Velocities of Strain Waves Resulting from Impact.* Textile Research Journal, 1960. **30**(10): p. 752-760.
27. Gu, B., *Analytical modeling for the ballistic perforation of planar plain-woven fabric target by projectile.* Composites Part B: Engineering, 2003. **34**(4): p. 361-371.
28. Chen, X., Zhu, F., and Wells, G., *An analytical model for ballistic impact on textile based body armour.* Composites Part B: Engineering, 2013. **45**(1): p. 1508-1514.
29. Vinson, J.R. and TAYLOR, W.J., *Modeling ballistic impact into flexible materials.* AIAA journal, 1990. **28**(12): p. 2098-2103.
30. Parga-Landa, B. and Hernandez-Olivares, F., *An analytical model to predict impact behaviour of soft armours.* International Journal of Impact Engineering, 1995. **16**(3): p. 455-466.
31. Hetherington, J., *Energy and momentum changes during ballistic perforation.* International Journal of Impact Engineering, 1996. **18**(3): p. 319-337.
32. Chocron-Benloulo, I.S., Rodriguez, J., and Sánchez-Gálvez, V., *A simple analytical model to simulate textile fabric ballistic impact behavior.* Textile Research Journal, 1997. **67**(7): p. 520-528.
33. Billon, H. and Robinson, D., *Models for the ballistic impact of fabric armour.* International Journal of Impact Engineering, 2001. **25**(4): p. 411-422.
34. Porwal, P.K. and Phoenix, S.L., *Modeling system effects in ballistic impact into multi-layered fibrous materials for soft body armor.* International journal of fracture, 2005. **135**(1-4): p. 217-249.
35. Mamivand, M. and Liaghat, G., *A model for ballistic impact on multi-layer fabric targets.* International Journal of Impact Engineering, 2010. **37**(7): p. 806-812.
36. Duan, Y., Keefe, M., Bogetti, T., and Cheeseman, B., *Modeling friction effects on the ballistic impact behavior of a single-ply high-strength fabric.* International Journal of Impact Engineering, 2005. **31**(8): p. 996-1012.

37. Rao, M.P., Duan, Y., Keefe, M., Powers, B.M., and Bogetti, T.A., *Modeling the effects of yarn material properties and friction on the ballistic impact of a plain-weave fabric.* Composite Structures, 2009. **89**(4): p. 556-566.
38. Duan, Y., Keefe, M., Bogetti, T.A., Cheeseman, B.A., and Powers, B., *A numerical investigation of the influence of friction on energy absorption by a high-strength fabric subjected to ballistic impact.* International Journal of Impact Engineering, 2006. **32**(8): p. 1299-1312.
39. Roylance, D., Wilde, A., and Tocci, G., *Ballistic impact of textile structures.* Textile Research Journal, 1973. **43**(1): p. 34-41.
40. Roylance, D. and Wang, S.-S., *Influence of fibre properties on ballistic penetration of textile panels.* Fibre Science and Technology, 1981. **14**(3): p. 183-190.
41. Ting, C., Ting, J., Cunniff, P., and Roylance, D., *Numerical characterization of the effects of transverse yarn interaction on textile ballistic response*, in *30 th International SAMPE Technical Conference*. 1998. p. 57-67.
42. Liu, D., ed. *Dynamic Effect in Composites*. ed. W.Hyer, M. Vol. 1. 2012, DEStech Publications: Lancaster,Pennsylvania. p.104.
43. Roylance, D. and Wang, S.-S., *Penetration mechanics of textile structures*, in *Ballistic Materials and Penetration Mechanics*, Laible, R.C., Editor. 1980, DTIC Document: New York.
44. Shim, V., Tan, V., and Tay, T., *Modelling deformation and damage characteristics of woven fabric under small projectile impact.* International Journal of Impact Engineering, 1995. **16**(4): p. 585-605.
45. Termonia, Y., *Impact resistance of woven fabrics.* Textile Research Journal, 2004. **74**(8): p. 723-729.
46. Tan, V. and Khoo, K., *Perforation of flexible laminates by projectiles of different geometry.* International Journal of Impact Engineering, 2005. **31**(7): p. 793-810.
47. Zeng, X., Shim, V., and Tan, V., *Influence of boundary conditions on the ballistic performance of high-strength fabric targets.* International Journal of Impact Engineering, 2005. **32**(1): p. 631-642.
48. Novotny, W., Cepuš, E., Shahkarami, A., Vaziri, R., and Poursartip, A., *Numerical investigation of the ballistic efficiency of multi-ply fabric armours*

during the early stages of impact. International Journal of Impact Engineering, 2007. **34**(1): p. 71-88.

49. Shockey, D.A., Erlich, D.C., and Simons, J.W. *Lightweight fragment barriers for commercial aircraft*. in *Proceedings of the 18th International Symposium on Ballistics, San Antonio, Texas*. 1999.
50. Shockey, D.A., Erlich, D.C., and Simons, J.W., *Improved barriers to turbine engine fragments: interim report III*. 2001, DTIC Document.
51. Gu, B., *Ballistic penetration of conically cylindrical steel projectile into plain-woven fabric target–a finite element simulation.* Journal of Composite Materials, 2004. **38**(22): p. 2049-2074.
52. Duan, Y., Keefe, M., Bogetti, T., and Cheeseman, B., *Modeling the role of friction during ballistic impact of a high-strength plain-weave fabric.* Composite Structures, 2005. **68**(3): p. 331-337.
53. Duan, Y., Keefe, M., Bogetti, T.A., and Powers, B., *Finite element modeling of transverse impact on a ballistic fabric.* International Journal of Mechanical Sciences, 2006. **48**(1): p. 33-43.
54. Zhang, G., Batra, R., and Zheng, J., *Effect of frame size, frame type, and clamping pressure on the ballistic performance of soft body armor*. Composites Part B: Engineering, 2008. **39**(3): p. 476-489.
55. Rao, M., Nilakantan, G., Keefe, M., Powers, B., and Bogetti, T., *Global/local modeling of ballistic impact onto woven fabrics.* Journal of Composite Materials, 2009. **43**(5): p. 445-467.
56. Talebi, H., Wong, S., and Hamouda, A., *Finite element evaluation of projectile nose angle effects in ballistic perforation of high strength fabric.* Composite Structures, 2009. **87**(4): p. 314-320.
57. Chocron, S., Figueroa, E., King, N., Kirchdoerfer, T., Nicholls, A.E., Sagebiel, E., Weiss, C., and Freitas, C.J., *Modeling and validation of full fabric targets under ballistic impact.* Composites Science and Technology, 2010. **70**(13): p. 2012-2022.
58. Nilakantan, G., Keefe, M., Bogetti, T.A., Adkinson, R., and Gillespie, J.W., *On the finite element analysis of woven fabric impact using multiscale modeling techniques.* International Journal of Solids and Structures, 2010. **47**(17): p. 2300-2315.

59. Nilakantan, G., Keefe, M., Bogetti, T.A., and Gillespie, J.W., *Multiscale modeling of the impact of textile fabrics based on hybrid element analysis.* International Journal of Impact Engineering, 2010. **37**(10): p. 1056-1071.
60. Nilakantan, G., Keefe, M., Wetzel, E.D., Bogetti, T.A., and Gillespie, J.W., *Computational modeling of the probabilistic impact response of flexible fabrics.* Composite Structures, 2011. **93**(12): p. 3163-3174.
61. Jin, L., Sun, B., and Gu, B., *Finite element simulation of three-dimensional angle-interlock woven fabric undergoing ballistic impact.* Journal of the Textile Institute, 2011. **102**(11): p. 982-993.
62. Chen, X., Zhou, Y., and Wells, G., *Numerical and experimental investigations into ballistic performance of hybrid fabric panels.* Composites Part B: Engineering, 2014. **58**(0): p. 35-42.
63. Grujicic, M., Arakere, G., He, T., Gogulapati, M., and Cheeseman, B., *A numerical investigation of the influence of yarn-level finite-element model on energy absorption by a flexible-fabric armour during ballistic impact.* Proceedings of the Institution of Mechanical Engineers, Part L: Journal of Materials Design and Applications, 2008. **222**(4): p. 259-276.
64. Ha-Minh, C., Boussu, F., Kanit, T., Crepin, D., and Imad, A., *Analysis on failure mechanisms of an interlock woven fabric under ballistic impact.* Engineering Failure Analysis, 2011. **18**(8): p. 2179-2187.
65. Barauskas, R. and Abraitienė, A., *Computational analysis of impact of a bullet against the multilayer fabrics in LS-DYNA.* International Journal of Impact Engineering, 2007. **34**(7): p. 1286-1305.
66. Zhou, Y., *Development of lightweight soft body armour for ballistic protechtion*, in *The University of Manchester*. 2013: Manchetser.
67. Hivet, G., Wendling, A., Vidal-Salle, E., Laine, B., and Boisse, P., *Modeling strategies for fabrics unit cell geometryapplication to permeability simulations.* International Journal of Material Forming, 2010. **3**(1): p. 727-730.
68. Lomov, S.V., Huysmans, G., Luo, Y., Parnas, R.S., Prodromou, A., Verpoest, I., and Phelan, F.R., *Textile composites: modelling strategies.* Composites Part A: Applied Science and Manufacturing, 2001. **32**(10): p. 1379-1394.
69. Kawabata, S., Niwa, M., and Kawai, H., *3—THE FINITE-DEFORMATION THEORY OF PLAIN-WEAVE FABRICS PART I: THE BIAXIAL-*

DEFORMATION THEORY. Journal of the Textile Institute, 1973. **64**(1): p. 21-46.

70. Grujicic, M., Bell, W., Arakere, G., He, T., Xie, X., and Cheeseman, B., *Development of a meso-scale material model for ballistic fabric and its use in flexible-armor protection systems.* Journal of materials engineering and performance, 2010. **19**(1): p. 22-39.
71. Kawabata, S., Niwa, M., and Kawai, H., *4—THE FINITE-DEFORMATION THEORY OF PLAIN-WEAVE FABRICS. PART II: THE UNIAXIAL-DEFORMATION THEORY.* Journal of the Textile Institute, 1973. **64**(2): p. 47-61.
72. Kawabata, S., Niwa, M., and Kawai, H., *5—THE FINITE-DEFORMATION THEORY OF PLAIN-WEAVE FABRICS. PART III: THE SHEAR-DEFORMATION THEORY.* Journal of the Textile Institute, 1973. **64**(2): p. 62-85.
73. Ivanov, I. and Tabiei, A., *Loosely woven fabric model with viscoelastic crimped fibres for ballistic impact simulations.* International journal for numerical methods in engineering, 2004. **61**(10): p. 1565-1583.
74. King, M., Jearanaisilawong, P., and Socrate, S., *A continuum constitutive model for the mechanical behavior of woven fabrics*. International Journal of Solids and Structures, 2005. **42**(13): p. 3867-3896.
75. Shahkarami, A. and Vaziri, R., *A continuum shell finite element model for impact simulation of woven fabrics.* International Journal of Impact Engineering, 2007. **34**(1): p. 104-119.
76. Grujicic, M., Bell, W., Arakere, G., He, T., and Cheeseman, B., *A meso-scale unit-cell based material model for the single-ply flexible-fabric armor.* Materials & Design, 2009. **30**(9): p. 3690-3704.
77. Lin, C.C., Lin, J.H., and Chang, C.C., *Fabrication of Compound Nonwoven Materials for Soft Body Armor*.* Journal of forensic sciences, 2011. **56**(5): p. 1150-1155.
78. Roylance, D., *Ballistics of transversely impacted fibers.* Textile Research Journal, 1977. **47**(10): p. 679-684.
79. Cheeseman, B.A. and Bogetti, T.A., *Ballistic impact into fabric and compliant composite laminates.* Composite Structures, 2003. **61**(1): p. 161-173.

80. Cunniff, P.M., *An analysis of the system effects in woven fabrics under ballistic impact.* Textile Research Journal, 1992. **62**(9): p. 495-509.
81. Roylance, D., *Stress wave propagation in fibres: effect of crossovers.* Fibre Science and Technology, 1980. **13**(5): p. 385-395.
82. Freeston, W.D. and Claus, W.D., *Strain-wave reflections during ballistic impact of fabric panels.* Textile Research Journal, 1973. **43**(6): p. 348-351.
83. Shahkarami, A., Cepus ,E.,Vaziri, R. and Poursartip, A., *Material Responses To Ballistic Impact*, in *Lightweight Ballistic Composite*, Bhatnagar, A., Editor. 2006, Woodhead Publishing Limited and CRC Press LLC:Cambridge: Cambridges. p. p.82-95.
84. Lee, B.L., Walsh, T.F., Won, S.T., Patts, H.M., Song, J.W., and Mayer, A.H., *Penetration failure mechanisms of armor-grade fiber composites under impact.* Journal of Composite Materials, 2001. **35**(18): p. 1605-1633.
85. Prosser, R.A., Cohen, S.H., and Segars, R.A., *Heat as a factor in the penetration of cloth ballistic panels by 0.22 caliber projectiles.* Textile Research Journal, 2000. **70**(8): p. 709-722.
86. Cunniff, P., *Dimensionless Parameters for Optimization of Textile-Based Body Armor Systems in Proceedings of the 18th International Symposium on Ballistics*. 1999, San Antonio, United States of America.
87. Shin, H.-S., Erlich, D., and Shockey, D., *Test for measuring cut resistance of yarns.* Journal of Materials Science, 2003. **38**(17): p. 3603-3610.
88. Zhou, Y., Chen, X., and Wells, G., *Influence of yarn gripping on the ballistic performance of woven fabrics from ultra-high molecular weight polyethylene fibre.* Composites Part B: Engineering, 2014. **62**(0): p. 198-204.
89. Ha-Minh, C., Imad, A., Boussu, F., Kanit, T., and Crépin, D., *Numerical study on the effects of yarn mechanical transverse properties on the ballistic impact behavior of textile fabric.* The Journal of Strain Analysis for Engineering Design, 2012: p. 524-534.
90. Song, J.W., *Fabrics and composites for balllistic protection of personnel*, in *Lightweight ballistic composites Military and law-enforcement application*, Bhatnagar, A., Editor. 2006, Woodhead publising in materials. p. 212.
91. *A History of Body Armor- Bullet Proof Vest.* 2012; Available from: http://inventors.about.com/library/inventors/blforensic3.htm

92. Machalaba, N., Budnitskii, G., and Shchetinin, A., *Trends in the development of synthetic fibres for armor material.* Fibre Chemistry, 2001. **33**(2): p. 117-126.
93. Stein, H.L., *Ultrahigh molecular weight polyethylenes(uhmwpe).* ASM International, Engineering Plastics. Engineered Materials Handbook, 1988. **2**: p. 167-171.
94. Wong, D.W., Camirand, W.M., and Pavlath, A.E., *Development of edible coatings for minimally processed fruits and vegetables.* Edible coatings and films to improve food quality, 1994: p. 65-88.
95. *Dyneema* Available from: http://www.tote.com.au/dyneema.htm.
96. Tam T. and Bhatnagar A., *High performance ballsitic fibers*, in *Lighweight ballistic composites Military and law-enforcement applications*, Bhatnagar, A., Editor. 2006, Woodhead publishing in materials. p. 193.
97. Ran, S., Burger, C., Fang, D., Cookson, D., Yabuki, K., Teramoto, Y., Cunniff, P., Viccaro, P., Hsiao, B., and Chu, B., *Structure formation in high-performance PBO fibers.* NSLS Activity Report2001, 2001: p. 2-147.
98. Yamashita, Y., Kawabata, S., Minami, H., Okada, S., and Tanaka, A., *Fatigue property of PRO fiber.* Published on-line http://www. mat. usp. ac. jp/polymer-composite.
99. TOYOBO. *PBO FIBER ZYLON*. 2005; Available from: http://www.toyobo-global.com/seihin/kc/pbo/zylon-p/bussei-p/technical.pdf.
100. Thomas, H.L., *Non-woven ballistic composites*, in *Lightweight ballistic composites Military and law-enforcement applications*, Bhatnagar, A., Editor. 2006, Woodhead publishing in materials: Abington. p. 249.
101. Scott, R.A., *Textiles for protection*. 2005: Elsevier.
102. Song, J.W., *Fabrics and composites for ballistic protection of personnel*, in *Lightweight ballistic composites Military and law-enforcement applications*, A.Bhatnagar, Editor. 2006, Woodhead publishing in materials: Abington. p. 213.
103. *Hybrid ballistic fabric*. 1993, Google Patents.
104. Laible, R., *Ballistic materials and penetration mechanics*. Vol. 5. 2012: Elsevier.
105. Lyons, J., *Impact phenomena in textiles*. 1962, DTIC Document.

106. Riewald, P., Folgar, F., Yang, H., and Shaughnessy, W., *Lightweight helmet from a new aramid fiber.* Advanced Materials/Affordable Processes., 1991. **23**: p. 684-695.
107. Scott, B.R., *New ballistic products and technologies*, in *Lightweight ballistic composites Military and law-enforcement application*, A.Bhatnagar, Editor. 2006, Woodhead publishing in materials: Abington. p. 347.
108. Thomas, G., *Non-woven fabrics for military applications.* The Textile Institute and Woodhead Publishing, 2008: p. 17.
109. Thomas, G., *Non-woven fabrics for military applications.* Military Textile, A volume in Woodhead Publishing Series in Textiles, 2008: p. 17-48.
110. Sun, D. and Chen, X., *13 - Three-dimensional textiles for protective clothing*, in *Advances in 3D Textiles*, Chen, X., Editor. 2015, Woodhead Publishing. p. 341-360.
111. Lim, J.S., Lee, B.H., Lee, C.B., and Han, I.-S., *Effect of the weaving density of aramid fabrics on their resistance to ballistic impacts.* 2012.
112. Bhatnagar, A., *Bullets, fragments and bullet deformation*, in *Lightweight ballistic composites Military and law-enforcement applications*, Bhatnagar, A., Editor. 2006, Woodhead publishing in materials: Abington. p. 63.
113. Shahkarami, A., Cepus ,E.,Vaziri, R. and Poursartip, A., *Material responses to ballistic impact*, in *Lightweight ballistic composites Military and law-enforcement applications*, Bhatnagar, A., Editor. 2006, Woodhead publishing in materials: Abington. p. 77.
114. Briscoe, B. and Motamedi, F., *The ballistic impact characteristics of aramid fabrics: the influence of interface friction.* Wear, 1992. **158**(1): p. 229-247.
115. Bazhenov, S., *Dissipation of energy by bulletproof aramid fabric.* Journal of Materials Science, 1997. **32**(15): p. 4167-4173.
116. Tan, V. and Ching, T., *Computational simulation of fabric armour subjected to ballistic impacts.* International Journal of Impact Engineering, 2006. **32**(11): p. 1737-1751.
117. Montgomery, T., Grady, P., and Tomasino, C., *The effects of projectile geometry on the performance of ballistic fabrics.* Textile Research Journal, 1982. **52**(7): p. 442-450.

118. Tan, V., Lim, C., and Cheong, C., *Perforation of high-strength fabric by projectiles of different geometry.* International Journal of Impact Engineering, 2003. **28**(2): p. 207-222.
119. Lim, C., Tan, V., and Cheong, C., *Perforation of high-strength double-ply fabric system by varying shaped projectiles.* International Journal of Impact Engineering, 2002. **27**(6): p. 577-591.
120. Bhatnagar, A., *Bullets, fragments and bullet deformation*, in *Lightweight ballistic composites Military and law-enforcement applications*, Bhatnagar, A., Editor. 2006, Woodhead publishing in materials: Abington. p. 52.
121. Pierson, M., Delfosse, D., Vaziri, R., and Poursartip, A. *Penetration of laminated composite plates due to impact*. in *14th International Symposium on Ballistics, Québec, Canada*. 1993.
122. Ellis, R.L., *Ballistic Impact Resistance of Graphite Epoxy Composites with Shape Memory Alloy and Extended Chain Polyethylene Spectra™ Hybrid Components*. 1996, Virginia Polytechnic Institute and State University.
123. Carr, D., *Failure mechanisms of yarns subjected to ballistic impact.* Journal of materials science letters, 1999. **18**(7): p. 585-588.
124. Starratt, D., Pageau, G., Vaziri, R., and Poursartip, A. *An instrumented experimental study of the ballistic impact response of Kevlar fabric*. in *Proceedings of the 18th International Symposium on Ballistics*. 1999.
125. Carr, D., Lankester, C., Peare, A., Fabri, N., and Gridley, N., *Does quilting improve the fragment protective performance of body armour?* Textile Research Journal, 2012: p. 0040517512436827.
126. Stuart, I., *Capstan equation for strings with rigidity.* British Journal of Applied Physics, 1961. **12**(10): p. 559.
127. Bilisik, K., *Properties of yarn pull-out in para-aramid fabric structure and analysis by statistical model.* Composites Part A: Applied Science and Manufacturing, 2011. **42**(12): p. 1930-1942.
128. Bilisik, K. and Korkmaz, M., *Single and multiple yarn pull-outs on aramid woven fabric structures.* Textile Research Journal, 2011. **81**(8): p. 847-864.
129. Dong, Z. and Sun, C., *Testing and modeling of yarn pull-out in plain woven Kevlar fabrics.* Composites Part A: Applied Science and Manufacturing, 2009. **40**(12): p. 1863-1869.

130. Sun, D., Chen, X., and Wells, G., *Engineering and analysis of gripping fabrics for improved ballistic performance.* Journal of Composite Materials, 2013: p. 0021998313485997.
131. X. Chen, D.S., Y. Wang, Y. Zhou. *2D/3D Woven Fabrics for Ballistic Protection. Proceedings to the 4th World Conference on 3D Fabrics and Their Application,*. 2012. RWTH Aachen University, Germany.
132. Sun, D., Chen, X., and Mrango, M., *Investigating ballistic impact on fabric targets with gripping yarns.* Fibers and Polymers, 2013. **14**(7): p. 1184-1189.
133. Hearle, J., Leech, C., Adeyefa, A., and Cork, C., *Ballistic impact resistance of multi-layer textile fabrics*. 1981, DTIC Document.
134. Ahmad, M., Ahmad, W., Samsuri, A., Salleh, J., and Abidin, M. *Blunt Trauma Performance of Fabric Systems Utilizing Natural Rubber Coated High Strength Fabrics*. in *INTERNATIONAL CONFERENCE ON ADVANCEMENT OF MATERIALS AND NANOTECHNOLOGY:(ICAMN—2007)*. 2010: AIP Publishing.
135. Wilson, T.V. *How Liquid Body Armor Works*. 26 February 2007 [cited 2015 06 August]; Available from: http://science.howstuffworks.com/liquid-body-armor.htm.
136. Lee, Y.S., Wetzel, E.D., and Wagner, N.J., *The ballistic impact characteristics of Kevlar® woven fabrics impregnated with a colloidal shear thickening fluid.* Journal of Materials Science, 2003. **38**(13): p. 2825-2833.
137. Wetzel, D., Wagner, J., Lee, Y.S., Egres, R., Kirkwood, K., Kirkwood, J., and Matthews, P., *Novel flexible body armor utilizing shear thickening fluid (STF) composites.* 2003.
138. Wetzel, E.D., Lee, Y., Egres, R., Kirkwood, K., Kirkwood, J., and Wagner, N. *The effect of rheological parameters on the ballistic properties of shear thickening fluid (STF)-Kevlar composites*. in *AIP Conference Proceedings*. 2004: IOP INSTITUTE OF PHYSICS PUBLISHING LTD.
139. Bhatnagar, A., *Standard and specifications for lightweight ballistic materials*, in *Lightweight ballistic composites Military and law-enforcement applications*, Bhatnagar, A., Editor. 2006, Woodhead publishing in materials: Abington. p. 127.
140. Zee, R.H. and Hsieh, C.Y., *Energy loss partitioning during ballistic impact of polymer composites.* Polymer Composites, 1993. **14**(3): p. 265-271.

141. Lee, B., Song, J., and Ward, J., *Failure of Spectra® polyethylene fiber-reinforced composites under ballistic impact loading.* Journal of Composite Materials, 1994. **28**(13): p. 1202-1226.
142. Sun, C. and Potti, S., *A simple model to predict residual velocities of thick composite laminates subjected to high velocity impact.* International Journal of Impact Engineering, 1996. **18**(3): p. 339-353.
143. Starratt, D., Sanders, T., Cepuš, E., Poursartip, A., and Vaziri, R., *An efficient method for continuous measurement of projectile motion in ballistic impact experiments.* International Journal of Impact Engineering, 2000. **24**(2): p. 155-170.
144. Zeng, X., Tan, V., and Shim, V., *Modelling inter-yarn friction in woven fabric armour*. International journal for numerical methods in engineering, 2006. **66**(8): p. 1309-1330.
145. Gogineni, S., Gao, X.-L., David, N., and Zheng, J., *Ballistic impact of Twaron CT709® plain weave fabrics.* Mechanics of Advanced Materials and Structures, 2012. **19**(6): p. 441-452.
146. Bhatnagar, A., *Lightweight ballistic composites: military and law-enforcement applications*. 2006: Woodhead Publishing.
147. Justice, N.I.o., *Ballistic Resistance of Body Armor NIJ Standard-0101.06*, in *Ballistic Test Method*. 2008, U.S. Department of Justice.
148. Croft, J. and Longhurst, D., *HOSDB Body Armour Standards for UK Police (2007) Part 2: Ballistic Resistance.* C) Crown Copyright, 2007.
149. Metker, L.W., Prather, R.N., and Johnson, E.M., *A Method for Determining Backface Signatures of Soft Body Armors*. 1975, DTIC Document.
150. Prather, R.N., Swann, C.L., and Hawkins, C.E., *Backface Signatures of Soft Body Armors and the Associated Trauma Effects*. 1977, DTIC Document.
151. Gower, H., Cronin, D., and Plumtree, A., *Ballistic impact response of laminated composite panels.* International Journal of Impact Engineering, 2008. **35**(9): p. 1000-1008.
152. Lomakin, E., Mossakovsky, P., Bragov, A., Lomunov, A., Konstantinov, A.Y., Kolotnikov, M., Antonov, F., and Vakshtein, M., *Investigation of impact resistance of multilayered woven composite barrier impregnated with the*

shear thickening fluid. Archive of applied mechanics, 2011. **81**(12): p. 2007-2020.

153. Bilisik, K. and Korkmaz, M., *Multilayered and multidirectionally-stitched aramid woven fabric structures: experimental characterization of ballistic performance by considering the yarn pull-out test.* Textile Research Journal, 2010. **80**(16): p. 1697-1720.
154. Karahan, M., *Comparison of ballistic performance and energy absorption capabilities of woven and unidirectional aramid fabrics.* Textile Research Journal, 2008. **78**(8): p. 718-730.
155. Pandya, K.S., Pothnis, J.R., Ravikumar, G., and Naik, N., *Ballistic impact behavior of hybrid composites.* Materials & Design, 2013. **44**: p. 128-135.
156. Villanueva, G.R. and Cantwell, W., *The high velocity impact response of composite and FML-reinforced sandwich structures.* Composites Science and Technology, 2004. **64**(1): p. 35-54.
157. Wen, H., *Predicting the penetration and perforation of FRP laminates struck normally by projectiles with different nose shapes.* Composite Structures, 2000. **49**(3): p. 321-329.
158. Standard, D.o.D.T.M., *V50 Ballistic Test For Armor*, in *MIL-STD-662F*. 1997.
159. Nilakantan, G. and Gillespie, J.W., *Ballistic impact modeling of woven fabrics considering yarn strength, friction, projectile impact location, and fabric boundary condition effects.* Composite Structures, 2012. **94**(12): p. 3624-3634.
160. Abiru, S. and Iizuka, K., *Bulletproof fabric and process for its production*. 1999, Google Patents.
161. Price, A.L. and Young, S.A., *Ballistic vest*. 1999, Google Patents.
162. Cunniff, P.M. *Decoupled response of textile body armor*. in *Proceedings of the 18th International Symposium of Ballistics*. 1999: CRC, Boca Raton, FL.
163. Figucia, F., *Energy absorption of Kevlar fabrics under ballistic impact.* US Army Natick Research and Development Command, 1980.
164. Ahmed, A.Y., *Physical Properties of Leno Fabrics* in *in Institute of Science and Technology*. 1972, Victoria Univeristy of Manchester: Manchester.
165. Sondhelm, W.S., *Technical fabric structures–1. Woven fabrics.* Handbook of technical textiles, 2000. **12**: p. 62.
166. Peirce, F.T., *5—The geometry of cloth structure.* Journal of the Textile Institute Transactions, 1937. **28**(3): p. T45-T96.

167. Kemp, A., *An extension of Peirce's cloth geometry to the treatment of non-circular threads.* 1958.
168. Xiong, J., Shenoi, R., and Cheng, X., *A modified micromechanical curved beam analytical model to predict the tension modulus of 2D plain weave fabric composites.* Composites Part B: Engineering, 2009. **40**(8): p. 776-783.
169. Hearle, J.W., *High-performance fibres*. 2001: Elsevier.
170. CHU, Y., *Surface Modification to Aramid and UHMWPE Fabrics to Increase Inter-yarn Friction for Improved Ballistic Performance*. 2015, The University of Manchester.
171. Lim, C., Shim, V., and Ng, Y., *Finite-element modeling of the ballistic impact of fabric armor.* International Journal of Impact Engineering, 2003. **28**(1): p. 13-31.
172. Sabet, A., Fagih, N., and Beheshty, M.H., *Effect of reinforcement type on high velocity impact response of GRP plates using a sharp tip projectile.* International Journal of Impact Engineering, 2011. **38**(8): p. 715-722.
173. Sun, D., Chen, X., Lewis, E., and Wells, G., *Finite element simulation of projectile perforation through a ballistic fabric.* Textile Research Journal, 2012: p. 0040517512464295.
174. Wang, Y. and Xia, Y., *The effects of strain rate on the mechanical behaviour of kevlar fibre bundles: an experimental and theoretical study.* Composites Part A: Applied Science and Manufacturing, 1998. **29**(11): p. 1411-1415.

Appendix

Table 1 single layer ballistic tests for BPW

Test number	*Impact velocity (m/s)*	*Residual velocity (m/s)*	*Projectile kinetic energy loss (J)*
1	465	445	9.56
2	494	476	8.84
3	488	471	8.45
4	483	467	7.47
5	476	457	9.08
6	492	478	6.63
7	485	469	7.58
8	476	456	9.35
9	475	456	9.15
10	488	471	8.45

Table 2 single layer ballistic tests of BPL2

Test number	*Impact velocity (m/s)*	*Residual velocity (m/s)*	*Projectile kinetic energy loss (J)*
1	476	457	8.85
2	485	466	8.73
3	478	459	8.94
4	491	474	8.50
5	472	456	7.27
6	475	459	7.53
7	488	477	5.21
8	494	473	10.65
9	475	460	7.26
10	472	459	6.20
11	475	462	6.43
12	485	466	9.02
13	490	481	4.37
14	484	468	7.38

Table 3 single layer ballistic tests of BPC2

Test number	*Impact velocity (m/s)*	*Residual velocity (m/s)*	*Projectile kinetic energy loss (J)*
1	478.1282	458.2278	9.484602
2	475.2275	462.9156	5.879116
3	472.837	451.3716	10.09782
4	482.0513	458.8086	11.13086
5	486.0393	478.836	3.537704
6	487.0466	464.6983	10.82637
7	483.0421	467.0968	7.711508
8	488.5655	469.5201	9.287778
9	471.4142	453.0663	8.633804
10	478.1282	457.6485	9.754661
11	478.6151	453.0663	12.11587
12	476.6734	453.6341	10.90974
13	474.7475	458.2278	7.844914
14	469.5305	453.0663	7.731588

Table 4 single layer ballistic tests of BPD2

Test number	*Impact velocity (m/s)*	*Residual velocity (m/s)*	*Projectile kinetic energy loss (J)*
1	490.6054	471.3542	9.426138
2	480.0817	465.2956	7.115021
3	487.5519	471.9687	7.610752
4	485.0361	470.1299	7.247113
5	477.6423	456.4943	10.05533
6	479.5918	465.8945	6.591894
7	489.0739	478.2034	5.352001
8	485.0361	469.5201	7.538753
9	463.9684	439.8542	11.09364
10	483.0421	468.3053	7.136103
11	476.6734	455.3459	10.11773
12	484.5361	467.7003	8.160127
13	477.6423	460.5598	8.15765
14	488.0582	468.9119	9.326088

Table 5 single layer ballistic tests of BPL2C

Test number	*Impact velocity (m/s)*	*Residual velocity (m/s)*	*Projectile kinetic energy loss (J)*
1	492.1466	475.0656	8.409155
2	481.5574	464.6983	8.120061
3	493.6975	478.836	7.356733
4	484.5361	469.5201	7.291978
5	482.5462	465.2956	8.322564
6	487.5519	471.3542	7.905825
7	485.5372	469.5201	7.786293
8	492.6625	474.443	8.968663
9	482.5462	465.2956	8.322564
10	496.8288	477.5726	9.550499
11	484.0371	464.6983	9.338802
12	482.5462	470.7412	5.728051
13	485.5372	466.4948	9.227621
14	484.5361	470.1299	7.000338

Table 6 single layer ballistic tests of BPL2D

Test number	*Impact velocity (m/s)*	*Residual velocity (m/s)*	*Projectile kinetic energy loss (J)*
1	458.9844	443.0845	7.300496
2	486.0393	465.2956	10.0447
3	486.5424	470.1299	7.99204
4	481.0645	466.4948	7.027048
5	478.6151	458.8086	9.450622
6	491.1181	474.443	8.195316
7	491.1181	471.9687	9.387234
8	489.0739	475.6899	6.572411
9	483.0421	462.9156	9.690776
10	484.5361	465.2956	9.302073
11	486.5424	470.1299	7.99204
12	486.0393	468.9119	8.325108
13	486.5424	468.9119	8.574188
14	492.1466	479.4702	6.26915

Table 7 EV_{50} ballistic tests for 2 layers of plain fabric

Test number	*T1 (ms)*	*T2 (ms)*	*Vi (m/s)*	*Vr (m/s)*
1	0.965	0.797	487.0466	454.2033
2	0.962	0.789	488.5655	458.8086
3	0.981	0.8	479.103	452.5
4	0.98	0.821	479.5918	440.9257
5	0.964	0.79	487.5519	458.2278
6	0.983	0.8	478.1282	452.5
7	0.96	0.78	489.5833	464.1026

Table 8 EV_{50} ballistic tests for 4 layers of plain fabric

Test number	*T1 (ms)*	*T2 (ms)*	*Vi (m/s)*	*Vr (m/s)*
1	1.033	0.895	454.9855	404.4693
2	1.009	0.848	465.8077	426.8868
3	0.988	0.822	475.7085	440.3893
4	0.965	0.847	487.0466	427.3908
5	0.967	0.841	486.0393	430.44
6	0.948	0.838	495.7806	431.9809
7	0.98	0.889	479.5918	407.1991

Table 9 EV_{50} ballsitc tests for 2 layers of leno fabric with 2cm gap

Test number	*T1 (ms)*	*T2 (ms)*	*Vi (m/s)*	*Vr (m/s)*
1	0.99	0.817	474.7475	443.0845
2	0.989	0.813	475.2275	445.2645
3	0.964	0.821	487.5519	440.9257
4	0.975	0.792	482.0513	457.0707
5	0.962	0.795	488.5655	455.3459
6	0.963	0.82	488.0582	441.4634

Table 10 EV_{50} ballstic tests for 4 layers of leno fabric with 2cm gap

Test number	*T1 (ms)*	*T2 (ms)*	*Vi (m/s)*	*Vr(m/s)*
1	0.986	0.862	476.6734	419.9536
2	0.987	0.888	476.1905	407.6577
3	1.006	0.867	467.1968	417.5317
4	0.989	0.849	475.2275	426.384
5	0.966	0.924	486.5424	391.7749
6	0.985	0.886	477.1574	408.5779

Table 11 EV_{50} ballstic tests for 2 layers of leno fabric with 4cm gap

Test number	*T1(ms)*	*T2(ms)*	*V1(m/s)*	*V2(m/s)*
1	0.942	0.783	498.9384	462.3244
2	0.942	0.771	498.9384	469.5201
3	0.952	0.781	493.6975	463.5083
4	0.977	0.806	481.0645	449.1315
5	0.951	0.784	494.2166	461.7347

Table 12 EV_{50} ballistic tests for 4 layers of leno fabric with 4cm gap

Test number	*T1 (ms)*	*T2 (ms)*	*V1 (m/s)*	*V2(m/s)*
1	0.949	0.891	495.2582	406.2851
2	0.96	0.865	489.5833	418.4971
3	0.931	0.789	504.8335	458.8086
4	0.957	0.823	491.1181	439.8542
5	0.951	0.811	494.2166	446.3625